Phylogeny, histological observation, and *in vitro* fungicide screening and field trials of multiple *Colletotrichum* species, the causal agents of grape ripe rot

Charlotte Oliver

Dissertation submitted to the faculty of the Virginia Polytechnic Institute and State University in partial fulfillment of the requirements for the degree of

Doctor of Philosophy
In
Plant Pathology, Physiology, and Weed Science

Mizuho Nita, Committee Chair
Anton Baudoin
Guido Schnabel
Boris Vinatzer
Keith Yoder

December 12, 2018
Blacksburg, VA

Keywords: Grape ripe rot, *Colletotrichum* spp., histology, fungicide resistance, fungicide screening, Virginia

Phylogeny, histological observation, and *in vitro* fungicide screening and field trials of multiple *Colletotrichum* species, the causal agents of grape ripe rot

Charlotte Oliver

ABSTRACT

Colletotrichum acutatum and *C. gloeosporioides* are fungal plant pathogens that have a global distribution, extensive host range, and convoluted taxonomy. Both species can cause grape ripe rot and are considered endemic to Virginia US. In 2012, *C. acutatum* and *C. gloeosporioides* were reclassified into species complexes that consist of 31 and 22 accepted species, respectively. The objectives of this study were to: 1) survey Virginia vineyards for grape ripe rot, and morphologically and phylogenetically identify isolates to the species within the complexes, 2) conduct an *in vitro* fungicide assay to screen fifteen commercial fungicides and combinations of two fungicides for efficacy to control isolates from seven *Colletotrichum* species from Virginia vineyards, 3) sequence gene fragments from three subunits of the SDH enzyme in the fungicide-screened isolates to observe potential resistance mutations, 4) investigate the susceptibility of three grapevine tissues to *Colletotrichum* species, 5) observe potential infection structures before and after the application of fungicides, 6) evaluate the efficacy of commercial fungicide controls of grape ripe rot in the field, and determine the most advantageous timing of applications. In my studies, I identified six *Colletotrichum* species: *C. aenigma, C. conoides, C. fioriniae, C. gloeosporioides¸ C. kahawae,* and *C. nymphaeae.* I also found two additional groups; an isolate similar to *C. limetticola* and *C. melonis* and a group of isolates that are similar to *C. alienum, C. fructicola,* and *C. nupharicola*. I also identified captan, and mancozeb as two potential active ingredients for control of grape ripe rot isolates from Virginia via the *in vitro* fungicide assay. Additionally, I found that combinations of two active ingredients could increase the efficacy of benzovindiflupyr, copper, and polyoxin-D. *C. fioriniae g*ermination and production of melanized appressoria was documented on leaves. I observed appressorium formation with isolates of two *C. fructicola*-like genotypes and *C. nymphaeae,* as well as secondary conidiation with isolates of *C. aenigma, C. fructicola*-like genotype 3, and *C. nymphaeae* on blooms. And finally, benzovindiflupyr, cyprodinil + fludioxonil pre-mix, and potassium phosphite + tebuconazole were identified as candidates for chemical control for grape ripe rot in the field.

Phylogeny, histological observation, and *in vitro* fungicide screening and field trials of multiple *Colletotrichum* species, the causal agents of grape ripe rot

Charlotte Oliver

PUBLIC ABSTRACT

Colletotrichum acutatum and *C. gloeosporioides* are two fungal plant pathogens that are found on a wide range of crops around the globe. Both fungal species cause the disease grape ripe rot and have been found in Virginia (VA) USA since the late 1800s. Originally, grape ripe rot was considered a minor disease in VA; however, based on communications with local VA vineyard managers, grape ripe rot was found to cause up to 30% direct crop loss. Further indirect economic loss occurs during wine production due to the production of unpalatable, tobacco-like, off flavors from the infected grapes. Sensory studies found this wine flavor change occurred with as little as 3% of the total crushed grapes being infected. Grape ripe rot appears as a sunburn-like, tan injury on the surface of white-fruited grape berries. As the disease progresses, the dark injury expands across the surface of the berry and rings of salmon-colored spore masses form. On red-fruited grapes, the formation of spore masses is usually the first observable sign. Over time, the infected berries will shrivel down to a soft, pustule-covered raisin. Both *C. acutatum* and *C. gloeosporioides* cause the same grape ripe rot symptoms on fruit and overlap in fungal appearance. In addition, investigations of these pathogens using molecular techniques have revealed that each consists of a number of genetically distinct groups that are difficult to distinguish by appearance. Therefore, in 2012, *C. acutatum* and *C. gloeosporioides* were reclassified into 31 and 22 newly accepted species, respectively, using molecular techniques.

The objectives of this study were to: 1) survey VA vineyards for grape ripe rot, and visually and molecularly identify isolates to the species within the new complexes, 2) conduct a laboratory fungicide assay to screen fifteen commercial fungicides and combinations of two fungicides for control of isolates from VA vineyards, 3) sequence gene fragments from three subunits of the SDH enzyme in the fungicide-screened isolates to observe potential resistance mutations, 4) investigate the susceptibility of three grapevine tissues to *Colletotrichum* species, 5) observe potential infection structures before and after the application of fungicides, 6) evaluate the efficacy of commercial fungicide controls of grape ripe rot in the field, and determine the most advantageous timing of applications. In my studies, I identified six *Colletotrichum* species: *C. aenigma, C. conoides, C. fioriniae, C. gloeosporioides¸ C. kahawae,* and *C. nymphaeae.* I also found two additional groups; an isolate similar to *C. limetticola* and *C. melonis* and a group of isolates that are similar to *C. alienum, C. fructicola,* and *C. nupharicola*. Our lab also identified four active ingredients as potential controls of grape ripe rot in the laboratory fungicide assay; captan, mancozeb, tetraconazole and thiophanate-methyl. Additionally, combinations of two compounds can increase the effectiveness of benzovindiflupyr, copper, and polyoxin-D. of *C. fructicola*-like isolates, and *C. nymphaeae* formed infection structures on blooms. of *C. aenigma*, *C. fructicola*-like genotype 3, and *C. nymphaeae* formed spores on blooms without producing symptoms. *C. fioriniae* spores *g*erminated and produced infection structures on leaves without producing symptoms.

Acknowledgements

I would like to thank my advisor, Dr. Mizuho Nita, for his help and direction with these projects over the last four years. I would also like to thank the members of my committee, Dr. Anton Baudoin, Dr. Boris Vinatzer, Dr. Guido Schnabel, and Dr. Keith Yoder, for their support and guidance throughout these projects and, my sources of funding; The Virginia Wine Board, VDACS SCRI block grants and Virginia Tech CALS. Many thanks to the current and past lab members of the Grape Pathology lab at the Alson H. Smith Jr. AREC who have helped me with lab assays, fungal isolation, fungicide applications, vineyard maintenance, sanity retention, etc.: Amanda Bly, Sabrina Hartley, Whitney Berry, Akiko Mangan, Alex Wong, Morgan Gannon, Vanette Trumm, Diana McHenry, Dana Melby, and Binbin Lin. I am grateful for the support of my partner, Curtis Ogle, over the last seven years, and for the gallons of coffee that have been consumed to survive.

Table of Contents

List of Figures

List of Tables

Chapter 1.

Literature Review

1.1. Colletotrichum *epidemiology and global impact*

1.1.1 Global importance

The filamentous, asexual fungal genus *Colletotrichum* has a worldwide distribution and economic significance due in part to *Colletotrichum's* vast host range which encompasses cereals, tree fruit, woody ornamentals, and vegetables in the majority of agricultural areas (Hyde et al. 2009; Prusky et al. 2000; Peres et al. 2005; Wharton & Dieguez-Uribeondo 2004). This genus is generally associated with the sexual genus *Glomerella* (Hyde et al. 2009). The *Colletotrichum* genus is considered to be the eighth most important plant pathogen group, and has been extensively studied as a model organism for genetics and host interaction since the mid-1900s (Bailey & Jeger 1992; Cannon et al. 2012; Dean et al. 2012; Hyde et al. 2009; Prusky et al. 2000).

1.1.2 Pathogen description

Colletotrichum acutatum and *C. gloeosporioides* have extensive overlapping host ranges (Hyde et al. 2009; Peres et al. 2005). Both species are notable pathogens of tree fruits such as apple (Shane & Sutton 1981; Southworth 1891), avocado (Binyamini & Schiffmann-Nadel 1972), and mango (Dodd et al. 1992), small fruits such as strawberry (Maas 1998), blueberry (Hartung et al. 1981; Verma et al. 2007), and grapes (Greer et al. 2014; Simmonds 1965; Steel et al. 2012), and vegetables such as green pepper (Harp et al. 2014). For several crops, such as apple and mango, these *Colletotrichum* species are an important post-harvest pathogen due to the prevalence of asymptomatic, latent infections (Biggs 1995; Dodd et al. 1991; Prusky et al. 2000).

For the rest of this dissertation, the focus will be on grape ripe rot, a disease caused by multiple *Colletotrichum* species.

1.1.3 Symptomology and disease cycle

Both *C. acutatum* and *C. gloeosporioides* cause identical symptoms on mature grape berries (Sutton 2015a). The symptoms are more apparent on white-fruited cultivars where symptoms appear as sunburn-like, tan lesions on berry surfaces. As the disease progresses, the lesion expands across the surface of the berry and concentric rings of acervuli, filled with masses of salmon-colored conidia, form. The formation of salmon-colored, conidial masses generally is the first observable sign on red-fruited cultivars, since the fruit color obscures observation of the lesion (Fig. 1.1). Over time, the infected berries will shrivel to form a soft, pustule-covered raisin.

The disease cycle of ripe rot of grape is not well understood. There are two large gaps in knowledge that will be focused on in this dissertation; the source of initial inoculum in a growing season and how these pathogens behave during the extended latency between infection and symptom development. The hypothesized cycle begins as resting inoculum overwintering in several locations; as dormant conidia or mycelia in infected tissues, on the woody tissues, or conidia in dormant grapevine buds (Samuelian et al. 2012; Sutton 2015a). As the weather warms in the spring, early season rainfall washes the overwintering conidia and mycelia onto new tissues, such as the blooms, young clusters and leaves (Steel et al. 2012). Once the conidia germinate or the mycelium breaks dormancy, the elongating mycelium penetrates grape cluster tissues via an appressorium or a natural opening any time between bloom and two weeks before harvest (Daykin & Milholland 1984; Oliver 2016). As the berries enter veraison (= color change), the first symptoms of grape ripe rot, as described above, appear. Additional, secondary

infections occur when late season rains wash the conidia out of the active acervuli and down the rest of the berries in a cluster (Fig. 1.2).

Colletotrichum sp. on other hosts, such as strawberry (Maas 1998), blueberry (Wharton & Dieguez-Uribeondo 2004), or apple (Sutton 2014), have a better understood disease cycle, including information on initial inoculum source. For all three hosts, one consistent source of initial inoculum is infected debris and fruit mummies left in the field from the previous season (Maas 1998; Milholland 1995; Sutton 2014). Additional sources include inoculum inside dormant blueberry buds, and new transplants with debris in the soil or petiole and stolon lesions for strawberry (Maas 1998; Wharton & Dieguez-Uribeondo 2004). Additionally, on both apple and strawberry, leaves can have asymptomatic, sporulating *Colletotrichum* infection (Borve & Stensvand 2017; Leandro et al. 2003).

1.1.4 Asymptomatic infections

A latent infection occurs when a delay occurs between the initial infection and when symptoms, or obvious signs of fungal colonization, develop (Agrios 2005a). The ability to form asymptomatic, or latent, infections is common for species in the *Colletotrichum* genus (Peres et al. 2005; Prusky & Plumby 1992). Certain chemical or physiological triggers are required for latency to be broken such as a shift in sugar content or disruption of epidermal integrity (Biggs 1995; Mertely & Legard 2004). *C. gloeosporioides* and *acutatum* have been observed to have an extended latent period on the fruit of a variety of hosts such as strawberry (Leandro et al. 2003), olive (Moral et al. 2012), apple (Sutton 2014), and blueberry (Hartung et al. 1981; Milholland 1995; Verma et al. 2007), where infection can begin during bloom but the symptoms are delayed until harvest or during storage (Bailey & Jeger 1992). Daykin and Milholland (1984), in their study of infection by *Colletotrichum* species on grape tissue, showed that *C. gloeosporioides*

infect muscadine grape at any growth stage from green berry until ripening with the formation of appressoria and penetrative hyphae. More recently, *C. acutatum* has been found to infect wine grape inflorescences, and immature table grapes (Greer et al. 2014; Shiraishi et al. 2007; Steel et al. 2012). Additionally, an extended latent period has been observed for *C. acutatum* and *C. siamense* isolates from Virginia (VA) vineyards on infected wine grape clusters (Oliver 2016). However, the behavior between the initial infection event and symptom development of these fungi, and potentially other species of *Colletotrichum* found in VA, is unknown.

1.2. *Taxonomy and Species complex formation*

1.2.1 Historical taxonomy

Historically, *Colletotrichum* species that cause anthracnose diseases on fruit crops were classified as *C. gloeosporioides* (Simmonds 1965; Sutton 1992). However, in the 1960s, *C. acutatum* was described as a separate species (Simmonds 1965). This resulted in overlapping morphology and host range between the two species. In general, the colonies of *Colletotrichum gloeosporioides* on potato dextrose agar (PDA) are flat and gray in culture with aerial conidia, whereas *C. acutatum* appears pink and gray with pink pigmentation in PDA medium (Peres et al. 2005) (Fig. 1. 3, A). The conidia of *C. acutatum* and *C. gloeosporioides* are clear and hyaline and salmon colored en masse. The differentiating feature of the conidia is their shape. *C. acutatum* conidia are oval with one or both ends acute whereas *C. gloeosporioides* conidia are only oval. The size range for the two species overlaps and is 8.5 - 16.5 x 2.5 - 4 µm and 12-21 x 3.5-6 µm, respectively (Maas 1998; Sutton 2015a) (Fig. 1.3, B, C). Unfortunately, when these two fungi are extensively cultured on artificial media, these conidial features become less apparent as the conidia of *C. acutatum* will lose their pointed ends and the *C. gloeosporioides*

conidia lose size (Damm et al. 2012; Weir et al. 2012). The expansive, overlapping host range of both species made the species identification process even more complicated (Peres et al. 2005; Weir et al. 2012; Wharton & Dieguez-Uribeondo 2004).

1.2.2 Multilocus sequence typing and Colletotrichum *species complex formation*

The multiple attempts from many different studies for clarifying *Colletotrichum* species (Hyde et al. 2009; Maharaj & Rampersad 2012; Sreenivasaprasad & Talhinhas 2005) has led to an accumulation of partially or poorly identified gene fragments in open repositories (Hyde et al. 2009). Multilocus sequence typing (MLST) is a newer method for molecular taxonomic identification (Gil-Lamaignere et al. 2003). This method has successfully identified multiple bacterial pathogens such as *Pseudomonas syringae* (Sarkar & Guttman 2004) and *Xylella fastidiosa* (Scally et al. 2005). More recently, MLST has been adapted to fungal pathogens such as *Fusarium solani* (O'Donnell et al. 2008) and multiple *Phytophthora* species (Blair et al. 2008).

MLST functions by amplifying conserved gene fragments of housekeeping genes (Gil-Lamaignere et al. 2003). In 2012, two labs developed MLST schemes to restructure the *C. acutatum* and *C. gloeosporioides* species into large species complexes of 31 and 22 species, respectively (Damm et al. 2012; Weir et al. 2012). The restructuring of *C. acutatum* relied on the following housekeeping genes: internal spacer unit, β-tubulin, chitin synthase 1, glyceraldehyde-3-phosphate dehydrogenase, histone 3, and actin, as well as traditional morphological techniques (Damm et al. 2012). The restructuring of *C. gloeosporioides* relied on similar housekeeping genes including internal spacer unit, β-tubulin, chitin synthase 1, glyceraldehyde-3-phosphate dehydrogenase, and actin, with the addition of calmodulin, glutamine synthetase, and manganese-superoxide dismutase (Weir et al. 2012). Both of these studies contain samples from

a wide range of hosts and global locations; however, *Colletotrichum* species have a very wide hose range and are omnipresent. Localized studies that target a specific host could bring useful information to both scientists and stakeholders about the species within an area.

1.3. *Importance of Fungicides*

1.3.1 Modes of action

The way fungicides inhibit fungal cellular function is called the mode of action (MOA). The MOA of a fungicide generally consists in inhibiting conidial germination or mycelial elongation (Agrios 2005b). Since fungi have rapid generation times and are subject to pressures from fungicide applications, fungicide resistance is a rising issue (Hobbelen et al. 2014). To monitor and mitigate resistance, the international organization Fungicide Resistance Action Committee (FRAC) was formed in the early 1980s (FRAC 2016). This committee manages a MOA fungicide classifications list and assesses the potential for resistance development by each fungicide MOA group. The numbering system, or FRAC group, will be referenced throughout this dissertation.

In this dissertation, ten fungicide chemical groups that are commonly used in wine grape production in the USA are investigated: methyl-benzimidazole carbamates (MBC) (FRAC 1), demethylase inhibitors (DMI) (FRAC 3), succinate dehydrogenase inhibitors (SDHI) (FRAC 7), quinone outside inhibitors (QoI) (FRAC 11), chitin synthase (FRAC 19), aryl-phenyl-ketone (FRAC 50), inorganic coppers (FRAC M1), ethylene-bis-dithiocarbamates (EBDC) (FRAC M3), phthalimides (FRAC M4), and a phosphonate (FRAC P07) (FRAC 2018).

The multi-site MOA compounds EBDC, phthalimide, and inorganic fungicides are three of the oldest chemical classes still available for use (Morton & Staub 2008). These classes are

non-specific protectant chemicals with modes of action that are not fully understood, but are assumed to interact with sulfhydryl groups (–SH) in different ways (McCallan 1949). The major theorized MOA of EBDCs is the formation of isothiocyanate (-N=C=S) radicals which interfere with sulfhydryl groups (McCallan 1949). Sulfhydryl groups that are part of the phthalimide chemical structure are presumed to inhibit the separation of chromosomes during cellular division (McCallan 1949). In the case of copper, the assumed MOA is denaturing of proteins and enzymes by interacting with the sulfur groups (McCallan 1949). Although all three chemical groups have overlapping modes of action, these compounds fall into three different FRAC groups; FRAC M1 for copper, FRAC M3 for EBDC, and FRAC M4 for phthalimides (FRAC 2018).

The MBC (FRAC 1) fungicide class was introduced in the mid-1960s as the first broad-spectrum systemic compounds (Morton & Staub 2008). MBC compounds begin as the chemical benzimidazole; however, *in planta*, benzimidazole unfolds into the active MBC molecule (methyl benzimidazole carbamate). The MBC molecule disrupts microtubule formation by binding to beta-tubulin subunits (Hollomon 2010).

DMIs, most of which are triazoles, are part of the sterol biosynthesis inhibitor (SBI) group (FRAC 3) and currently constitutes the largest class of fungicides available (Morton & Staub 2008). The MOA of DMIs is disruption of sterol formation by inhibiting demethylation of precursors that would normally lead to ergosterol. Cells that failed to properly form sterol become unable to manage the permeability of the cell membrane (Montgomery & Paulsrud 2006).

Many newly introduced fungicides belong to the succinate dehydrogenase inhibitor (SDHI) (FRAC 7) fungicide class and the first compound, carboxin, was released in 1966 as a

cereal seed coating. Originally named the carboxamides, this class was renamed by FRAC during the late 2000s (FRAC 2016). The first compound in this class was only efficacious against basidiomycetes such as bunts, and smuts (Morton & Staub 2008). However, boscalid, which was introduced in 2003, was the first compound in the class to have efficacy on a wide range of pathogens such as *Alternaria alternata* (Avenot et al. 2008), *Monilinia fructicola* (Amiri et al. 2010), *Rhizoctonia solani* (Zhang et al. 2009), and *Sclerotinia sclerotiorum* (Stammler et al. 2007). SDHIs achieve their activity by inhibiting the function of succinate dehydrogenase, an enzyme required for cellular respiration. Recently introduced products include: fluopyram, isofetamid, benzovindiflupyr, pydiflumetofen, and several others. The majority of these new compounds are broad spectrum in action and are labeled for use on multiple crops.

The strobilurins, or QoI class (FRAC 11), is the second largest group of fungicides available and is one of the newest classes (Morton & Staub 2008). The first products, azoxystrobin and kresoxim-methyl, were introduced in 1992 (Morton & Staub 2008). The MOA of QoIs is to involves binding to the quinone 'outer' (Qo) binding site of the cytochrome bc1 complex (Bartlett et al. 2002). This leads to the blocking of electron transfer and arrest of ATP production thereby stopping mitochondrial respiration. This group of fungicides works particularly well against germinating spores (Vincelli 2002). As with the DMIs and SDHIs, QoI fungicides have a broad efficacy range on fungal diseases, including diseases caused by water molds, downy mildews, powdery mildews, fruit rots, and even rusts (Morton & Staub 2008).

Polyoxin-D is a peptidyl pyrimidine nucleoside (FRAC 19) with chitin-synthase inhibition as a mode of action. This is an older compound, with the first introduction in Japan in 1965 (Endo et al. 1970). However, a new line of products was released in the USA in early 2012.Pyriofenone (FRAC 50) was made available 2018 to commercial growers in the USA in

2018. The mode of action of pyriofenone is inhibition of appressorium formation, particularly for powdery mildew (Erysiphales) fungi (FRAC 2018).

1.3.2 Fungicide resistance

The multi-site MOA compounds such as mancozeb (FRAC M3) or captan (FRAC M4) are generally robust to the formation of molecular resistance. Unfortunately, there was a report of an isolate of *C. gloeosporioides* that was insensitive to captan (Greer et al. 2011). Moreover, several vineyards in VA reported outbreaks of grape ripe rot where the grower's spray programs relied heavily on applications of captan (Nita, *personal communication*). The DMI fungicide class has been classified as a medium risk for fungicide resistance (FRAC 2018). Despite the lower risk of fungicide resistance when compared to the QoI fungicides, variable *Colletotrichum* sensitivity has been observed in recent years (Chen et al. 2016; Xu et al. 2014). In the work by Chen et al. (2016), sensitivity differences were observed between species to the six tested fungicides, for example, *C. nymphaeae* was insensitive to fenbuconazole and flutriafol while *C. fioriniae* and *C. fructicola* were sensitive. Additionally, differences in sensitivity were observed within *C. fioriniae* where one of the sub-groups was found to be less sensitive to all tested fungicides compared to the other sub-group (Chen et al. 2016).

Newer chemical classes such as the QoIs (FRAC 11), and the SDHIs (FRAC 7), are classified as single- site MOA, where a single mutation is required to confer fungicide resistance. This makes these compounds vulnerable to the rise of resistant strains. For both of these fungicide classes, plant pathogens such as *Botrytis cinerea* and *Alternaria alternata* (Ishii 2009; Sierotzki & Scalliet 2013) have already been reported as resistant. In the case of QoIs, a single-point mutation at the G143A location in the *cyt*-B gene is enough to form resistance (Ishii 2009). For *Colletotrichum* species, studies have been completed on isolates from peach in South

Carolina. Hu et al. 2015 found the presence of the G143A point-mutation in isolates of *C. siamense*.

The molecular basis of resistance for the SDHI chemical class is still a single mutation, but with multiple potential locations (Sierotzki & Scalliet 2013). There are four subunits that make up the succinate dehydrogenase enzyme, the binding site for the MOA of SDHIs. The most common mutation for resistance is located in the *sdh*-B subunit at the H272Y/R/L/V location in the protein sequence (Sierotzki & Scalliet 2013; Von Schmeling & Kulka 1966). There are multiple other mutations that have also been identified farther from the binding site and on additional subunits (Sierotzki & Scalliet 2013). Studies on the presence of resistance mutations are limited in *Colletotrichum*. Ishii et al. 2016 sequenced gene fragments of *sdh*-B, *sdh*-C, and *sdh*-D. The gene fragments contained multiple polymorphisms; however, no resistance mutations leading to resistance were found (Ishii et al. 2016).

1.4. *The Virginia Wine Industry*

1.4.1 Introduction to the Virginia wine industry

The VA wine industry has grown quickly from just six wineries on 286 acres in the late 1970s to over 270 wineries and more than 3,000 bearing acres in 2017 (Dunham 2017; Wood et al. 2018). With an annual fruit production of ~7,800 tons, VA is now tied for eighth in the nation in wine production (NASS 2016; Wood et al. 2018). Between tourism and wine sales, VA wine now contributes $1.4 billion to the local economy and employs approximately 8,000 individuals (Rimerman 2017). Additionally, in 2012, VA was listed as one of the top ten wine destinations in the world by Wine Enthusiast magazine (VDACS 2017). The industry is still relatively small,

with the majority (~64%) of vineyards containing 10 acres of bearing vines, but there is a continued potential for growth (Rephann 2017; Wood et al. 2018; VDACS 2017).

1.4.2 Impact of grape ripe rot

C. acutatum and *C. gloeosporioides* are endemic to the Mid-Atlantic US, and have been reported as bitter rot on apples in VA since the late 1800s (Schrenk & Spaulding 1903; Southworth 1891). Grape ripe rot is often confused with other late season rots such as bitter rot (*Greeneria uvicola*) (Sutton 2015b) and sour rot (caused by a complex of 70 species of fungi and bacteria) (McFadden-Smith & Gubler 2015), due to the timing of symptom development and/or similarity of symptom appearance. Until recently, the impact of grape ripe rot on wine grape yield has been regarded as minor. However, it has been observed in some VA vineyards that there may be up to 30% direct crop loss (Nita, *personal communication*). Indirect economic loss can occur during wine production due to the production of unpalatable, tobacco-like, off flavors from the infected grapes (Meunier & Steel 2009). Sensory analysis studies showed that this change in flavor in wines occurred with as little as 3% of the total crushed grapes being infected (Meunier & Steel 2009).

1.4.3 Current chemical controls for grape ripe rot

Basic information for control of *C. acutatum* and *C. gloeosporioides* is limited, especially in a vineyard setting. The majority of field trials for control of grape ripe rot were completed before 2010 (Travis et al. 2006a; Travis et al. 2006b; Travis et al. 2007a; Travis et al. 2007b; Travis et al. 2008). Since 2010, a limited number of field trials have been completed in the Mid-Atlantic region with one trial in North Carolina (Anas & Sutton 2011) and two in Pennsylvania (Halbrent et al. 2012; Halbrent et al. 2013). These studies were also mainly focused on controlling other cluster rot pathogens such as Botrytis gray mold (*B. cinerea*), therefore the

focus was on materials to control gray mold such as a pre-mix of pyraclostrobin and fluxapyroxad (Merivon, BASF, Research Triangle Park, NC), or fenhexamid (Elevate, Arysta LifeScience, LLC, Cary, NC).

The current recommendations for grape ripe rot control in VA are EBDC materials, such as mancozeb (FRAC M3), captan (FRAC M1), and the QoIs, such as azoxystrobin (FRAC 11) fungicide classes (Pfeiffer et al. 2018). Each of these compound classes have limitations such as the long pre-harvest interval of mancozeb (66 days), reports of captan insensitivity in *C. gloeosporioides*, and reports of *Colletotrichum* QoI fungicide resistance in the Mid-Atlantic (FRAC 2018; Greer et al. 2011; Hu et al. 2015).

1.5. *Project objectives*

This dissertation encompasses several projects and objectives that are discussed in the following four chapters. The objectives of these projects are:

Chapter 2: Five Colletotrichum species were identified from grape ripe rot symptomatic berries in Virginia vineyards

- Objective 1: survey VA vineyards for the presence of symptomatic fruit,
- Objective 2: morphologically and phylogenetically characterize the *C. acutatum* and *C. gloeosporioides* complex species from across the state
- Objective 3: investigate the intra-state spatial distribution of species.

Chapter 3: Screening commercial fungicides for control of seven *Colletotrichum* species, the causal agents of grape ripe rot, from VA vineyards

- Objective 1: screen fifteen commercial fungicides and two active ingredient combinations of eight commercial fungicides via two *in vitro* fungicide-amended

media assay for control of *Colletotrichum* species isolated from grapes grown in Virginia

- Objective 2: sequence the gene fragments of three of the four SDH enzyme subunits (*sdh*-B, *sdh*-C, and *sdh*-D) to identify a potential molecular basis for SDHI fungicide resistance.

Chapter 4: Potential survival phases of Colletotrichum species in three wine grape tissues

- Objective 1: initial infection stages of *Colletotrichum* species on grape leaf, flowers, and young berries
- Objective 2: the effect of fungicides on flower infection
- Objective 3: capability of *Colletotrichum* species to infect woody grape tissues as a potential means of winter survival

Chapter 5: Evaluation of commercial fungicides at different wine grape phenological stages for control of grape ripe rot caused by the *Colletotrichum acutatum* and *C. gloeosporioides* species complexes

- Objective 1: evaluate the efficacy of ten commercial fungicides and examine the most advantageous timing of applications

These studies seek to elucidate issues for managing grape ripe rot in VA by investigating the *Colletotrichum* species present in VA (Chapter 2), examine fungicide chemical controls (Chapter 3 & 5) and observe the importance of grape vine phenological stage on control of *Colletotrichum* species (Chapter 4 & 5).The information from our studies will impact not only VA vineyards where ripe rot of grape has become a recurring issue, but also many other growing regions, including Australia and New Zealand where grape ripe rot has become an economically important disease (Meunier & Steel 2009; Steel et al. 2007; Steel et al. 2012).

1.6. *References*

Agrios, G. ed. (2005)a. Glossary. in *Plant Pathology.* Sonnack, K., ed. Burlington, MA: Elsevier Academic Publishing.

Agrios, G. ed. (2005)b. Control of plant diseases - direct protection of plants from pathogens. in *Plant Pathology.* Sonnack, K., ed. Burlington, MA: Elsevier Academic Publishing.

Amiri, A., Brannen, P., & Schnabel, G. (2010). Reduced sensitivity in *Monilinia fructicola* field isolates from South Carolina and Georgia to respiration inhibitor fungicides. *Plant Disease*, *94*, 737–743.

Anas, O., & Sutton, T. (2011). Effect of spray volume on control of bunch rot in Sauvignon blanc, 2010. *Plant Disease Management Reports, 5,* SMF025.

Avenot, H., Morgan, D., & Michailides, T. (2008). Resistance to pyraclostrobin, boscalid and multiple resistance to Pristine® (pyraclostrobin+ boscalid) fungicide in *Alternaria alternata* causing Alternaria late blight of pistachios in California. *Plant Pathology*, *57*, 135–140.

Bailey, J., & Jeger, M. (1992). Preface. in *Colletotrichum: Biology, Pathology and Control*, Bailey, J., & Jeger, M. eds. Melksham, UK: CAB International.

Bartlett, D., Clough, J., Godwin, J., Hall, A., Hamer, M., & Parr-Dobrzanski, B. (2002). The strobilurin fungicides. *Pest Management Science*: formerly *Pesticide Science*, *58,* 649–662.

Biggs, A. (1995). Detection of latent infections in apple fruit with paraquat. *Plant Disease*, *7*9, 1062–1067.

Binyamini, N. & Schiffmann-Nadel, M. (1972). Latent infection in avocado fruit due to *Colletotrichum gloeosporioides*. *Phytopathology*, *62*, 592–594.

Blair, J., Coffey, M., Park, S., Geiser, D., & Kang, S. (2008). A multi-locus phylogeny for Phytophthora utilizing markers derived from complete genome sequences. *Fungal Genetics and Biology*, *45*, 266–277.

Børve, J., & Stensvand, A. (2017). *Colletotrichum acutatum* occurs asymptomatically on apple leaves. *European Journal of Plant Pathology*, *147*, 943–948.

Cannon, P., & Bridge, P. (2008). Linking the past, present and future of *Colletotrichum* systematics. in *Colletotrichum: Host Specificity, Pathology and Host-pathogen Interaction*, Prusky, D., Freeman, S., & Dickman, M. ed. St. Paul, MN: American Phytopathology Society.

Chen, S., Luo, C., Hu, M., & Schnabel, G. (2016). Sensitivity of *Colletotrichum* species, including *C. fioriniae* and *C. nymphaeae*, from peach to demethylation inhibitor fungicides. *Plant Disease*, *100*, 2434–2441.

Damm, U., Cannon, P., Woudenberg, J., & Crous, P. (2012). The *Colletotrichum acutatum* species complex. *Studies in Mycology*, *73*, 37–113.

Daykin, M., & Milholland, R. (1984). Histopathology of ripe rot caused by *Colletotrichum gloeosporioides* on muscadine grape. *Phytopathology*, *74*, 1339–1341.

Dean, R., Van Kan, J., Pretorius, Z., Hammond-Kosack, K., Di Pietro, A., Spanu, P., Rudd, J., Dickman, M., Kahmann, R., Ellis, J. & Foster, G. (2012). The Top 10 fungal pathogens in molecular plant pathology. *Molecular Plant Pathology*, *13*, 414–430.

Dodd, J., Estrada, A., & Jeger, M. (1992). Epidemiology of *Colletotrichum gloeosporioides* in the tropics. in *Colletotrichum: Biology, Pathology and Control.* Bailey, J., & Jeger, M. eds. Melksham, UK: CAB International

Dodd, J., Estrada, A., Matcham, J., Jeffries, P., & Jeger, M. (1991). The effect of climatic factors on *Colletotrichum gloeosporioides*, causal agent of mango anthracnose, in the Philippines. *Plant Pathology*, *40*, 568–575.

Dunham, N., & Associates. (2017). 2017 economic report on wine. *Study for the National Association of American Wineries.*

Endo, A., Kakiki, K., & Tomomasa, M. (1970). Mechanism of action of the antifungal agent polyoxin D. *Journal of Bacteriology*, *104*, 189–196.

FRAC, 2016. *About FRAC*. In: International CL, ed. http://www.frac.info/. (2018.)

FRAC. (2018). FRAC Code List 2018: Fungicides sorted by mode of action. In.: FRAC.

Gil-Lamaignere, C., Roilides, E., Hacker, J., & Müller, F. (2003). Molecular typing for fungi—a critical review of the possibilities and limitations of currently and future methods. *Clinical Microbiology and Infection*, *9*, 172–185.

Greer, L., Harper, J., & Steel, C. (2014). Infection of *Vitis vinifera* (cv. Chardonnay) inflorescences by *Colletotrichum acutatum* and *Greeneria uvicola*. *Journal of Phytopathology*, *162*, 407–410.

Greer, L., Harper, J., Savocchia, S., Samuelian, S., & Steel, C. (2011). Ripe rot of south-eastern Australian wine grapes is caused by two species of *Colletotrichum*: *C. acutatum* and *C. gloeosporioides* with differences in infection and fungicide sensitivity. *Australian Journal of Grape and Wine Research*, *17*, 123–128.

Gunnell, P., & Gubler, W. (1992). Taxonomy and morphology of *Colletotrichum* species pathogenic to strawberry. *Mycologia*, *84*, 157–165.

Halbrent, N., Ngugi, J., Halbrent, J. & Jarjour, B. (2012). Evaluation of fungicides for management of bunch rots on Pinot Noir and Cabernet Franc in PA, 2011. *Plant Disease Management Report, 6*, SMF027.

Halbrent, N., Halbrent, J., & Jarjour, B. (2013). Evaluation of experimental and existing fungicides for management of bunch rots on Cabernet Franc in PA, 2012. *Plant Disease Management Report, 7*, SMF028.

Harp, T., Kuhn, P., Roberts, P., & Pernezny, K. (2014). Management and cross-infectivity potential of *Colletotrichum acutatum* causing anthracnose on bell pepper in Florida. *Phytoparasitica, 42*, 31–39.

Hartung, J., Burton, C., & Ramsdell, D. (1981). Epidemiological studies of blueberry anthracnose disease caused by *Colletotrichum gloeosporioides*. *Phytopathology, 71*, 449–459.

Hobbelen, P., Paveley, N., & van den Bosch, F. (2014). The emergence of resistance to fungicides. *PLoS One, 9*, e91910.

Hollomon, D. (2010). New fungicide modes of action strengthen disease control strategies. *Outlooks on Pest Management, 21*, 108–112.

Hu, M., Grabke, A., Dowling, M., Holstein, H., & Schnabel, G. (2015). Resistance in *Colletotrichum siamense* from peach and blueberry to thiophanate-methyl and azoxystrobin. *Plant Disease, 99*, 806–814.

Hyde, K., Cai, L., McKenzie, E., Yang, Y., Zhang, J., & Prihastuti, H., (2009). *Colletotrichum*: a catalogue of confusion. *Fungal Diversity, 39*, 1–17.

Ishii, H. (2009). QoI fungicide resistance: current status and the problems associated with DNA-based monitoring. in *Recent Developments in Management of Plant Diseases*: Gisi, U.,

Chet, I., & Gullino, M. ed. Springer Netherlands, 37–45.Ishii, H., Zhen, F., Hu, M., Li, X., & Schnabel, G. (2016). Efficacy of SDHI fungicides, including benzovindiflupyr, against *Colletotrichum* species. *Pest Management Science*, *72*, 1844–1853.

Leandro, L., Gleason, M., Nutter, F., Wegulo, S., & Dixon, P. (2003). Ecology and population biology strawberry plant extracts stimulate secondary conidiation by *Colletotrichum acutatum* on symptomless leaves. *Phytopathology*, *93*, 1285–1291.

Maas, J. (1998). Anthracnose fruit rot (black spot). in *Compendium of Strawberry Diseases*. 2nd ed. Maas, J. ed. St. Paul, MN: American Phytopathological Society.

Maharaj, A., & Rampersad, S. (2012). Genetic differentiation of *Colletotrichum gloeosporioides*; and *C. truncatum* associated with anthracnose disease of papaya (*Carica papaya* L.) and bell pepper (*Capsicum annuum* L.) based on ITS PCR-RFLP fingerprinting. *Molecular Biotechnology*, *50*, 237–249.

McCallan, S. (1949). The nature of the fungicidal action of copper and sulfur. *The Botanical Review*, *15*, 629–643.

McFadden-Smith, W., & Gubler, W. (2015). Sour rot. in *Compendium of Grape Diseases, Disorders, and Pests*. Wilcox, W., Gubler, W., & Uyemoto, J. eds. St. Paul, MN: American Phytopathological Society.

Mertely, J., & Legard, D. (2004). Detection, isolation, and pathogenicity of *Colletotrichum* spp. from strawberry petioles. *Plant Disease*, *88*, 407–412.

Mertely, J., Seijo, T., & Peres, N. (2015). Evaluation of products for anthracnose and Botrytis fruit rot control in annual strawberry, 2013-14. *Plant Disease Management Reports*, *9*, SMF007.

Meunier, M., & Steel, C. (2009). Effect of *Colletotrichum acutatum* ripe rot on the composition and sensory attributes of Cabernet Sauvignon grapes and wine. *Australian Journal of Grape and Wine Research*, *15*, 223–227.

Milholland, R. (1995). Anthracnose fruit rot (ripe rot). in *Compendium of blueberry and cranberry diseases*. Caruso, F., & Ramsdell, D. eds. St. Paul, MN: American Phytopathological Society.

Montgomery, M., & Paulsrud, B. (2006). *Beyond Strobys and Triazoles: How Do Fungicides Work?*: University of Illinois Extension.

Moral, J., Jurado-Bello, J., Sánchez, M., & De Oliveira, R. (2012). Effect of temperature, wetness duration, and planting density on olive anthracnose caused by *Colletotrichum* spp. *Phytopathology, 102*, 974–981.

Morton, V., & Staub, R. (2008). A short history of fungicides. In. *APSnet Features.* Online: American Phytopathological Society.

NASS, 2016. *Census of Agriculture*. Virginia Census Statistics.

O'Donnell, K., Sutton, D., Fothergill, A., McCarthy, D., Rinaldi, M., Brandt, M., Zhang, N., & Geiser, D. (2008). Molecular phylogenetic diversity, multilocus haplotype nomenclature, and in vitro antifungal resistance within the *Fusarium solani* species complex. *Journal of Clinical Microbiology*, *46*, 2477–2490.

Oliver, C. (2016). Effects of cultivar and cluster developmental stage of wine grapes to infection by ripe rot of grape, caused by *Colletotrichum gloeosporioides* and *C. acutatum* species complexes. Ch. 2. (Master's Thesis, Virginia Tech).

Peres, N., Timmer, L., Adaskaveg, J., & Correll, J. (2005). Lifestyles of *Colletotrichum acutatum*. *Plant Disease*, *89*, 784–796.

Pfeiffer, D., Baudoin, A., Bergh, J., & Nita, M. (2018). Grapes: diseases and insects in vineyards. in *Pest Management Guide: Horticultural and Forest Crops*. Hong, C., & Day, E. eds. Virginia Cooperative Extension. Pub. 456-017.

Prusky, D., Freeman, S., & Dickman, M. (2000). Preface. in *Colletotrichum: host specificity, pathology, and host-pathogen interaction*. Prusky, D., Freeman, S., & Dickman, M. ed. St. Paul, MN: American Phytopathology Society.

Prusky, D., & Plumby, R. (1992). Quiescent infection of *Colletotrichum* in tropical and subtropical fruits. in *Colletotrichum: Biology, Pathology and Control.* Bailey, J., & Jeger, M. eds. Melksham, UK: CAB International.

Rephann, T. (2017). The economic impact of Virginia's agriculture and forest industries: 2017. *Weldon Cooper Center for Public Service*. University of Virginia, Charlottesville, VA.

Rimerman, F. & Co., LLP. (2017). The economic impact of wine and wine grapes on the state of Virginia: 2015. *Study for the Virginia Wine Board*.

Samuelian, S., Greer, L., Savocchia, S., & Steel, C. (2012). Overwintering and presence of *Colletotrichum acutatum* (ripe rot) on mummified bunches, dormant wood, developing tissues and mature berries of *Vitis vinifera*. *Vitis, 51*, 33–37.

Sarkar, S., & Guttman, D. (2004). Evolution of the core genome of *Pseudomonas syringae*, a highly clonal, endemic plant pathogen. *Applied and Environmental Microbiology, 70*, 1999–2012.

Scally, M., Schuenzel, E.L., Stouthamer, R., & Nunney, L. (2005). Multilocus sequence type system for the plant pathogen *Xylella fastidiosa* and relative contributions of recombination and point mutation to clonal diversity. *Applied and Environmental Microbiology, 71*, 8491–8499.

Schrenk, H., & Spaulding, P. (1903). *The bitter rot of apples*. United States Department of Agriculture

Shane, W., & Sutton, T. (1981). Germination, appressorium formation, and infection of immature and mature apple fruit by *Glomerella cingulata*. *Phytopathology*, *71*, 454–457.

Shiraishi, M., Koide, M., Itamura, H., Yamada, M., Mitani, N., Ueno, T., Nakaune, R., & Nakano, M. (2007). Screening for resistance to ripe rot caused by *Colletotrichum acutatum* in grape germplasm. *Vitis*, *46*, 196–200.

Sierotzki, H., & Scalliet, G. (2013). A review of current knowledge of resistance aspects for the next-generation succinate dehydrogenase inhibitor fungicides. *Phytopathology*, *103*, 880–887.

Simmonds, J. (1965). A study of *Colletotrichum* causing ripe fruit rots in Queensland. *Queensland Journal of Agricultural and Animal Science*, *22*, 437–459.

Southworth, E. (1891). Ripe rot of grapes and apples. *The Journal of Mycology*, *6*, 164–173.

Sreenivasaprasad, S. & Talhinhas, P. (2005). Genotypic and phenotypic diversity in *Colletotrichum acutatum*, a cosmopolitan pathogen causing anthracnose on a wide range of hosts. *Molecular Plant Pathology*, *6*, 361–374.

Stammler, G., Benzinger, G., & Speakman, J. (2007). A rapid and reliable method for monitoring the sensitivity of *Sclerotinia sclerotiorum* to boscalid. *Journal of Phytopathology*, *155*, 746–748.

Steel, C., Greer, L., & Savocchia, S. (2007). Studies on *Colletotrichum acutatum* and *Greeneria uvicola*: Two fungi associated with bunch rot of grapes in sub-tropical Australia. *Australian Journal of Grape and Wine Research*, *13*, 23–29.

Steel, C., Greer, L., & Savocchia, S. (2012). Grapevine inflorescences are susceptible to the bunch rot pathogens, *Greeneria uvicola* (bitter rot) and *Colletotrichum acutatum* (ripe rot). *European Journal of Plant Pathology, 133*, 773–778.

Sutton, B. (1992). The Genus *Glomerella* and its anamorph *Colletotrichum.* in *Colletotrichum: Biology, Pathology and Control*. Bailey, J., & Jeger, M. eds. Melksham, UK: CAB International.

Sutton, T. (2014). Bitter rot. in *Compendium of Apple and Pear Diseases*. Sutton, T., Aldwinckle H., Agnello A., & Walgenbach J. eds. St. Paul, MN: American Phytopathological Society.

Sutton, T. (2015)a. Ripe rot. in *Compendium of Grape Diseases, Disorders, and Pests*. Wilcox, W., Gubler, W., & Uyemoto, J. eds. St. Paul, MN: American Phytopathological Society.

Sutton, T. (2015)b. Bitter rot. in *Compendium of Grape Diseases, Disorders, and Pests*. Wilcox, W., Gubler, W., & Uyemoto, J. eds. St. Paul, MN: American Phytopathological Society.

Travis, J., Halbrent, N., Lehman, B., Hed, B., & Jarjour, B. (2006)a. Efficacy of cultivars and alternative fungicide programs for control of harvest bunch rots on American hybrid grapes, 2005. *Plant Disease Management Reports, B&C Tests 21*, N007.

Travis, J., Halbrent, N., Lehman, B., Hed, B., & Jarjour, B. (2006)b. Evaluation of alternative materials for control of grape harvest bunch rots in Pennsylvania, 2005. *Plant Disease Management Reports, B&C Tests 21*, N005.

Travis, J., Halbrent, N., Lehman, B., & Jarjour, B. (2007)a. Evaluation of conventional and alternative materials for control of grape cluster diseases, 2006. *Plant Disease Management Reports, 1*, SMF035.

Travis, J., Halbrent, N., Lehman, B., & Jarjour, B. (2007)b. Evaluation of fungicide application timing and cultivar susceptibility for control of ripe rot of grapes, 2006 *Plant Disease Management Reports, 1*, SMF036.

Travis, J., Halbrent, N., Lehman, B., & Jarjour, B. (2008). Evaluation of materials for control of grape cluster rots, 2007. *Plant Disease Management Reports, 2*, STF023.

VDACS (2017). Virginia agriculture--facts and figures. in http://www.vdacs.virginia.gov/agfacts/index.shtml.

Verma, N., Macdonald, L., & Punja, Z. (2007). Environmental and host requirements for field infection of blueberry fruits by *Colletotrichum acutatum* in British Columbia. *Plant Pathology, 56*, 107–113.

Vincelli, P. (2012). QoI (strobilurin) fungicides: benefits and risks. In. *The Plant Health Instructor*.http://www.apsnet.org/edcenter/advanced/topics/Pages/StrobilurinFungicides.aspx: APSnet.

Von Schmeling, B., & Kulka, M. (1966). Systemic fungicidal activity of 1, 4-oxathiin derivatives. *Science, 152*, 659–660.

Weir, B., Johnston, P., & Damm, U. (2012). The *Colletotrichum gloeosporioides* species complex. *Studies in Mycology, 73*, 115–180.

Wharton, P., & Dieguez-Uribeondo, J. (2004). The biology of *Colletotrichum acutatum*. *Anales Del Jardín Botánico de Madrid, 61*, 3–22.

Wood, V., Custer, S., Watson, K., & Chibbaro, B. (2018). Virginia 2017 commercial grape report. *Study for the Virginia Wine Board*.

Xu, X., Lin, T., Yuan, S., Dai, D., Shi, H., Zhang, C., & Wang, H. (2014). Characterization of baseline sensitivity and resistance risk of *Colletotrichum gloeosporioides* complex

isolates from strawberry and grape to two demethylation-inhibitor fungicides, prochloraz and tebuconazole. *Australasian Plant Pathology*, *43*, 605–613.

Zhang, C., Liu, Y., Ma, X., Feng, Z., & Ma, Z. (2009). Characterization of sensitivity of *Rhizoctonia solani*, causing rice sheath blight, to mepronil and boscalid. *Crop Protection*, *28*, 381–386.

Figure 1.1: Visual symptoms of grape ripe rot in the field. Symptoms and pustule formation on cv. Merlot [A] and cv. Traminette [B]. Distribution of disease signs on cv. Traminette clusters across a cordon [C].

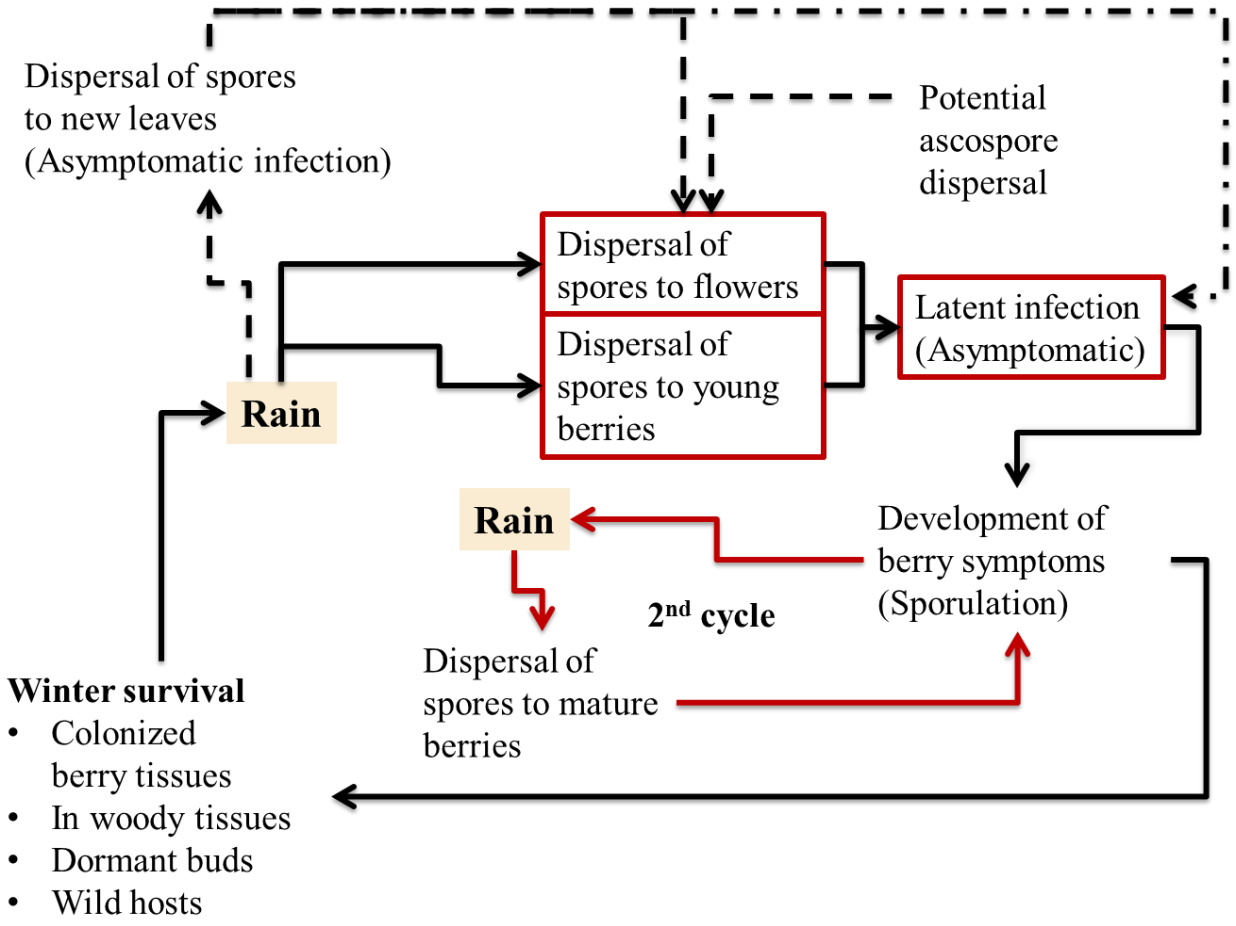

Figure 1.2: Disease cycle of grape ripe rot. The resting mycelia and conidia overwinter in several ways: In colonized grape tissues, in woody tissues, in dormant grapevine buds or on wild hosts. During warm, spring rains, the conidia and mycelia are washed onto new tissues, such as the blooms, young clusters, or leaves. The conidia germinate and form latent infections on the tissues. When the berries begin to change color (veraison), salmon-colored acervuli form on the surface of the berry. As the season progresses, the berry shrivels as the acervuli form in concentric rings around the berry. Secondary infection occurs when rains wash the conidia out of these acervuli and down the ripening cluster. Rain also washes mycelia and conidia into the woody tissues and dormant buds to colonize and overwinter.

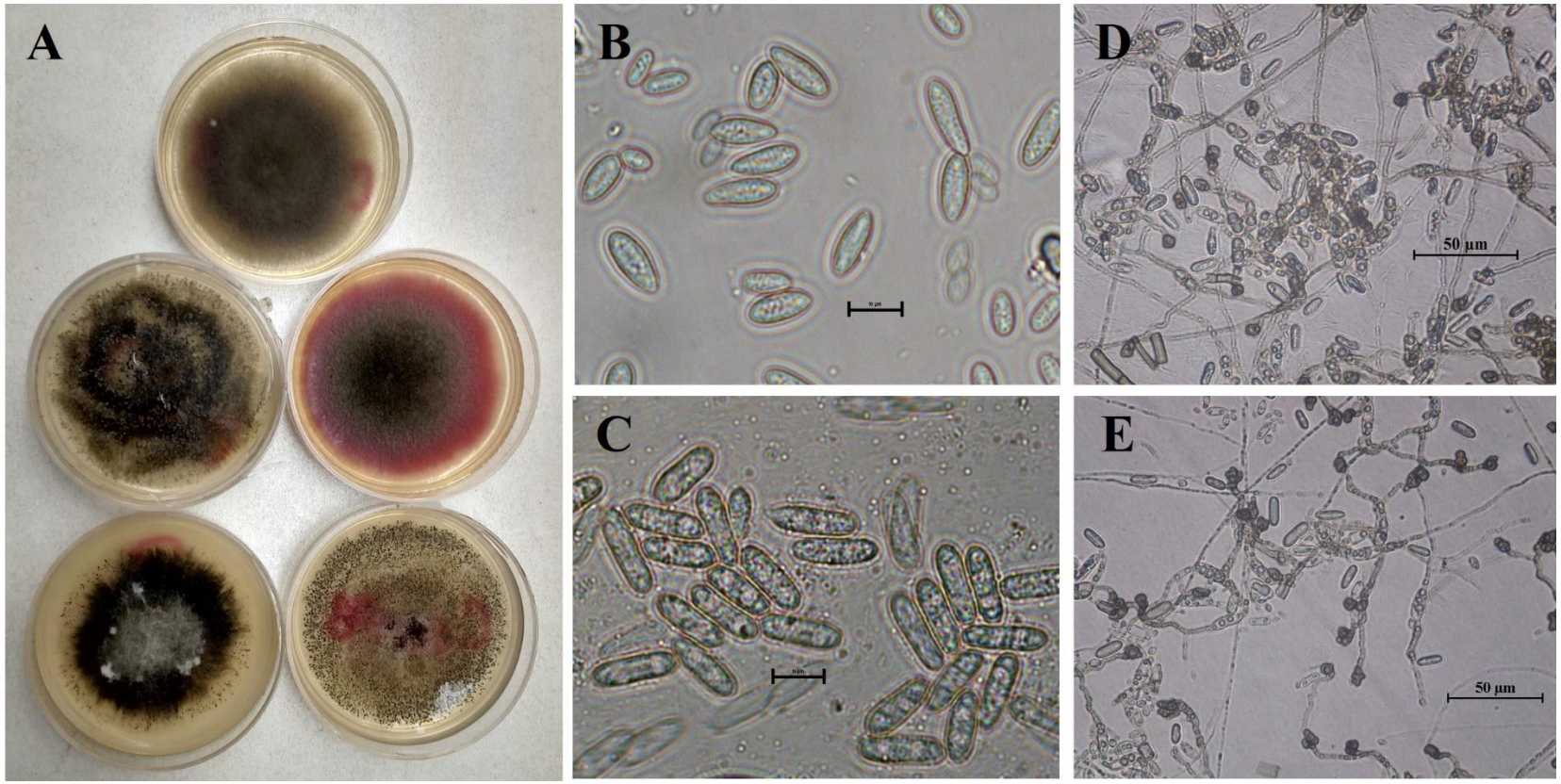

Figure 1.3: Morphology of isolates collected from VA vineyards in 2013-2014. Colors and textures of 14-day old cultures on amended-¼ PDA plates [A]. Size and shape of 14-day old culture conidia produced by species within the *C. acutatum* species complex [B] and species within the *C. gloeosporioides* species complex [C]. Appressorial shapes from a suspension of 14-day old cultures of two isolates within the *C. gloeosporioides* complexes [D, E]. The size bar represents 10 µm [B, C] or 50 µm [D, E].

Chapter 2.

Five *Colletotrichum* species were identified from grape ripe rot symptomatic berries in Virginia vineyards

Abstract

Colletotrichum acutatum and *C. gloeosporioides* are fungi that are prevalent on a global scale with a wide host range and a convoluted taxonomic history. Advances in molecular techniques, such as multilocus sequence typing (MLST), are important tools for elucidating species with overlapping morphology. With traditional morphological characteristics and molecular techniques, *C. acutatum* and *C. gloeosporioides* were reclassified into species complexes that consist of 31, and 22 new accepted species, respectively. The objectives of this study were to 1) survey VA vineyards for the presence of symptomatic fruit, 2) morphologically and phylogenetically characterize the *C. acutatum* and *C. gloeosporioides* complex species from across the state, and 3) investigate the intra-state spatial distribution of species. In this study, I surveyed thirty-two vineyards, encompassing eight out of the nine Virginia wine regions, and identified six *Colletotrichum* species: *C. aenigma, C. conoides, C. fioriniae, C. gloeosporioides, C. kahawae,* and *C. nymphaeae.* I also found two additional groups; an isolate similar to *C. limetticola* and *C. melonis* and a group of isolates that are similar to *C. alienum, C. fructicola,* and *C. nupharicola*. On average, 2.5 *Colletotrichum* species were present in the sampled Virginia vineyards with variability by region as to which of the species were present. *C. fioriniae* was the only species that was omnipresent throughout the state.

2.1. Introduction

Colletotrichum acutatum and *C. gloeosporioides* are two filamentous fungi with a global host range encompassing tropical and temperate hosts such as apple (Southworth 1891), avocado (Everett 2003), grape (Sutton 2015a), mango (Fitzell et al. 1984), and strawberry (Maas 1998). These fungi have a history of convoluted taxonomy with multiple attempts of rearrangement via morphological techniques (Cannon & Bridge 2008; Prusky et al. 2000; Sutton 1992). With the current advances in molecular techniques, additional attempts were made to clarify the phylogenetic relationships between these species (Hyde et al. 2009; Maharaj & Rampersad 2012; Sreenivasaprasad & Talhinhas 2005). Unfortunately, this has led to an abundance of incorrectly and limitedly identified gene fragments in repositories such as NCBI GenBank (Benson et al. 1993; Hyde et al. 2009). In 2012, the taxonomies of both *C. acutatum* and *C. gloeosporioides* were extensively restructured using a multilocus sequence typing (MLST) approach in addition to traditional morphology (Damm et al. 2012; Weir et al. 2012). The two species were divided into species complexes of 31 (*C. acutatum*) and 22 (*C. gloeosporioides*) new accepted species, respectively, with additional subspecies (Damm et al. 2012; Weir et al. 2012).

Grape ripe rot is a cluster rot disease caused by *C. acutatum* and *C. gloeosporioides* (Greer et al. 2011; Samuelian et al. 2012; Simmonds 1965). These *Colletotrichum* species are endemic to Virginia (VA), and have been observed as apple bitter rot since the late 1800s (Southworth 1891). The impact of *Colletotrichum* species on the wine grape industry was considered minor since grape ripe rot is often confused with other late season diseases, such as bitter rot (*Greeneria uvicola*) and sour rot, due to similar appearance time and symptomology (McFadden-Smith & Gubler 2015; Sutton 2015b). However, in communicating with local VA vineyard managers, grape ripe rot was found to cause up to 30% direct crop loss with additional

economic losses due to undesirable, tobacco-like flavors that occur during wine production (Meunier & Steel 2009; Nita, *personal communication*).

Grape ripe rot symptoms appear after the fruit begins to color (veraison) (Sutton 2015a). Lesions form on the berry skin surface and appear either as round to irregular-shaped tan lesions for white-fruited cultivars or mild discoloration on red-fruited cultivars. As the disease progresses, salmon-colored, conidial masses form in concentric rings of acervuli, and infected berries shrivel to raisin-like texture. Conidial mass formation is generally the first easily observed sign on red-fruited cultivars. Differentiation of the causal fungus on symptomatic fruit is difficult since both species complexes cause the same lesions and conidial masses (Daykin & Milholland 1984). Additionally, cultures of *Colletotrichum* species have overlapping morphological characteristics that are influenced by environmental factors, such as growth medium, light exposure and temperature (Damm et al. 2012; Peres et al. 2005; Wharton & Dieguez-Uribeondo 2004). Molecular confirmation is required to properly identify *Colletotrichum* species.

Differences were observed between the optimum growing conditions required by the *Colletotrichum* species within the complexes (Diéguez-Uribeondo et al. 2011; Steel et al. 2011; Wilson et al. 1990). Different wine growing regions are subject to distinct climatic conditions in VA. These conditions could influence which species are present in a region or even a specific vineyard. Additionally, vineyards, especially in the northern section of the state, border orchards, other hosts, and woodlands. Despite the young age of the VA wine industry, fungicide usage on *Colletotrichum* species on alternative hosts, such as apple and strawberry, could influence the efficacy of fungicide applications within vineyards. Additionally, recent studies have observed differences in fungicide sensitivity between the *Colletotrichum* species complexes and between

the species within the *Colletotrichum* species complexes (Hu et al. 2015a; Ishii et al. 2016; Munir et al. 2016). These differences can have a strong impact on the chemical requirements for control of grape ripe rot depending on the location of a vineyard within the state.

The objectives of this study were to: 1) survey VA vineyards for the presence of symptomatic fruit, 2) morphologically and phylogenetically characterize the *C. acutatum* and *C. gloeosporioides* complex species from across the state, and 3) investigate the intra-state spatial distribution of species.

2.2. Materials and methods

2.2.1 Sample collection and fungal isolation

Thirty-two commercial vineyards were surveyed between 2013 and 2014 for the presence of symptomatic fruit in the two weeks before harvest. The collections encompassed 20 wine grape cultivars from 8 of the 9 VA wine regions; Blue Ridge Region (1 vineyard), Central VA Region (11), Chesapeake Bay Region (2), Eastern Shore Region (2), Heart of Appalachia Region (1), Northern VA Region (8), Shenandoah Valley Region (3), and Southern VA (4) (Fig. 2.2). No samples were taken from the Hampton Roads Region. Fungal colonies were isolated from berries by submerging whole, symptomatic berries in 10% bleach for 1 min, followed by three rinses of sterile water. Approximately 4x4 mm square of skin tissue was cut from the advancing lesion edge and placed in acidified potato dextrose agar (APDA) (Acumedia®, Neogen Company, Lansing, MI). Plates were incubated at 25 °C (Precision™ 818, Thermo Scientific Inc., Waltham, MA) with a diurnal light cycle (12 h light /12 h dark) for 7-14 days until sporulation in the form of aerial conidia was observed. To obtain pure cultures, a sterile wire loop was used to transfer a clump of conidia to a water agar (WA) (BD Difco™, Becton

Dickinson Co., Franklin Lakes, NJ) plate in a T pattern. Plates were incubated overnight at 25 °C with a diurnal light cycle (12 h light /12 h dark). Individual germinated conidia were transferred to quarter-strength potato dextrose agar (amended-¼ PDA) amended with streptomycin and chloramphenicol, 100 mg/mL each. Before storage, gala apples from the Alson H Smith Jr. Agricultural Research and Extension Center orchard were stab-inoculated with mycelia from individual conidium colonies. Colonies were recovered from actively sporulating lesions on the apple surface. Each isolate was stored as dry agar plugs on 0.1 ppm azoxystrobin (Abound®, Syngenta Crop Protection, LLC, Greensboro, NC) amended-¼ PDA at -20 °C and as 20% (w/v) glycerol suspension of hypha and conidia in Nunc® CryoTubes® (Thermo Scientific, Waltham, MA) at -80 °C (Sinclair & Dhingra 1995).

2.2.2 DNA extraction, and Colletotrichum *species complex confirmation*

Plates of 14-day old amended-¼ PDA were flooded with sterile distilled water to suspend fungal structures. The fungal suspension was transferred to a sterile 1.5 mL microcentrifuge tube and the water was removed by centrifugation and pipetting. A total of 100 mg of dried fungal mass was transferred to a FastPrep® 2 mL grinder tube (MP Biomedicals, LLC, Santa Ana, CA) containing one 5-mm and 4-6 2.5-mm glass beads. After overnight storage at -20 °C, samples were ground for 60 s at 4.5 m/s in a FastPrep®-24 (MP Biomedicals, LLC, Santa Ana, CA). Total genomic DNA was extracted using the DNeasy Plant Mini Kit (QIAGEN Sciences, Germantown, MD) according to the manufacturer's protocol.

To confirm the *Colletotrichum* species complex identification from morphological assessment, the beta-tubulin (*TUB2*) gene was amplified and sequenced for all tested isolates (Table 2.1). Polymerase chain reaction (PCR) reactions were prepared at a volume of 25 µL containing: 1X GoTaq® Green (Promega Corp., Madison, WI), 0.25 µM per primer, 2.61 µM

bovine serum albumin (BSA) (New England BioLabs Inc., Ipswich, MA) and 2 µL of DNA extraction in a StepOnePlus™ (Applied Biosystems™, Foster City, CA). The PCR conditions had a denaturation step of 3 min at 94 °C, followed by 35 cycles of 40 s at 94 °C, 40 s at 55 °C, and 1 min at 72 °C with a final extension of 10 min at 72 °C. When reactions resulted in low amplification, the BSA concentration was increased to 4.81 µM and annealing temperature was increased to 60 °C. Products were cleaned before submission to Eurofins Genomics (Eurofins MWG Operon, Louisville, KY) using Exonuclease I and rSAP (New England BioLabs Inc., Ipswich, MA) by the protocol provided by the manufacturer. Sequences were aligned using the Geneious (Kearse et al. 2012) and ClustalW (Larkin et al. 2007) alignment programs in Geneious® 11.1 (Biomatters Inc., Newark, NJ).

2.2.3 Species within the Colletotrichum *complex identification*

After examining the *TUB2* gene, a subset of representative *Colletotrichum* isolates from across the state were chosen (Table 2.2 & 2.3). Additional genes were then used for species delineation within each species complex (Damm et al. 2012; Weir et al. 2012). For the isolates within the *C. acutatum* complex, the internal transcribed spacer unit (*ITS*), and histone-3 (*HIS3*) were amplified, and for the isolates within the *C. gloeosporioides* complex, the calmodulin (*CAL*), and glyceraldehyde-3-phosphate dehydrogenase (*GAPDH*) fragments were amplified (Table 2.1). PCR reactions were prepared as described above in an ABI StepOnePlus™. The conditions for the PCR reactions were the same except for the annealing temperature: 59 °C for *CAL*, 64 °C for *GAPDH*, 58 °C for *HIS3*, and 52 °C for *ITS*. PCR products were cleaned before submission as described above, and sent to the same facility described above.

2.2.4 Phylogenetic analyses

Gene sequences were trimmed and calls were validated with Geneious® 11.1 and aligned via the Geneious (Kearse et al. 2012) and ClustalW (Larkin et al. 2007) alignments within Geneious® 11.1. The validated gene sequences were concatenated by *Colletotrichum* species complex in the order of *ITS*, *HIS3*, and *TUB2* for the *C. acutatum* complex (Fig. 2.2) and *CAL*, *GAPDH*, and *TUB2* for the *C. gloeosporioides* complex (Fig. 2.3). The concatenated sequences were used for phylogenetic tree construction using reference sequences from GenBank (Clark et al. 2015) and Q-bank (Bonants et al. 2013) (Table 2.4). Trees were constructed via three methods: neighbor-joining using Geneious Tree Builder (Kearse et al. 2012) with the HKY 85 substitution model, Bayesian inference using MrBayes 3.2.6 (Ronquist & Huelsenbeck 2003), plug-in in Geneious® 11.1.3, with the HKY 85 substitution model, and maximum likelihood using the online PhyML 3.0 interface (Guindon et al. 2010).

2.2.5 Morphological analyses

An initial *Colletotrichum* species complex identification of the fungal isolate was obtained from the morphological characteristics. After obtaining single-conidium cultures, isolates were plated on amended-¼ PDA and incubated at 25 °C with a diurnal light cycle (12 h light /12 h dark) for 14 days. Visual assessments of colony characteristics (colony surface, colony top color, and bottom color) were recorded. After recording the colony characteristics, the colony surface was flooded with 2 mL of sterile 20% glycerol (w/v), and the surface was gently rubbed to suspend conidia. The conidial suspensions were filtered through two layers of autoclaved Miracloth (EMD Millipore, Germany) to remove mycelia. Microscopic preparations of conidia were made and the length (µm), and width (µm) of 20 conidia were measured with a Nikon Eclipse Ci microscope (Nikon Instrument Inc., Tokyo, Japan).

To observe appressorial characteristics, 100 µL of a $5x10^5$ conidia/mL suspension made by flooding 14-day old plates with 2 mL sterile distilled water was placed in the center of a circle of dialysis tubing affixed to a glass slide. The dialysis tubing slides were incubated in a container with moist, sterile Kimwipes™ (Kimtech Science, Kimberly-Clark™ Co., Irving, TX) to keep the relative humidity high. The container was placed in an incubator set to 25 ℃ with a diurnal light cycle (12 h light/12 h dark) for four days. Slides were then removed from the container and observed via Nikon Eclipse Ci microscope (Fig. 2.3, D, E).

2.3. Results

2.3.1 Phylogenetics

Using Bayesian inference, two species in the *C. acutatum* species complex were identified; *C. fioriniae,* and *C. nymphaeae*, with additional isolates that were closely related to *C. limetticola* and *C. melonis* (Fig. 2.2). For this dissertation, these isolates will be referred to as "*C. melonis*-like". For the *C. gloeosporioides* complex isolates, four definitive species were identified; *C. aenigma, C. conoides, C. gloeosporioides sensu stricto, C. kahawae* (Fig. 2.3). Additionally, there was one group of isolates that were closely related to *C. alienum, C. fructicola*, and *C. nupharicola* (Fig. 2.3). For this dissertation, these isolates will be referred to as "*C. fructicola*-like" due to the observation of *C. fructicola* on tree-fruits in the Mid-Atlantic (Hu et al. 2015b). There was one unidentified *C. acutatum* complex isolate which was associated with the *C. nymphaeae* clade but further work is required to properly the isolate to a species (Fig. 2.2).

2.3.2 Morphology

Colony characteristics such as colony top, bottom, surface, and conidial shape varied between isolates within a *Colletotrichum* species (Fig. 2.6). *C. fioriniae* colonies were mostly pink with a gray rim and produced with oval conidia with acute ends, however, *C. fioriniae* also had conidia with both acute and oval ends as well as other colors for colony tops (Fig. 2.6, A, C). Overall, morphology was inconsistent for the rest of the *Colletotrichum* species (Fig. 2.6). Additionally, the appressorial morphology of the *C. fructicola*-like isolates and the *C. aenigma* isolates was determined. No patterns in appressorial shape were informative in separating the *C. fructicola*-like isolates into *C. alienum, C. fructicola,* and *C. nupharicola* species (*Data not shown*).

2.3.3 Species distribution in the state

The identified species and groups of partially identified species were not found in all wine regions (Table 2.5). On average, there were 3.5 species or partially identified species found within a wine region (Table 2.5). *C. fioriniae* and *C. aenigma* were the most prevalent across the state and were found in seven and six wine regions, respectively. The *C. fructicola*-like isolates and *C. nymphaeae* were the next most common, being present in five and four wine regions, respectively. *C. conoides* was found in two wine regions. *C. gloeosporioides sensu stricto*, *C. kahawae*, and *C. melonis*-like isolates were found in only one wine region each (Table 2.5). The number of species per vineyard ranged from one to five with an average of 2.5 species per vineyard. Additionally, there were instances of two species being recovered from the same grape cluster. For example, the isolates KPTR01A12A and KPTR01C13A, a *C. fructicola*-like isolate and a *C. aenigma* isolate respectively, were recovered from the top and bottom of the same cluster.

2.4. Discussion

Historical research on grape ripe rot state that *C. acutatum* and *C. gloeosporioides* are the causal agents of the disease in the Mid-Atlantic. Few studies on wine grape have been completed since the taxonomic revisions in 2012. Surveys of *Colletotrichum* species on other hosts such as tree fruits have been completed in the Mid-Atlantic US. In South Carolina, *C. acutatum*, *C. fructicola*, *C. siamense*, and *C. truncatum* were isolated from lesions on peach fruit (Munir et al. 2016; Hu et al. 2015b). Munir et al. 2016 surveyed orchards in Kentucky and identified *C. fioriniae, C. fructicola*, *C. nymphaeae, C. siamense,* and *C. theobromicola* on apple. Surveys of grape ripe rot have been completed in China where *C. aenigma, C. fructicola, C. gloeosporioides sensu stricto, C. hebeiense,* and *C. viniferum* were found (Peng et al. 2013; Yan et al. 2015). To our knowledge, this is the first survey of VA vineyards for grape ripe rot identification and the first report of *C. aenigma*, *C. conoides*, *C. fioriniae,* and *C. nymphaeae* causing grape ripe rot the US.

The distribution of the *Colletotrichum* species found in Kentucky was considered to be random (Munir et al. 2016). In our survey, there was more of a pattern to the distribution of the *Colletotrichum* species. *C. fioriniae* was the most wide-spread species in the state and was found in all regions but the Chesapeake Bay region which had only three isolates total (Fig. 2.5). This species also has the most diverse host range including pear, rhododendron, tulip, and hemlock scale (Cannon et al. 2012; Damm et al. 2012), and poison ivy (Kasson et al. 2014). Additionally, studies prior to the taxonomic reconstruction of *C. acutatum* found that the optimum temperature for growth and sporulation was 24-28 ℃ (Maas 1998; Miles et al. 2013), whereas *C. gloeosporioides* exhibited a slightly higher optimum in the range of 25-30 ℃ (Dodd et al. 1991; Estrada et al. 2000). This difference in temperature optimum could explain the geographic

distribution of species in the *C. gloeosporioides* complex in which was found to be limited to the cooler, more mountainous regions, such as the Heart of Appalachia, and the distribution of species in the *C. acutatum* complex in the warmer regions, such as the Southern and Chesapeake Bay regions (Fig. 2.5).

On average, the number of species within a VA vineyard is 2.5 species. This result shows that the presence of multiple species within a vineyard is very common. Additionally, there were instances of two species being recovered from the same grape cluster, such as the isolates KPTR01A12A (*C. fructicola*-like) and KPTR01C13A (*C. aenigma*). Recent studies have observed differences in fungicide sensitivity between the *Colletotrichum* species complexes that were isolated from fruit grown in the Mid-Atlantic region (Hu et al. 2015a; Ishii et al. 2016; Munir et al. 2016). The prior reports of variability in fungicide sensitivity, and my findings of the presence of multiple species within a vineyard, and potentially the same cluster, create an increasingly complex issue of grape ripe rot control within VA vineyards. In a next step, further studies will be required to evaluate differences in fungicide sensitivity between the isolates of *Colletotrichum* species from VA vineyards.

Recovering only a low number of isolates in some regions, such as the Chesapeake Bay region, where I collected only three isolates (Table 2.4), may not have been sufficient to obtain a representative sample of the diversity of *Colletotrichum* species in the region. Additionally, regions where only one vineyard was sampled, such as the Heart of Appalachia region, may have affected our results as well, even though the number of isolates collected was 66 (Table 2.4). Generally, when the number of vineyards sampled was more than two, the number of *Colletotrichum* species identified per region was three or more (Table 2.4). Expanded surveys

are required to increase low vineyard numbers in specific regions and low isolate numbers to uncover additional species within these regions.

Sequencing of additional genes is required to further elucidate the identification of the subspecies of the *C. kahawae* isolates that were found. *C. kahawae* subspecies can be fully separated with the glutamine synthase gene (Weir et al. 2012). Additional work is also required to fully identify the *C. melonis*-like isolates and the group of *C. fructicola*-like isolates. Since the morphology of the *C. fructicola*-like isolates overlapped, morphology did not add to the identification process. Therefore, sequencing of additional gene fragments , such as Ap/MAT, is required to resolve the species affiliation of the *C. fructicola*-like isolates (Jayawardena et al. 2016).

Acknowledgements

This research was financially supported by the Virginia Wine Board (VWB, 449036, 449204, and 449338), and Virginia Department of Agriculture and Consumer Services (VDACS, FYY-2015 544). We thank Amanda Bly, and Sabrina Hartley, members of the Grape Pathology lab, for assisting with sample collection and fungal collection creation. We also thank Akiko Mangan, Whitney Berry, and Vanette Trumm, additional members of the Grape Pathology lab, for assisting with fungal collection maintenance, DNA extraction, and PCR.

2.5. References

Benson, D., Lipman, D., & Ostell, J. (1993). GenBank. *Nucleic Acids Research, 21*, 2963–2965.

Bonants, P., Edema, M., & Robert, V. (2013). Q-bank, a database with information for identification of plant quarantine plant pest and diseases. *EPPO Bulletin*, *43*, 211–215.

Cannon, P., & Bridge, P. (2008). Linking the past, present and future of *Colletotrichum* systematics. in *Colletotrichum: host specificity, pathology and host-pathogen interaction*, Prusky, D., Freeman, S., & Dickman, M. eds. St. Paul, MN: American Phytopathology Society.

Cannon, P., Damm, U., Johnston, P., & Weir, B. (2012). *Colletotrichum*–current status and future directions. *Studies in Mycology*, *73*, 181–213.

Clark, K., Karsch-Mizrachi, I., Lipman, D., Ostell, J., & Sayers, E. (2015). GenBank. *Nucleic Acids Research*, *44*, D67–72.

Damm, U., Cannon, P., Woudenberg, J., & Crous, P. (2012). The *Colletotrichum acutatum* species complex. *Studies in Mycology*, *73*, 37–113.

Daykin, M., & Milholland, R. (1984). Ripe rot of muscadine grape caused by *Colletotrichum gloeosporioides* and its control. *Phytopathology, 74*, 710–714.

Diéguez-Uribeondo, J., Förster, H., & Adaskaveg, J. (2011). Effect of wetness duration and temperature on the development of anthracnose on selected almond tissues and comparison of cultivar susceptibility. *Phytopathology*, *101*, 1013–1020.

Dodd, J., Estrada, A., Matcham, J., Jeffries, P., & Jeger, M. (1991). The effect of climatic factors on *Colletotrichum gloeosporioides*, causal agent of mango anthracnose, in the Philippines. *Plant Pathology*, *40*, 568–575.

Everett, K. (2003). The effect of low temperatures on *Colletotrichum acutatum* and *Colletotrichum gloeosporioides* causing body rots of avocados in New Zealand. *Australasian Plant Pathology, 32*, 441–448.

Estrada, A., Dodd, J., & Jeffries, P. (2000). Effect of humidity and temperature on conidial germination and appressorium development of two Philippine isolates of the mango anthracnose pathogen *Colletotrichum gloeosporioides*. *Plant Pathology, 49*, 608–618.

Fitzell, R. & Peak, C. (1984). The epidemiology of anthracnose disease of mango: inoculum sources, spore production and dispersal. *Annals of Applied Biology*, *104*, 53–59.

Gardes, M., & Bruns, T. (1993). ITS primers with enhanced specificity for basidiomycetes - application to the identification of mycorrhizae and rusts. *Molecular Ecology, 2*, 113–118.

Glass, N., & Donaldson, G. (1995). Development of primer sets designed for use with the PCR to amplify conserved genes from filamentous ascomycetes. *Applied and Environmental Microbiology*, *61*, 1323–1330.

Greer, L., Harper, J., Savocchia, S., Samuelian, S., & Steel, C. (2011). Ripe rot of South-eastern Australian wine grapes is caused by two species of *Colletotrichum*: *C. acutatum* and *C. gloeosporioides* with differences in infection and fungicide sensitivity. *Australian Journal of Grape and Wine Research*, *17*, 123–128.

Guindon, S., Dufayard, J.F., Lefort, V., Anisimova, M., Hordijk, W., & Gascuel, O. (2010). New algorithms and methods to estimate maximum-likelihood phylogenies: assessing the performance of PhyML 3.0. *Systematic Biology*, *59*, 307–321.

Hu, M., Grabke, A., Dowling, M., Holstein, H., & Schnabel, G. (2015)a. Resistance in *Colletotrichum siamense* from peach and blueberry to thiophanate-methyl and azoxystrobin. *Plant Disease*, *99*, 806–814.

Hu, M., Grabke, A., & Schnabel, G. (2015)b. Investigation of the *Colletotrichum gloeosporioides* species complex causing peach anthracnose in South Carolina. *Plant Disease*, *99*, 797–805.

Hyde, K., Cai, L., McKenzie, E., Yang, Y., Zhang, J., & Prihastuti, H. (2009). Colletotrichum: a catalogue of confusion. *Fungal Diversity*, *39*, 1–17.

Ishii, H., Zhen, F., Hu, M., Li, X., & Schnabel, G. (2016). Efficacy of SDHI fungicides, including benzovindiflupyr, against *Colletotrichum* species. *Pest Management Science*, *72*, 1844–1853.

Jayawardena, R., Hyde, K., Damm, U., Cai, L., Liu, M., Li, X.H., Zhang, W., Zhao, W., & Yan, J. (2016). Notes on currently accepted species of *Colletotrichum*. *Mycosphere*, *7*, 1192–1260.

Kasson, M., Pollok, J., Benhase, E., & Jelesko, J. (2014). First report of seedling blight of eastern poison ivy (*Toxicodendron radicans*) by *Colletotrichum fioriniae* in Virginia. *Plant Disease*, *98*, 995.

Kearse, M., Moir, R., Wilson, A., Stones-Havas, S., Cheung, M., Sturrock, S., Buxton, S., Cooper, A., Markowitz, S., Duran, C., Thierer, T., Ashton, B., Mentjies, P., & Drummond, A. (2012). Geneious Basic: an integrated and extendable desktop software platform for the organization and analysis of sequence data. *Bioinformatics*, *28*, 1647–1649.

Larkin, M., Blackshields, G., Brown, N., Chenna, R., McGettigan, P., McWilliam, H., Valentin, F., Wallace, I., Wilm, A., Lopez, R., Thompson, J., Gibson, T., & Higgins, D. (2007). Clustal W and Clustal X version 2.0. *Bioinformatics*, *23*, 2947–2948.

Maas, J. (1998). Anthracnose fruit rot (black spot). in *Compendium of Strawberry Diseases*. 2nd ed. Maas, J. ed. St. Paul, MN: American Phytopathological Society.

Maharaj, A., & Rampersad, S. (2012). Genetic differentiation of *Colletotrichum gloeosporioides*; and *C. truncatum* associated with anthracnose disease of papaya (*Carica papaya* L.) and bell pepper (*Capsicum annuum* L.) based on ITS PCR-RFLP fingerprinting. *Molecular Biotechnology*, *50*, 237–249.

McFadden-Smith, W., & Gubler, W. (2015). Sour rot. in *Compendium of Grape Diseases, Disorders, and Pests*. Wilcox, W., Gubler, W., & Uyemoto, J. eds. St. Paul, MN: American Phytopathological Society.

Meunier, M., & Steel, C. (2009). Effect of *Colletotrichum acutatum* ripe rot on the composition and sensory attributes of Cabernet Sauvignon grapes and wine. *Australian Journal of Grape and Wine Research*, *15*, 223–227.

Miles, T., Gillett, J., Jarosz, A., & Schilder, A. (2013). The effect of environmental factors on infection of blueberry fruit by *Colletotrichum acutatum*. *Plant Pathology, 62*, 1238–1247.

Munir, M., Amsden, B., Dixon, E., Vaillancourt, L., & Ward Gauthier, N. (2016). Characterization of *Colletotrichum* species causing bitter rot of apple in Kentucky orchards. *Plant Disease*, *100*, 2194–2203.

O'Donnell, K., & Cignelnik, E. (1997). Two divergent intragenomic RDNA ITS2 types within a monophyletic lineage of the fungus *Fusarium* are nonorthologous. *Molecular Phylogenetics and Evolution*, *7*, 103–116.

Peng, L., Sun, T., Yang, Y., Cai, L., Hyde, K., Bahkali, A., & Liu, Z. (2013). *Colletotrichum* species on grape in Guizhou and Yunnan provinces, China. *Mycoscience, 54*, 29–41.

Peres, N., Timmer, L., Adaskaveg, J., & Correll, J. (2005). Lifestyles of *Colletotrichum acutatum*. *Plant Disease*, 89, 784–796.

Prusky, D., Freeman, S., & Dickman, M. (2000). Preface. in *Colletotrichum: host specificity, pathology, and host-pathogen interaction*. Prusky, D., Freeman, S., & Dickman, M. ed. St. Paul, MN: American Phytopathology Society.

Ronquist, F., & Huelsenbeck, J. (2003). MRBAYES 3: Bayesian phylogenetic inference under mixed models. *Bioinformatics, 19*, 1572–1574.

Samuelian, S., Greer, L., Savocchia, S., & Steel, C. (2012). Overwintering and presence of *Colletotrichum acutatum* (ripe rot) on mummified bunches, dormant wood, developing tissues and mature berries of *Vitis vinifera*. *Vitis, 51*, 33–37.

Simmonds, J. (1965). A study of *Colletotrichum* causing ripe fruit rots in Queensland. *Queensland Journal of Agricultural and Animal Science, 22*, 437–59.

Sinclair, J., & Dhingra, O. (1995). *Basic Plant Pathology Methods*. CRC press.

Southworth, E. (1891). Ripe rot of grapes and apples. *The Journal of Mycology*, *6*, 164–173.

Sreenivasaprasad, S. & Talhinhas, P. (2005). Genotypic and phenotypic diversity in *Colletotrichum acutatum*, a cosmopolitan pathogen causing anthracnose on a wide range of hosts. *Molecular Plant Pathology*, *6*, 361–74.

Steel, C., Greer, L., Savocchia, S., & Samuelian, S. (2011). Effect of temperature on *Botrytis cinerea*, *Colletotrichum acutatum* and *Greeneria uvicola* mixed fungal infection of *Vitis vinifera* grape berries. *Vitis*, *50*, 69–71.

Sutton, B. (1992). The Genus *Glomerella* and its anamorph *Colletotrichum.* in *Colletotrichum: Biology, Pathology and Control*, Bailey, J., & Jeger, M. eds. Melksham, UK: CAB International.

Sutton, T. (2015)a. Ripe rot. in *Compendium of Grape Diseases, Disorders, and Pests*. Wilcox, W., Gubler, W., & Uyemoto, J. eds. St. Paul, MN: American Phytopathological Society.

Sutton, T. (2015)b. Bitter rot. in *Compendium of Grape Diseases, Disorders, and Pests*. Wilcox, W., Gubler, W., & Uyemoto, J. eds. St. Paul, MN: American Phytopathological Society.

Templeton, M., Rikkerink, E., Solon, S., & Crowhurst, R. (1992). Cloning and molecular characterization of the glyceraldehyde-3-phosphate dehydrogenase-encoding gene and cDNA from the plant pathogenic fungus *Glomerella cingulata*. *Gene*, *122*, 225–230.

Weir, B., Johnston, P., & Damm, U. (2012). The *Colletotrichum gloeosporioides* species complex. *Studies in Mycology*, *73*, 115–180.

Wharton, P., & Dieguez-Uribeondo, J. (2004). The biology of *Colletotrichum acutatum*. *Anales Del Jardín Botánico de Madrid*, *61*, 3–22.

White, T., Bruns, T., Lee, S., & Taylor, J. (1990). Amplification and direct sequencing of fungal ribosomal RNA genes for phylogenetics. *PCR protocols: a guide to methods and applications*, *18*, 315–322.

Wilcox, W., Gubler, W., & Uyemoto, J. eds. (2015). Compendium of grape diseases, disorders, and pests. St Paul: APS Press.

Wilson, L., Madden, L., & Ellis, M. (1990). Influence of temperature and wetness duration on infection of immature and mature strawberry fruit by *Colletotrichum acutatum*. *Phytopathology*, *80*, 111–116.

Yan, J., Jayawardena, M., Goonasekara, I., Wang, Y., Zhang, W., Liu, M., Huang, J., Wang, Z., Shang, J., Peng, Y., & Bahkali, A. (2015). Diverse species of *Colletotrichum* associated with grapevine anthracnose in China. *Fungal Diversity*, *71*, 233–246.

Table 2.1: Primers for PCR amplification and sequencing.

Gene	Product name	Primer	Sequence (5'-3')	Reference
CAL	calmodulin	CL1C	GAA TTC AAG GAG GCC TTC TC	Weir et al. 2012
		CL2C	CTT CTG CAT CAT GAG CTG GAC	Weir et al. 2012
GAPDH	glyceraldehyde-3-phosphate dehydrogenase	GDF	GCC GTC AAC GAC CCC TTC ATT GA	Templeton et al. 1992
		GDR	GGG TGG AGT CGT ACT TGA GCT TGT	Templeton et al. 1992
HIS3	histone-3	HIS3F	AAG AAG CCT CAC CGC TAC AA	Swett, *personal communication*
		HIS3R	CTG AAT GGT GAC ACG CTT GG	Swett, *personal communication*
ITS	internal transcribed spacer	ITS-1F	CTT GGT CAT TTA GAG GAA GTA A	Gardes & Bruns 1993
		ITS-4	TCC TCC GCT TAT TGA TAT GC	White et al. 1990
TUB2	β-tubulin 2	T1	AAC ATG CGT GAG ATT GTA AGT	O'Donnell & Cigelnik 1997
		Bt2b	ACC CTC AGT GTA GTG ACC CTT GGC	Glass & Donaldson 1995

Table 2.2: Representative isolates obtained during the Virginia survey that belong to the *C. acutatum* species complex and were identified to the species within the complex by multi-locus sequence typing.

Species[a]		Isolate	Year	Origin (County)	Wine region	Cultivar	Colony characteristics: top	Colony characteristics: bottom	Colony characteristics: Surface	Conidium characteristics[b]
C. fioriniae	1	ABCY01B14C	2014	Washington	Blue Ridge	Cayuga	Pink & gray	Dark-pink	Flat	12.16 x 4.49 acute
		ABTR04A14B	2014	Washington	Blue Ridge	Traminette	Pink & gray	Dark-pink	Flat	11.30 x 5.09 acute and oval
		ABTR10A14A	2014	Washington	Blue Ridge	Traminette	Pink & gray	Black with a pink rim	Flat	12.48 x 4.85 acute and oval
		ABVR01B14C	2014	Washington	Blue Ridge	Viognier	Pink & gray	Pink & white	Flat	12.96 x 4.55 acute
		GWCH03B13B	2013	Halifax	Southern	Chardonnay	Pink	Pink	Woolly	9.28 x 3.78 acute
		LNRS01A13A	2013	Fauquier	Northern	Riesling	White & buff	White	Cottony	10.61 x 4.52 acute
		LNRS01B13A	2013	Fauquier	Northern	Riesling	Pink & white	White	Cottony	8.75 x 4.71 acute
		MRNI01A14A	2014	Wise	Heart of Appalachia	Niagara	Pink & gray	Dark-pink	Flat	13.75 x 4.35 acute
		NECH04A13A	2013	Loudoun	Northern	Chardonnay	Light-gray	Light-gray	Cottony	9.99 x 4.48 acute and oval
		OHCH10A14B	2014	Culpepper	Northern	Chardonnay	Pink & gray	Dark-pink	Flat	12.72 x 4.49 acute
		TACH02A13A	2013	Loudoun	Northern	Chardonnay	Pink & white	White	Cottony	11.71 x 4.22 acute
	2	BAVR01C13A	2013	Nottoway	Central	Viognier	Pink & light-gray	Pink & light-gray	Woolly	10.16 x 3.80 acute
		BYPV01A14A	2014	Maryland		Petit Verdot	Pink & gray	Dark-pink	Flat	10.59 x 4.01 acute
		GRVR02C13A	2013	Albemarle	Central	Viognier	Pink	Pink	Woolly	13.31 x 5.40 oval
		JRCH02D13B	2013	Hanover	Central	Chardonnay	Pink & light-gray	Pink	Woolly	10.64 x 4.24 acute and oval
		WCTR02C13A	2013	Loudoun	Northern	Traminette	Pink & white	Pink & white	Cottony	10.98 x 3.97 acute and oval
	N/A	BYPV03D14B	2014	Maryland		Petit Verdot	Pink & gray	Dark-pink	Flat	12.70 x 4.99 acute and oval
		CTME0814B	2014	Northampton	Eastern Shore	Merlot	Pink & gray	Pink with a black rim	Flat	10.01 x 4.18 oval
		MRTR01C14A	2014	Wise	Heart of Appalachia	Traminette	White & gray	White	Flat	10.52 x 4.17 oval
		SCPM01A13A	2013	Nelson	Central	Petit Manseng	White	White	Cottony	7.82 x 4.60 acute
C. nymphaeae	3	ABTR06A14B	2014	Washington	Blue Ridge	Traminette	Gray	Speckled white	Flat	15.31 x 5.61 acute
		BYPV05B14B	2014	Maryland		Petit Verdot	White & gray	White & gray	Cottony	14.10 x 5.62 acute
		BYPV06D14C	2014	Maryland		Petit Verdot	White & gray	White	Flat	15.72 x 4.87 acute
	4	GCVB02A13A	2013	Rappahannock	Northern	Vidal blanc	White	White	Cottony	12.88 x 5.32 oval
		TACH04C13A	2013	Loudoun	Northern	Chardonnay	Light-gray	Light-gray	Cottony	13.65 x 4.86 acute
	N/A	SHCY01A13A	2013	Shenandoah	Shenandoah	Cayuga	Light-gray	Light-gray	Flat	12.91 x 5.07 oval
		SHCY01C13A	2013	Shenandoah	Shenandoah	Cayuga	White	White	Cottony	12.43 x 4.83 oval
		TACH01D13B	2013	Loudoun	Northern	Chardonnay	Light-gray	Light-gray	Woolly	9.18 x 2.49 acute
C. melonis-like		MRTR01B14B	2014	Wise	Heart of Appalachia	Traminette	Gray	White	Flat	10.51 x 4.35 oval
N/A		OHCH01A14B	2014	Culpepper	Northern	Chardonnay	Gray	Gray & buff	Flat	14.33 x 7.46 acute

[a] Species identification from Bayesian inference phylogenetic tree construction using concatenated sequences of three primers (*ITS*, *HIS3*, *TUB2*) in the MrBayes 3.2.6 plug-in in Geneious® 11.1.3. Genotype lettering for delineation of genetic variation in VA isolates.

[b] Average length (µm), width (µm), and shape of twenty conidia from 14-day old cultures on amended-¼ PDA.

Table 2.3: Representative isolates obtained during the Virginia survey that belong to the *C. gloeosporioides* species complex and were identified to the species within the complex by multi-locus sequence typing.

Species[a]		Isolate	Year	Origin (County)	Wine region	Cultivar	Colony characteristics top	Colony characteristics bottom	Colony characteristics Surface	Conidium characteristics[b]			
C. aenigma	1	BAPM01B13B	2013	Nottoway	Central	Petit Manseng	Dark-gray	Dark-gray	Woolly	16.59	x	5.49	oval
		GMSB02A13A	2013	Warren	Shenandoah	Sauvignon blanc	White	Light-gray	Cottony	10.33	x	3.77	acute
		KPTR01C13A	2013	Mecklenburg	Southern	Traminette	Light-gray	Light-gray	Flat	16.82	x	4.92	oval
		PBCH04C13A	2013	Northampton	Eastern Shore	Chardonnay	Dark-gray	Dark-gray	Cottony	15.84	x	4.18	oval
		RMTR02A13A	2013	Mecklenburg	Southern	Traminette	White	Light-gray	Cottony	17.39	x	5.7	oval
	N/A	ACPM01A13B	2013	Frederick	Shenandoah	Petit Manseng	Clear	Clear	Flat	16.14	x	3.2	oval
		CTME14A14B	2014	Northampton	Eastern Shore	Merlot	Gray	Black	Flat	16.56	x	5.8	oval
C. fructicola-like	2	ABCL06A14A	2014	Washington	Blue Ridge	Chardonel	White & gray	Speckled gray	Woolly	15.06	x	5.43	oval
		ABRS02B14C	2013	Washington	Blue Ridge	Riesling	White & gray	White & black	Cottony	17.11	x	5.21	oval
		ABVB02A14C	2013	Washington	Blue Ridge	Vidal blanc	White & gray	White & gray	Cottony	15.58	x	5.54	oval
		BXCH01B13A	2013	Loudoun	Northern	Chardonnay	White	White	Cottony	15.05	x	4.52	oval
		SSTR02C13A	2013	Campbell	Central	Traminette	Light-gray	Light-gray	Woolly	15.99	x	5.69	acute and oval
	3	BXVR02A13A	2013	Loudoun	Northern	Viognier	Light-gray	Light-gray	Cottony	14.17	x	4.25	oval
		GRCH01D13A	2013	Albemarle	Central	Chardonnay	White	White	Cottony	8.49	x	2.96	oval
		HNPM01C13A	2013	Orange	Central	Petit Manseng	Light-gray	Light-gray	Cottony	12.78	x	4.08	acute and oval
		JNCH04A13A	2013	Albemarle	Central	Chardonnay	Light-gray & buff	Light-gray & buff	Woolly	15.49	x	5.77	oval
		NECH04B13B	2013	Loudoun	Northern	Chardonnay	Light-gray	Light-gray	Flat	13.56	x	4.48	oval
		PKCH01D13A	2013	Albemarle	Central	Chardonnay	Light-gray	Light-gray	Woolly	10.6	x	5.32	oval
		SSTR02B13A	2013	Campbell	Central	Traminette	Light-gray	Light-gray	Mottled	16.17	x	4.32	oval
	4	JRCH06A13B	2013	Hanover	Central	Chardonnay	Dark-gray	Dark-gray	Woolly	12.79	x	4.51	acute and oval
		RMVB02A13A	2013	Mecklenburg	Southern	Vidal blanc	Gray	Gray	Woolly	14.19	x	5.73	oval
	N/A	ACPM02B13B	2013	Frederick	Shenandoah	Petit Manseng	White	White	Cottony	13.1	x	3.88	oval
		AFCH02A13A	2013	Halifax	Southern	Chardonnay	Light-gray	Light-gray	Woolly	14.45	x	5.96	acute and oval
		BXCH01C13B	2013	Loudoun	Northern	Chardonnay	White	White	Cottony	12.13	x	3.11	oval
		GRVR03A13A	2013	Albemarle	Central	Viognier	White & light-gray	White & light-gray	Cottony	13.75	x	4.84	oval
		KPTR01A13A	2013	Mecklenburg	Southern	Traminette	White	White	Woolly	14.8	x	5.73	oval
		SSTR01D13A	2013	Campbell	Central	Traminette	White	White	Cottony	16.14	x	5.56	oval
C. conoides	5	BANN02A13A	2013	Nottoway	Central	Norton	Dark-gray	Dark-gray	Woolly	10.11	x	3.73	oval
		GCVB01C13A	2013	Rappahannock	Northern	Vidal blanc	Light-gray	Light-gray	Cottony	12.53	x	4.59	acute and oval
C. gloeosporioides		VECH01C13A	2013	Nelson	Central	Chardonnay	Light-gray	Light-gray	Flat	16.95	x	5.15	oval
C. kahawae	6	ABTR18A14B	2014	Washington	Blue Ridge	Traminette	White & Grey	White & Black	Cottony	16.11	x	4.76	oval
		ABTR19A14B	2014	Washington	Blue Ridge	Traminette	White & Grey	White & Black	Cottony	14.37	x	5.10	acute and oval
	N/A	GMSB02E13A	2013	Warren	Shenandoah	Sauvignon blanc	Light-gray	Light-gray	Cottony	12.03	x	3.57	oval

[a] Species identification from Bayesian inference phylogenetic tree construction using concatenated sequences of three primers (*CAL*, *GAPDH*, *TUB2*) in the MrBayes 3.2.6 plug-in in Geneious® 11.1.3. Genotype numbering for delineation of genetic variation in VA isolates.

[b] Average length (µm), width (µm), and shape of twenty conidia from 14-day old cultures on amended-¼ PDA.

Table 2.4: GenBank reference isolates used in phylogenetic tree construction.

C. acutatum reference isolates[a]					*C. gloeosporioides reference isolates*[b]				
Species	**Culture**	***ITS***	***HIS3***	***TUB2***	**Species**	**Culture**	***CAL***	***GAPDH***	***TUB2***
abscissum	CBS 134727	KC204988	KC205003	KC205056	*aenigma*	ICMP 18608	JX009683	JX010044	JX010389
acerbum	CBS 128530	JQ948459	JQ949450	JQ950110		ICMP 18686	JX009684	JX009913	JX010390
acutatum	CBS 127546	JQ948376	JQ949367	JQ950027	*aeschymenes*	ICMP 17673	JX009721	JX009930	JX010392
	CBS 127602	JQ948359	JQ949350	JQ950010	*alatae*	ICMP 17919	JX009738	JX009990	JX010383
	IMI 319423	JQ948399	JQ949390	JQ950050		ICMP 18122	JX009739	JX010011	JX010449
australe	CBS 116478	JQ948455	JQ949446	JQ950106	*alienum*	CBS 132880	KC297022	KC297005	KC297099
brisbanense	CBS 292.67	JQ948291	JQ949282	JQ949942		ICMP 12071	JX009654	JX010028	JX010411
cairnsense	BRIP 63641	KU923671	KU923721	KU923687		ICMP 18691	JX009664	JX010018	JX010385
chrysanthemi	CBS 126519	JQ948272	JQ949263	JQ949923	*aotearoa*	CBS 111965	KC297018	KC296995	KC297085
cosmi	CBS 853.73	JQ948274	JQ949265	JQ949925		CBS 132448	KC297020	KC296997	KC297089
costaricense	CBS 330.75	JQ948180	JQ949171	JQ949831		ICMP 18577	JX009612	JX009978	JX010417
cuscutae	IMI 304802	JQ948195	JQ949186	JQ949846	*asianum*	ICMP 18580	FJ917506	JX010053	JX010406
fioriniae	ATCC 28992	JQ948297	JQ949288	JQ949948		ICMP 18696	JX009723	JX009915	JX010384
	CBS 127537	JQ948318	JQ949309	JQ949969	*camelliae*	CGMCC 3.14924	KJ954633	KJ954781	KJ955229
	CBS 127599	JQ948309	JQ949300	JQ949960		LC3006	KJ954654	KJ954802	KJ955250
	CBS 127611	JQ948328	JQ949319	JQ949979	*clidemiae*	ICMP 18658	JX009645	JX009989	JX010438
	CBS 128517	JQ948292	JQ949283	JQ949943		ICMP 18706	JX009639	JX009909	JX010439
	CBS 129947	JQ948343	JQ949334	JQ949994	*conoides*	CAUG33	KP890151	KP890163	KP890175
	CBS 786.86	JQ948303	JQ949294	JQ949954	*cordylinicola*	ICMP 18579	HM470238	JX009975	JX010440
godetiae	CBS 131332	JQ948429	JQ949420	JQ950080	*endophytica*	CAUG28	KP145357	KP145413	KP145469
guajavae	IMI 350839	JQ948270	JQ949261	JQ949921	*fructicola*	ICMP 17921	JX009671	JX010035	JX010400
indonesiense	CBS 127551	JQ948288	JQ949279	JQ949939		ICMP 18645	JX009666	JX009992	JX010408
johnstonii	CBS 128532	JQ948444	JQ949435	JQ950095		ICMP 18727	JX009682	JX010035	JX010394
	IMI 357027	JQ948443	JQ949434	JQ950094		LC 3155	KJ954696	KJ954844	KJ955291
kinghornii	CBS 198.35	JQ948454	JQ949445	JQ950105		ICMP 19122	JX009744	JX009950	JX010433
laticiphilum	CBS 129827	JQ948290	JQ949281	JQ949941		LC3312	KJ954710	KJ954859	KJ955305
limetticola	CBS 114.14	JQ948193	JQ949184	JQ949844	*gloeosporioides*	LC3382	KJ954728	KJ954877	KJ955323
lupini	CBS 109226	JQ948158	JQ949149	JQ949809		LC3686	KJ954777	KJ954927	KJ955371
	CBS 122746	JQ948162	JQ949153	JQ949813	*henanense*	LC2820	KM610176	KM610178	KM610184
melonis	Col 22	KC204986	KC205006	KC205054		LC2821	KM610177	KM610179	KM610185
nymphaeae	CBS 126366	JQ948255	JQ949246	JQ949906	*horii*	ICMP 10492	JX009604	GQ329681	JX010450
	CBS 127612	JQ948230	JQ949221	JQ949881	*kahawae subsp.*	ICMP 12952	JX009648	JX009971	JX010426
	CBS 173.51	JQ948200	JQ949191	JQ949851	*ciggaro*	ICMP 18539	JX009635	JX009966	JX010434
	CBS 515.78	JQ948197	JQ949188	JQ949848	*kahawae subsp.*	ICMP 17816	JX009642	JX010012	JX010444
	CBS 526.77	JQ948199	JQ949190	JQ949850	*kahawae*	ICMP 17915	JX009638	JX010040	JX010435
	CSL 455	JQ948217	JQ949208	JQ949868	*musae*	ICMP 17817	JX009689	JX010015	JX010395
paxtonii	IMI 165753	JQ948285	JQ949276	JQ949936	*nupharicola*	ICMP 17940	JX009662	JX010031	JX010399
phormii	CBS 118194	JQ948446	JQ949437	JQ950097	*proteae*	CBS 132882	KC297032	KC297009	KC297101
pyricola	CBS 128531	JQ948445	JQ949436	JQ950096	*psidii*	ICMP 19120	JX009743	JX009967	JX010443
rhombiforme	CBS 131322	JQ948458	JQ949449	JQ950109	*queenslandicum*	ICMP 17708	JX009691	JX009934	JX010414
salicis	CBS 129972	JQ948466	JQ949457	JQ950117		ICMP 18705	JX009694	JX010036	JX010412
scovillei	CBS 126529	JQ948267	JQ949258	JQ949918	*salsolae*	ICMP 19051	JX009696	JX009916	JX010403
simmondsii	IMI 354381	JQ948280	JQ949271	JQ949931	*siamense*	CMM 3814	KC992372	KC702955	KC702922
sloanei	IMI 364297	JQ948287	JQ949278	JQ949938	*ti*	ICMP 4832	JX009649	JX009952	JX010442
tamarilloi	CBS 129811	JQ948185	JQ949176	JQ949836		ICMP 5285	JX009650	JX009910	JX010441
walleri	CBS 125472	JQ948275	JQ949266	JQ949926	*tropicale*	ICMP 18653	JX009719	JX010007	JX010407
						ICMP 18672	JX009722	JX010020	JX010396
					viniferum	GZAAS 5.08601	JQ309639	JN412798	JN412813
						GZAAS 5.08608	JN412782	JN412800	JN412811
					wuxiense	CGMCC 3.17894	KU251833	KU252045	KU252200
						JS1A44	KU251834	KU252046	KU252201
					xantharrhoeae	ICMP 17903	JX009653	JX009927	JX010448

[a] Internal transcribed spacer unit (*ITS*), histone-3 (*HIS3*), β-tubulin (*TUB2*)

[b] Calmodulin (*CAL*), glyceraldehyde-3-phosphate dehydrogenase (*GAPDH*), β-tubulin (*TUB2*)

Table 2.5: Number of *Colletotrichum* species found in each Virginia wine region.

Wine region[a]	No. of vineyards	No. of Isolates	Av. No. of species per vineyard	No. of species per region	Species
Heart of Appalachia	1	66	2.0	2	*C. fioriniae*, *C. melonis* strain
Blue Ridge	1	117	4.0	4	*C. fioriniae*, *C. fructicola*-like, *C. kahawae*, *C. nymphaeae*
Shenandoah Valley	3	25	2.7	5	*C. aenigma*, *C. fioriniae*, *C. fructicola*-like, *C. kahawae*, *C. nymphaeae*
Central VA	11	129	2.7	6	*C. aenigma*, *C. conoides*, *C. fioriniae*, *C. fructicola*-like, *C. gloeosporioides sensu stricto*, *C. nymphaeae*
Northern VA	8	68	2.8	5	*C. aenigma*, *C. conoides*, *C. fioriniae*, *C. fructicola*-like, *C. nymphaeae*
Southern VA	4	55	2.0	3	*C. aenigma*, *C. fioriniae*, *C. fructicola*-like
Chesapeake Bay	2	3	1.0	1	*C. aenigma*
Eastern Shore	2	8	1.5	2	*C. aenigma*, *C. fioriniae*

[a] Wine regions are arranged starting in the mountains (Heart of Appalachian, Blue Ridge, Shenandoah Valley, across the middle of the state (Central VA, Northern VA, Southern VA) to the coastline (Chesapeake Bay, Eastern Shore) to reflect the climate variability and topology changes within the state.

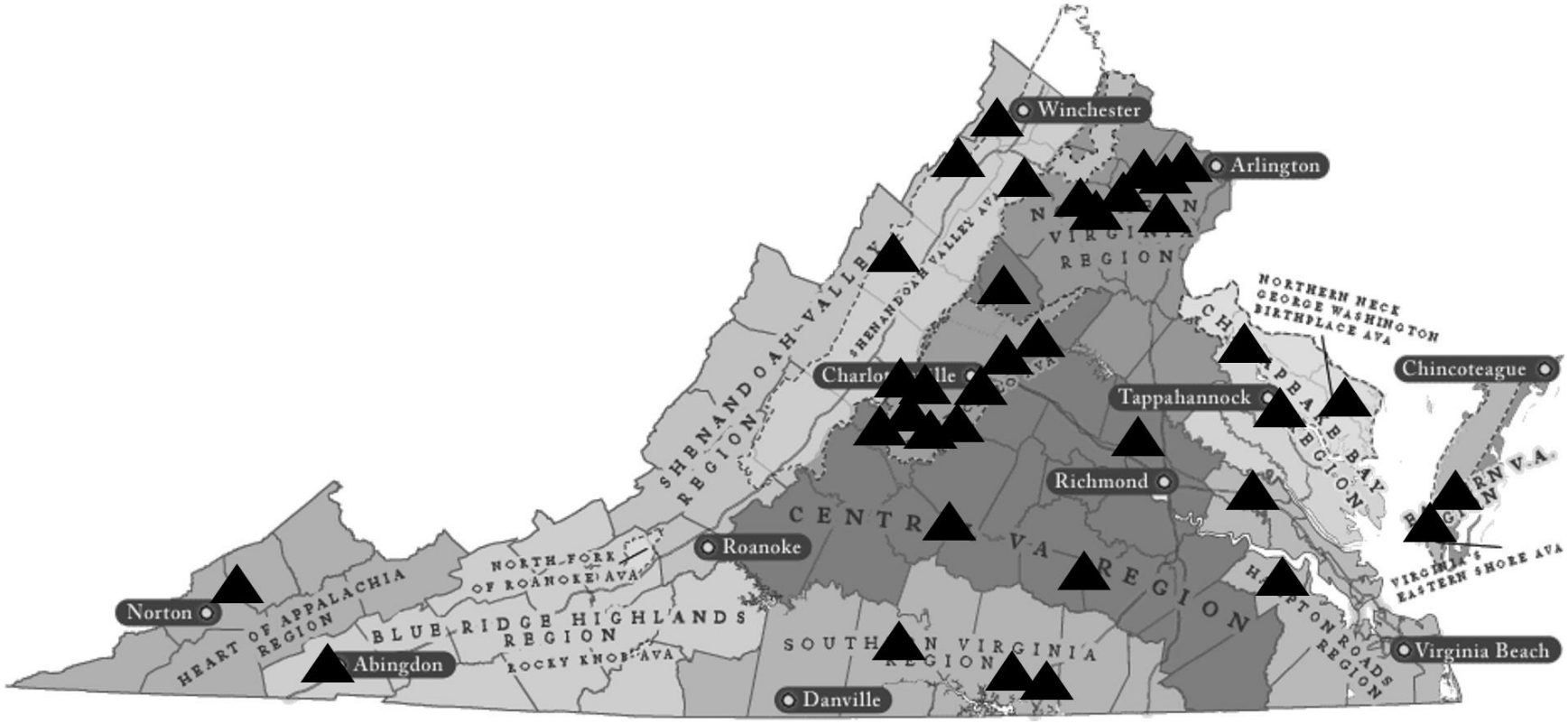

Figure 2.1: Locations of sampled vineyards from 2013-2014. Wine regions are displayed in various shades of gray. Vineyard locations are marked by the black triangles.

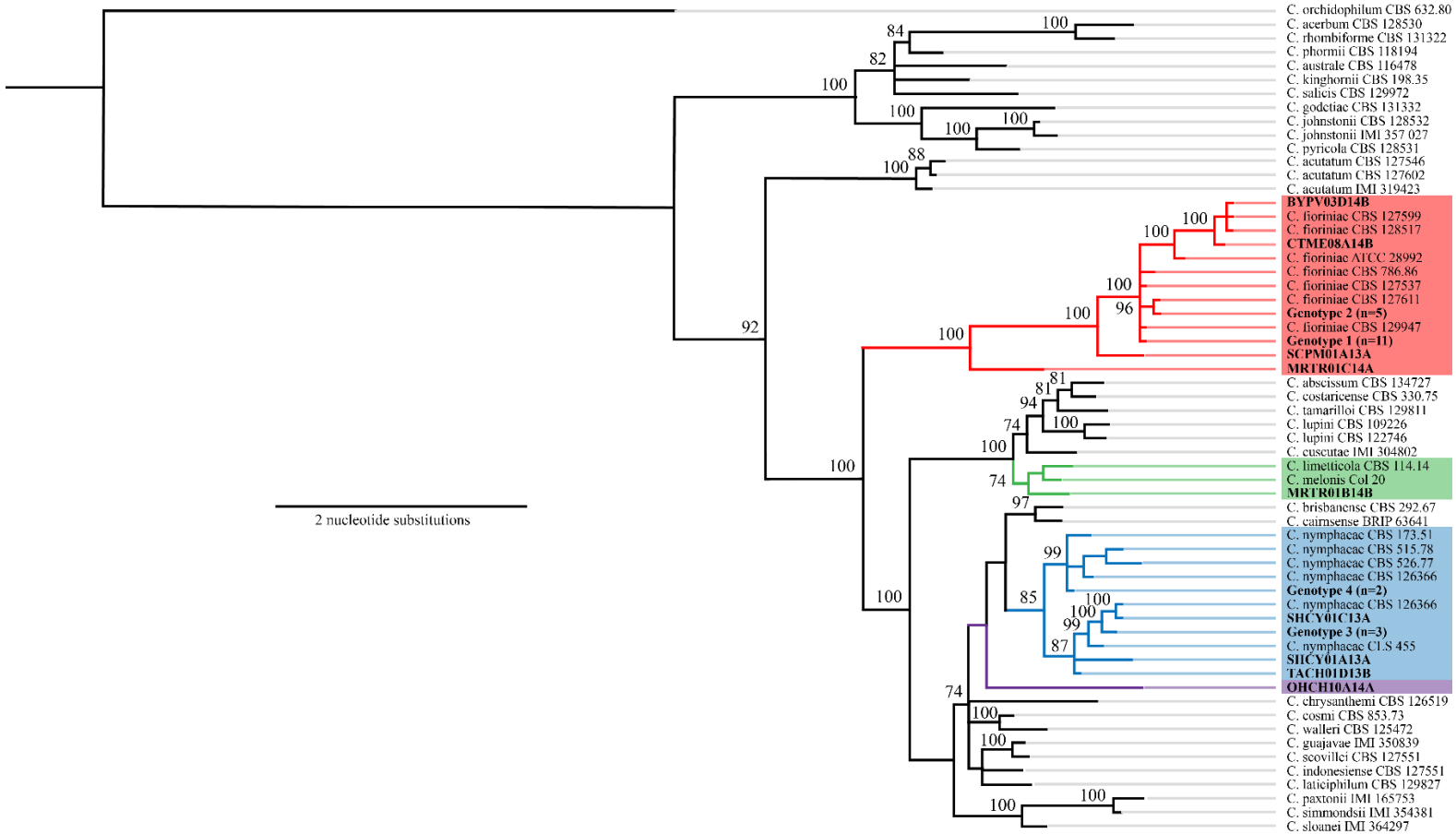

Figure 2.2: The rooted Bayesian inference phylogenetic tree constructed using *C. acutatum* species complex reference strains and putative *C. acutatum* isolates from VA. Clades containing isolates from VA vineyards are denoted by colored blocks; *C. fioriniae* in red, *C. limonetticola* and *C. melonis* in green, *C. nymphaeae* in blue, and an unidentified isolate in purple.

Figure 2.3: The rooted Bayesian inference phylogenetic tree constructed using *C. gloeosporioides* species complex reference strains and putative *C. gloeosporioides* isolates from VA. Clades containing isolates from VA vineyards are denoted by colored blocks; *C. kahawae* in red, *C. gloeosporioides sensu stricto* in yellow, *C. aenigma* in green, *C. conoides* in blue, and the undifferentiated grouping of *C. alienum*, *C. fructicola*, and *C. nupharicola* in purple.

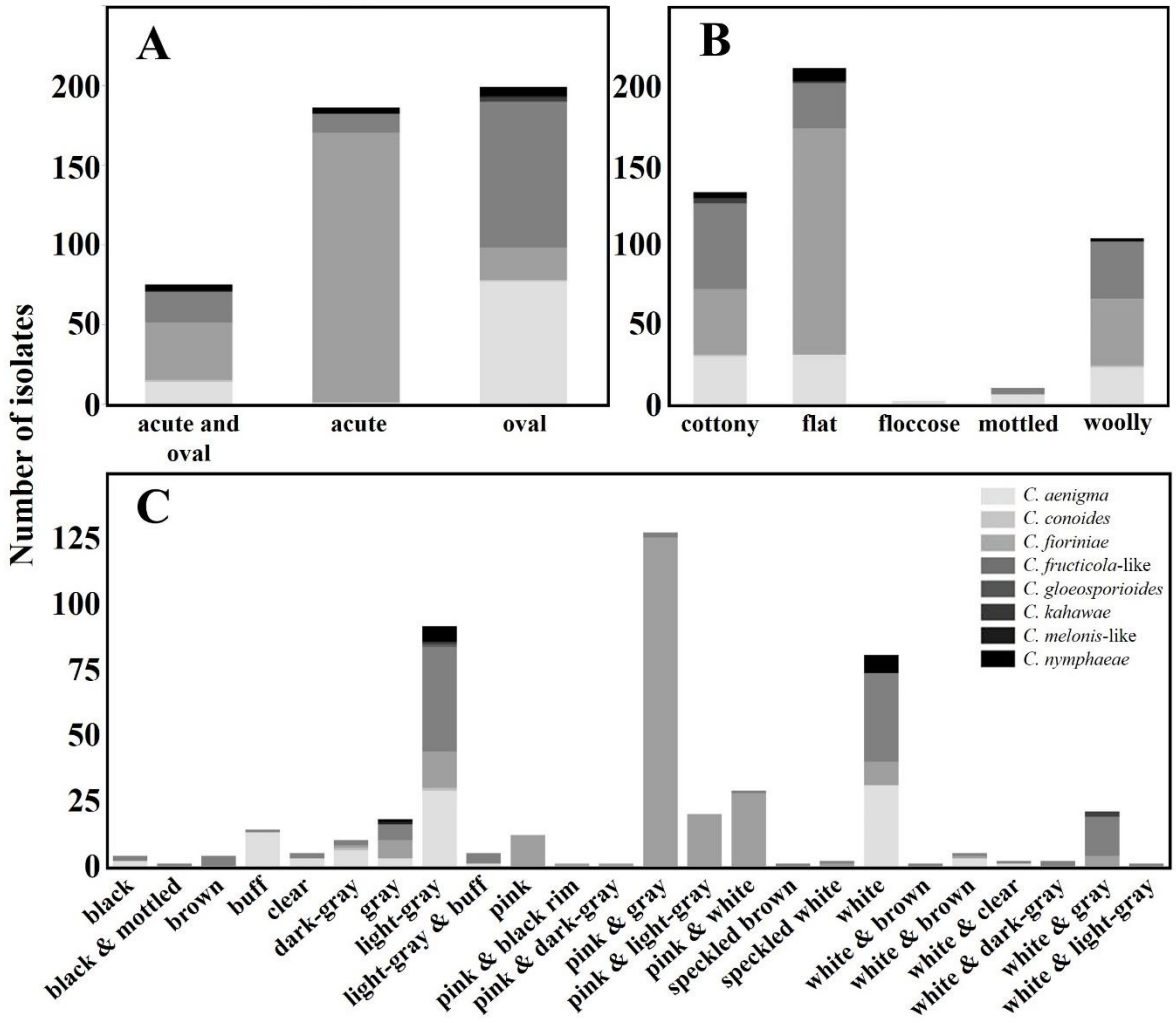

Figure 2.4: Proportion of isolates by *Colletotrichum* species and their morphological characteristics. Conidia came in three shapes [A]. Colony surfaces had five textures [B]. The first color in the colony top combinations corresponds to the most prevalent color that began in the center of the colony while the second color represents the colony edge [C]. The colors of the bars correspond to the *Colletotrichum* species with *C. aenigma* as the lightest gray and proceeding alphabetically to *C. nymphaeae,* which was the darkest. *C. fructicola*-like represents the grouping of isolates that were phylogenetically similar to *C. alienum, C. fructicola,* and *C. nupharicola. C. melonis*-like represents the isolates that were phylogenetically similar to *C. limetticola* and *C. melonis.*

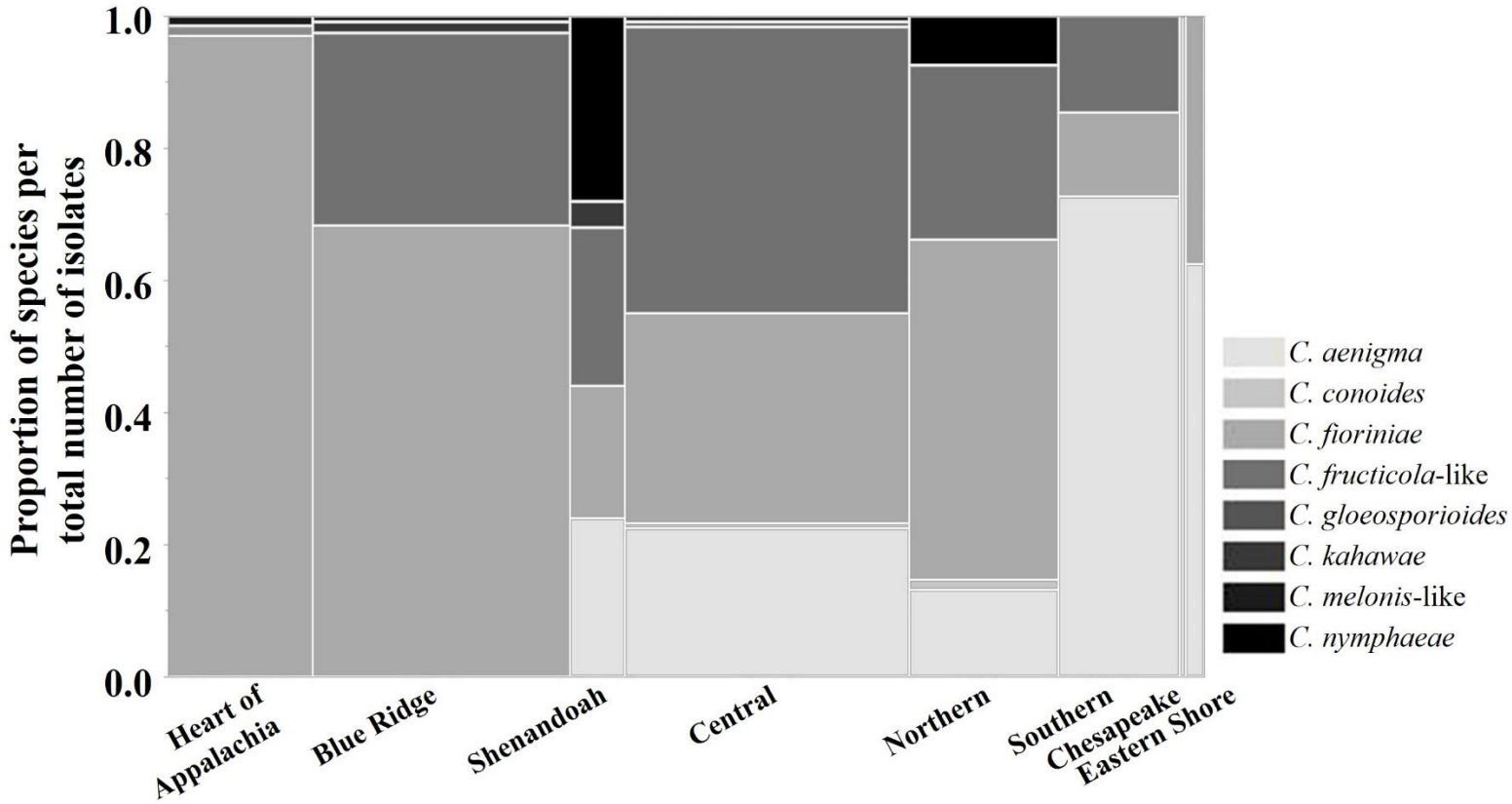

Figure 2.5: Proportion of isolates per *Colletotrichum* species within the total number of *Colletotrichum* isolates per wine region. The width of each bar corresponds to the number of samples collected from a wine region. The colors of the bars correspond to the *Colletotrichum* species with *C. aenigma* as the lightest gray and proceeding alphabetically to *C. nymphaeae*, which was the darkest. *C. fructicola*–like represents the grouping of isolates that were phylogenetically similar to *C. alienum*, *C. fructicola*, and *C. nupharicola*. *C. melonis*-like represents the isolates that were phylogenetically similar to *C. limetticola* and *C. melonis*.

Chapter 3.

Screening commercial fungicides for control of seven *Colletotrichum* species, the causal agents of grape ripe rot, from Virginia vineyards

Abstract

Grape ripe rot, a cluster rot disease caused by more than six *Colletotrichum* species within Virginia (Chapter 2), is endemic in the Mid-Atlantic region of the US. Since these pathogens were originally considered to be minor, there has been a limited investigation of chemical controls. The objectives of this study were to 1) screen fifteen commercial fungicides and two active ingredient combinations of eight commercial fungicides via two *in vitro* fungicide-amended media assay for control of *Colletotrichum* species isolated from grapes grown in Virginia, and 2) sequence the gene fragments of three of the four SDH enzyme subunits (*sdh*-B, *sdh*-C, and *sdh*-D) to identify a potential molecular basis for SDHI fungicide resistance. In my studies, I found that only four of the tested compounds resulted in EC50s below 100 µg/mL for conidial germination and mycelial elongation; captan, mancozeb, tetraconazole, and thiophanate-methyl. Captan and mancozeb effectively inhibited conidial germination and mycelial elongation of the majority of *Colletotrichum* species *in vitro,* whereas tetraconazole and thiophanate-methyl were effective for a limited number of *Colletotrichum* species. Additionally, we observed that the addition of captan and mancozeb increased the efficacy of azoxystrobin, benzovindiflupyr, copper octanoate, and polyoxin-D. The protein sequence of the *sdh*-B gene fragment did not have any of the known mutations; P225, N230, or H272.

3.1. Introduction

Colletotrichum acutatum and *C. gloeosporioides* are fungal pathogens with a wide range of hosts such as blueberry (Hu et al. 2015a), apple (Southworth 1891), mango (Fitzell et al. 1984), pepper (Higgins 1926), and grape (Sutton 2015). *Colletotrichum* species favor warm, humid environmental conditions which are common in most temperate climates such as the Mid-Atlantic USA (Greer et al. 2011; Melksham et al. 2002; Steel et al. 2007). Species formerly called *C. acutatum* and *C. gloeosporioides* have been re-classified into several different species (Damm et al. 2012, Weir et al. 2012). In a recent statewide survey (Chapter 2) we found six different *Colletotrichum* species from symptomatic grape berries sampled in Virginia, which is in the Mid-Atlantic USA.

Until recently, these fungal species were considered minor pathogens of wine grapes and the level of recognition by growers was low. Partially due to the lack of concern, the chemical controls available for control of grape ripe rot are limited to the ethylene-bis-dithiocarbamate (EBDC) (i.e. mancozeb, Fungicide Resistance Action Committee (FRAC) M3), the phthalimide (i.e. captan, FRAC M1), and the quinone outside inhibitor (QoI) (i.e. azoxystrobin, FRAC 11) fungicide classes. Each of these classes have limitations such as the long pre-harvest interval of mancozeb (66 days), reports of captan insensitivity in *C. gloeosporioides* (Greer et al. 2011), and reports of *Colletotrichum* QoI fungicide resistance in the Mid-Atlantic (FRAC 2018; Hu et al. 2015a). Additional field studies in other Mid-Atlantic states, such as Pennsylvania and North Carolina, have found inconsistent results for QoI for control of grape ripe rot (Halbrent et al. 2012; Hu et al. 2015a; Travis et al. 2008). More chemical control options are required for adequate control of these fungi over the course of the growing season, especially close to harvest when symptoms appear.

Additionally, the species of *Colletotrichum* found in VA were not evenly distributed across the state (Chapter 2). Recent studies with demethylase inhibitor (DMI, FRAC 3) fungicides observed variability in sensitivity between different *Colletotrichum* species and between isolates of the same species (Chen et al. 2016). For example, *C. nymphaeae* was found to be insensitive to fenbuconazole while *C. fioriniae* was found to be sensitive. In the same study, the two sub-groups of *C. fioriniae* exhibited differing levels of sensitivity to all tested fungicides where one of the sub-groups was overall more sensitive to all tested fungicides than the other sub-group.

In recent years, many fungicides that belong to succinate dehydrogenase inhibitor (SDHI, FRAC 7) fungicides have been introduced as new compounds for control of grape diseases. Until recently, boscalid (Endura, BASF Corp., Research Triangle Park, NC) introduced in 2003 (Walter 2011) was the only fungicide in the group, but the number of SDHI fungicides has grown rapidly with the introductions of benzovindiflupyr (Aprovia, Syngenta, Greensboro, NC), fluopyram (Luna Privilege, Bayer, Research Triangle Park, NC), isofetamid (Kenja, Summit Agro USA, Durham, NC), pydiflumetofen (Miravis, Syngenta), and several others. Although these compounds are labeled for application on wine grape, only isofetamid lists *Colletotrichum* as a target for disease control. *Colletotrichum* species have a history of being inherently insensitive to the majority of SDHIs, most notably boscalid (Greer et al. 2011; Ishii et al. 2016). However, recent studies have found that benzovindiflupyr is capable of controlling *Colletotrichum* sp. on apple and peach (Chapter 5; Ishii et al. 2016).

The SDHI fungicide chemical structure varies from compound to compound, however there is a shared, central structure (Sierotzki & Scalliet 2013). The MOA of the SDHIs is inhibition of cellular respiration by interference with the succinate dehydrogenase enzyme. This

enzyme is constructed of four subunits: SDH-A, the flavoprotein, SDH-B, the iron-sulfur protein, and SDH-C and -D, the hydrophobic anchoring regions. The molecular mechanisms of resistance have been documented in other plant pathogenic fungi, such as *Botrytis cinerea* and *Alternaria alternata* (Sierotzki & Scalliet 2013). The most common mutation for resistance is located in the *sdh*-B subunit at the H272Y/R/L/V location in the protein sequence (Sierotzki & Scalliet 2013; Von Schmeling & Kulka 1966). There are multiple other mutations that have also been identified farther from the binding site and on additional subunits (Sierotzki & Scalliet 2013).

Comparisons of fungal radial growth on fungicide-amended and fungicide-free media is the most common laboratory practice for evaluating fungicide efficacy screening (Amiri et al. 2008; Smilanick et al. 2010). Generally, six to 14 days are required to quantify fungal inhibition (Mondal et al. 2005; Peres et al. 2004; Shephard 1987; Xu et al. 2014). In recent years, media assays have been developed to reduce the time required for fungal inhibition calculation from over six days to less than four by methods such as 24-well plate assays and spiral plating (Fairchild et al. 2013; Fernández-Ortuño et al. 2014).

The objectives of this study were to 1) screen fifteen commercial fungicides and two active ingredient combinations of eight commercial fungicides via two *in vitro* fungicide-amended media assay for control of *Colletotrichum* species isolated from grapes grown in Virginia, and 2) sequence the gene fragments of three of the four SDH enzyme subunits (*sdh*-B, *sdh*-C, and *sdh*-D) to identify a potential molecular basis for SDHI fungicide resistance.

3.2. Materials and methods

3.2.1 Fungal isolate selection

Thirty-three representative isolates of seven *Colletotrichum* species (*C. aenigma, C. conoides, C. fioriniae,* the *C. fructicola*-like isolates*, C. gloeosporioides, C. kahawae,* and *C. nymphaeae*) identified from a survey of VA vineyards were used (Chapter 2) (Table 3.1). Several genotypes of *C. fioriniae, C. fructicola*-like isolates, and *C. nymphaeae* were observed in the Chapter 2 studies. Since previous literature had observed variations in fungicide sensitivity between *Colletotrichum* species isolates, these genotypes were tested separately and will be referred to as *C. fioriniae* genotype 1 and 2, *C. fructicola*-like genotype 1, 2, 3, and 4, and *C. nymphaeae* genotype 1 and 2 for these studies. Cultures were maintained as dry-agar plugs where were prepared in the following manner. Fourteen-day old single-conidium colonies grown on antibiotic amended [streptomycin and chloramphenicol (100 mg/mL each)] quarter strength potato dextrose agar (amended-¼ PDA) (Acumedia®, Neogen Company Lansing, MI). Agar plugs (3 mm) with a lawn of mycelia were cut and transferred to a sterile plastic petri dish for overnight desiccation in a laminar flow hood. The air-dried plugs were transferred to Nunc® CryoTube® (Thermo Scientific, Waltham, MA) and placed at -20 ℃ for long-term storage.

Prior to each experiment, dried agar plugs were placed into 7 mL of sterile potato dextrose broth (BD Difco™, Becton, Dickinson and Company, Franklin Lakes, NJ) in 15 mL conical tubes. The broth cultures were placed on a benchtop rocker (BenchRocker™ 3D, Benchmark Scientific, Edison, NJ) in an incubator (Precision™ 818, Thermo Scientific Inc, Waltham, MA) at 25 °C with a diurnal light cycle (12 h light /12 h dark). After 4 days, mycelia were pulled from the broth tubes and placed in the center of amended-¼ PDA plates. Cultures were grown for 7-14 days at 25 °C with a diurnal light cycle for conidial harvest.

3.2.2 Mycelium and conidium harvest

To obtain a conidial suspension, the surfaces of 7- to 14-day old cultures were flooded with 2 mL of sterile distilled water and the surface was gently rubbed to suspend conidia. The suspension was filtered through two layers of autoclaved Miracloth (EMD Millipore, Germany) to remove mycelia. The conidial suspension was then adjusted to $5x10^5$ conidia/mL with the aid of a hemocytometer (Neubauer Bright-line™, Hausser Scientific, Horsham, PA).

To harvest uniformly grown mycelia, a $5x10^5$ conidia/mL suspension was plated on water agar (BD Difco™, Becton Dickinson Co., Franklin Lakes, NJ) and spread until the liquid was absorbed to form an even lawn of conidia. The inoculated water agar plates were left at room temperature (20-25 ℃) for four days.

3.2.3 Single active ingredient plate layout and inoculations

The efficacy of fifteen active ingredients (a.i.) formulations (azoxystrobin, benzovindiflupyr, boscalid, captan, copper hydroxide, copper octanoate, fluopyram, isofetamid, mancozeb, polyoxin-D (two formulations), potassium phosphite, pyriofenone, tetraconazole, and thiophanate-methyl) (Table 3.2) were compared to a positive (= without a fungicide) control. The commercial fungicide formulations of the tested active ingredients were suspended in 2 mL of sterile distilled water and were diluted to 100 µg/mL (= ppm) by adding the solution to 25 mL aliquots of sterile, liquid potato dextrose agar (PDA). After the initial dilution, a serial dilution was completed to create a range of 100, 10, 1, 0.1, 0.01, 0 µg/mL of a.i. in 25 mL of sterile, liquid PDA. In order to inhibit the alternative oxidase respiratory pathway (Wood & Hollomon, 2003), salicylhydroxamic acid (SHAM) (Alfa Aesar, Ward Hill, MA) was added to each tube of liquid PDA that contained the a.i. azoxystrobin for a final concentration of 100 µg/Ml of SHAM. Prior to testing, *Colletotrichum* species sensitivity to SHAM was tested and was observed to have no effect on conidial germination or mycelial elongation (data not shown). One mL of the

liquid fungicide-amended media was transferred to wells in sterile, polystyrene 24-well culture plates with 2 mL wells (Falcon™, Corning Inc., Corning, NY). Plates were stored in a refrigerator (4 ℃) until use. All plates were used within five days of preparation.

The experimental design of the single-active-ingredient (a.i.) plate assay was a three-factor factorial design where *Colletotrichum* species (1-7 isolates per species (and subspecies), for a total of 33 isolates), inoculum type (conidia or mycelia), and a.i. concentration were examined for inhibition of fungal growth. Two rows of wells containing the full series of fungicide concentrations were inoculated with 5 µL of a 5 x 10^5 conidial suspension prepared as described above. The other two rows had 3 mm cores of the prepared WA plates (as described above) placed into the middle of each well (Fig. 3.1). Plates were visually assessed after three days of incubation at 25 ℃ with a diurnal light cycle (12 h light/12 h dark). The diameter of each colony was taken in two directions and recorded as the average. The inhibition of fungal activity was assessed as the proportion of fungal growth in the test well compared to the growth within the negative control well. The assay was repeated three times with each combination of a.i., *Colletotrichum* species, and propagule (conidia or mycelia) (minimum of three data points).

3.2.4 Two active ingredient plate assay layout and inoculations

The experimental design of the two a.i. plate assay was a three-factor factorial design where *Colletotrichum* species, inoculum type, and a.i. combination were examined for inhibition of fungal growth. The efficacy of the combination of nine a.i. formulations (azoxystrobin, benzovindiflupyr, captan, copper octanoate, mancozeb, polyoxin-D (Ph-D), potassium phosphite, tebuconazole, and thiophanate-methyl) (Table 3.2) was compared to a positive (mycelium or conidium without a fungicide) control for a subset of five isolates [BAVR01C13A (*C. fioriniae* genotype 2), GRVR03A13A (*C. fructicola*-like genotype 1), PBCH04C13A (*C. aenigma*),

PKCH01D13A (*C. fructicola*-like genotype 3), and TACH03A13A (*C. nymphaeae* genotype 2)] (Table 3.2). Fungicide stocks were prepared as described above and diluted to 100 µg/mL each for a total of 200 µg/mL of combined a.i. into a 25 mL aliquot of sterile, liquid PDA. SHAM was also added to all combinations containing azoxystrobin at a concentration of 100 µg/mL. Plates were prepared as described above.

Conidia and mycelia were tested on separate plates due to the layout of the combinations within the 24-well plates (Fig. 3.1, B). Plates were inoculated as described for the single a.i. plates and were visually assessed after three days of incubation at 25 ℃ with a diurnal light cycle (12 h light/12 h dark). The diameter of each colony was taken in two directions and recorded as the average. The inhibition of fungal activity was assessed as the proportion of fungal growth in the test well compared to the growth within the negative control well. The assay was repeated two times with each combination of a.i., *Colletotrichum* species, and inoculum type (conidia or mycelia) (minimum of four data points).

3.2.5 sdh-*fragment DNA extraction, amplification, and analysis*

Fourteen day-old cultures grown on amended-¼ PDA were flooded with 2 mL of sterile distilled water and the surface was gently rubbed to suspend fungal structures. The fungal suspension was transferred to a sterile 1.5 mL microcentrifuge tube, centrifuged, and the water was removed by pipetting. A pair of sterile forceps were used to pull the fungal mass from the 1.5 mL microcentrifuge tube, and tap to sterile Kimwipes™ (Kimtech Science, Kimberly-Clark™ Co., Irving, TX) to absorb the excess fluid. One hundred mg of fungal mass was transferred to a FastPrep® grinder tube (MP Biomedicals, LLC, Santa Ana, CA) containing one 5 mm and 4-6 2.5 mm glass beads. The samples were stored at -20 °C overnight, and then ground for 60 s at 4.5 m/s in a FastPrep®-24 (MP Biomedicals, LLC, Santa Ana, CA). Total

genomic DNA was extracted using the ISOLATE II Plant DNA Kit (Bioline, Meridian Bioscience, Cincinnati, OH) according to the manufacturer's instructions.

Three partial gene fragments of three subunits of the succinate dehydrogenase enzyme, *sdh*-B, *sdh*-C, and *sdh*-D, were amplified using the primer pairs listed in Table 3.3. Polymerase chain reaction (PCR) reactions for amplification of *sdh*-B were prepared at a volume of 25 µL containing1X GoTaq® Green (Promega Corp., Madison, WI), 0.4 µM of each primer, and 1 µL of DNA extraction in the StepOnePlus™ (Applied Biosystems™, Foster City, CA). The PCR conditions had a denaturation step of 2 min at 95°C, followed by 35 cycles of 1 min at 94 °C, 1 min at 58 °C, and 2 min at 72°C with a final extension of 10 min at 72°C. For amplification of *sdh*-D, reactions were prepared at a volume of 25 µL which contained 1X ImmoMix™ Red (Bioline, Meridian Bioscience, Cincinnati, OH), 0.25 µM of each primer, 2.61 µM bovine albumin serum (BSA) (New England BioLabs Inc., Ipswich, MA) and 2 µL of DNA extraction in the StepOnePlus™. The PCR conditions had a denaturation step of 5 min at 95°C, followed by 35 cycles of 30 s at 95 °C, 30 s at 60 °C, and 1 min at 72°C with a final extension of 10 min at 72°C. The *sdh*-B and *sdh*-D PCR products were cleaned before sequencing using Exonuclease I and rSAP (New England BioLabs Inc., Ipswich, MA) by the protocol provided by the manufacturer.

For amplification of *sdh*-C and all other low-yield reactions from *sdh*-B, and *sdh*-D, PCR reactions were prepared at a volume of 25 µL which contained 1X GoTaq® Green (Promega Corp., Madison, WI), 0.30 µM of each primer, and 2 µL of DNA extraction in the StepOnePlus™. The PCR conditions had a denaturation step of 5 min at 95°C, followed by 35 cycles of 30 s at 95 °C, 30 s at 52 °C or 56 °C, and 1 min at 72°C with a final extension of 10 min at 72°C. Products were run at 85V for 2.5 h on a 2% low melt agarose gel (Bio-Rad

Laboratories Co., Hercules, CA), bands were cut via platinum blade, and placed in a 1.5 mL microcentrifuge tube. The PCR products were extracted from the agarose blocks using the ISOLATE II PCR and Gel Kit (Bioline, Meridian Bioscience, Cincinnati, OH) according to the manufacturer protocol.

The cleaned PCR products of all three fragments were submitted to Eurofins Genomics (Eurofins MWG Operon, Louisville, KY) for sequencing. Sequences were trimmed and aligned using the Geneious (Kearse et al. 2012) and ClustalW (Larkin et al. 2007) alignment programs in Geneious® 11.1.3 (Biomatters Inc., Newark, NJ). Sequence similarities to previously identified samples from NCBI BLAST® (Altschul et al. 1990) were assessed with cleaned, consensus sequences.

3.2.6 Statistical analysis

For the single a.i. plate assay, the intercept and slope of the reaction of each *Colletotrichum* species against the active ingredient (a.i.) concentration was estimated using a generalized linear mixed model in SAS Studio (ver. 3.71, PROC GLIMMIX, SAS Institute Inc., Cary, NC). Since the dataset was composed of a binomial variable (yes or no on fungal presence), three common link functions for binomial data (logit, probit, and complementary log-log (CLL)) were used in the generalized linear mixed model (Bolker et al. 2009). The best link function was CLL for the majority of each *Colletotrichum* species, inoculum type, and single a.i. combination based on the comparisons of Akaike's Index of Criterion and deviance (Pearson's chi-square divided by degree of freedom) (SAS Institute, 2012). Using the intercept and slope from the CLL model, a nonlinear regression mixed model (PROC NLMIXED in SAS), was fitted to the actual data (Littell et al. 2006). The resulting model was used to calculate the

effective concentration for which 50% of samples are inhibited (EC50) for each *Colletotrichum* species, inoculum type, and single a.i. combination.

For the two a.i. plate assay, the effect of *Colletotrichum* species, inoculum type, two a.i. combination, and their interactions on the presence or absence of fungal growth were examined by generalized linear mixed model in SAS Studio (PROC GLIMMIX). For a multiple comparison, analysis of means was conducted using an option in PROC GLIMMIX to compare mean deviance of each species and fungicide treatment from the overall mean probability, 95% confidence interval was used as a threshold for a significant deviation from the overall mean. In short, the two a.i. combination was considered significant when the mean probability of one a.i. combination was lower than the low end of the 95% confidence interval.

3.3. Results

3.3.1 Single active ingredient plate assay

The effect of *Colletotrichum* species ($F = 5.19$, $P < 0.01$), and inoculum type ($F = 122.33$, $P < 0.01$) on the presence or absence of fungal inhibition were significant when the data was analyzed by fungicide. For inhibition of conidial germination, four compounds resulted in an EC50 below 100 µg/mL, which was the threshold I established for this assay, based on previous literature (Ishii et al. 2016). Mancozeb was the most active compound with a EC50 range of 1.1 µg/mL (*C. fructicola*-like genotype 2) to 30.0 µg/mL (*C. fructicola*-like genotype 4) µg/mL for all tested species and genotypes (Tables 3.4-3.6). Captan had a similar EC50 range of 3.2 µg/mL (*C. fructicola*-like genotype 2) to 30.0 µg/mL (*C. gloeosporioides*) for all species and genotypes tested with the exception of *C. fructicola*-like genotype 4, and *C. nymphaeae* genotype 1 (Tables 3.4-3.6). The EC50 of thiophanate-methyl was lower than 100 µg/mL with *C. aenigma, C.*

conoides, *C. fructicola*-like genotype 1, and *C. gloeosporioides*, with a range of 3.2 µg/mL (*C. gloeosporioides*) to 87.5 µg/mL (*C. conoides*) (Tables 3.5, 3.6). The EC50 of tetraconazole was lower than 100 µg/mL for *C. aenigma* (67.3 µg/mL) and *C. fioriniae* genotype 2 (87.8 µg/mL) (Tables 3.4, 3.5).

For inhibition of mycelial elongation, similarly to inhibition of conidial germination, the same four compounds reduced mycelial elongation and resulted in an EC50 below 100 µg/mL. Overall, the concentration of a.i. required to effectively inhibit mycelial elongation was higher than the concentration for inhibition of conidial germination. Mancozeb resulted in the lowest EC50 values ranging from 7.3 µg/mL (*C. aenigma*) to 97.6 µg/mL (*C. fioriniae* genotype 2) for tested species and genotypes with the exception of *C. nymphaeae* genotypes 1 and 2 (Tables 3.4-3.6). Captan resulted in an EC50 range of 9.4 µg/mL (*C. kahawae*) to 98.9 µg/mL (*C. fioriniae* genotype B) for seven out of twelve species and genotypes tested (Tables 3.4-3.6). The EC50 of thiophanate-methyl was lower than 100 µg/mL for *C. aenigma* (19.2 µg/mL), *C. fructicola*-like genotype 2 (1.2 µg/mL), and *C. gloeosporioides* (3.2 µg/mL) (Tables 3.5, 3.6). The EC50 of tetraconazole was lower than 100 µg/mL for *C. fioriniae* genotype 1 (98.9 µg/mL) and *C. fioriniae* genotype 2 (97.6 µg/mL) (Table 3.4). The additional eleven active ingredients, including all of the SDHI compounds, such as benzovindiflupyr, boscalid, fluopyram, and isofetamid, all resulted in estimated EC50s above 100 µg/mL.

3.3.2 Two active ingredient plate assay

I examined each factor and their combination, the interaction of a.i. combination and inoculum type ($F = 1.91$, $P < 0.01$), therefore, analyses were conducted separately for each inoculum type. For each inoculum type, both species (conidia $F = 5.50$, $P < 0.01$, mycelia $F = 4.14$, $P < 0.01$), and a.i. combination (conidia $F = 11.76$, $P < 0.01$, mycelia $F = 9.67$, $P < 0.01$)

significantly affected the probability of successful growth. Among tested species, *C. fructicola*-like isolates resulted in significantly lower probability of successful growth ($P \leq 0.05$) from conidia while *C. fioriniae* resulted in a significantly higher probability (i.e., tends to grow more than overall average) (Fig. 3.5, A). With mycelia, *C. nymphaeae* resulted in significantly lower probability of successful growth ($P \leq 0.05$) from conidia while the *C. fructicola*-like group resulted in a significantly higher probability, indicating that conidia are more sensitive to the tested compounds, but once germinated, mycelia are less sensitive (Fig. 3.5).

There were sixteen effective combinations that resulted in significantly lower probability of successful growth from conidia than the overall mean (= higher success rate for inhibition of conidial germination) (Fig. 3.6, A): eight combinations that contained captan (i.e., all tested combinations with captan); five combinations of mancozeb (with azoxystrobin, benzovindiflupyr, copper octanoate, polyoxin-D, and thiophanate-methyl); and three additional combinations that contained tebuconazole (with benzovindiflupyr, copper octanoate, and potassium phosphite) (Fig. 3.6, A).

There were fourteen effective combinations for inhibition of mycelial elongation (Fig. 3.6, B). Five combinations containing mancozeb (with azoxystrobin, benzovindiflupyr, captan, polyoxin-D, and thiophanate-methyl), five combinations containing tebuconazole (with benzovindiflupyr, captan, copper octanoate, potassium phosphite, and thiophanate-methyl), three additional thiophanate-methyl combinations (with captan, polyoxin-D, and potassium phosphite), and the azoxystrobin and benzovindiflupyr combination resulted in significantly lower probability ($P \leq 0.01$) mycelial elongation (Fig. 3.6, B).

3.2.4 sdh-fragment analysis

Based on NCBI BLAST®, the partial *sdh*-B gene sequences of VA isolates were 91% identical to *C. higginsianum* IMI349063 (GenBank XM 018295500) with a large gap in coverage (Altschul et al. 1990). The partial *sdh*-C gene sequences of VA isolates were 97% identical to *C. acutatum* HHBY48 (GenBank KU873019) with a gap in coverage, and the partial *sdh*-D was gene sequences of VA isolates were 90% identical to *C. orchidophilum* CORC01_11017 (GenBank XM 022622644). When the *sdh*-B gene sequences of the VA isolates were compared to sequences of *B. cinerea* BQ-3 (GenBank KR866382), and *B. cinerea* CAN 2 (GenBank KY499804), two resistant isolates, a 53 or 54 (genotype dependent) base-pair (bp) intron was observed at 108bp. Another large, 64 to 68 bp intron was observed in the sequences of *sdh*-D when compared to reference strains of *C. graminicola* M1.001 (GenBank XM 008091315) and *C. orchidophilum* CORC01 11017 (GenBank XM 0022622644) (Fig. 3.9). When the partial *sdh*-B gene sequence of VA isolates were translated into protein sequence, resistance mutations at P225, N230, or H272 were not observed.

3.4. Discussion

Captan (FRAC M4), and mancozeb (FRAC M3) were effective at inhibiting conidial germination and mycelial elongation of the tested *Colletotrichum* species and genotypes other than *C. nymphaeae*. Both captan and mancozeb are multi-site mode of action compounds, and are in the current recommendations for grape ripe rot management in the Mid-Atlantic USA (Pfeiffer et al. 2018). Additionally, we confirmed insensitivity of the *C. fructicola*-like genotypes 2, 3, and 4 to captan, which may explain recent outbreaks of grape ripe rot in vineyards where captan was prominently used. This also indicates that the already limited options against grape ripe rot are further restricted, especially for options to be used late in the season.

The lack of efficacy of azoxystrobin (FRAC 11) could be due to fungicide resistance. Studies in South Carolina have observed resistance to azoxystrobin in isolates of *C. siamense* isolated from symptomatic blueberries (Hu et al. 2015a). Additionally, QoI resistance has been confirmed in other wine grape pathogens such as downy mildew (*Plasmopara viticola*) and powdery mildew (*Erysiphe necator*) in VA (Colcol & Baudoin 2016). Preliminary sequencing of several VA *Colletotrichum* species isolates have exhibited G143A point-mutations in the *cyt*-B gene as well as the potential for gene region introns (data not shown) (Hu et al. 2015a; Ishii 2009). Further studies are required to fully confirm the presence of molecular resistance as well as plate assays.

In our studies, we used two different DMI compounds; tetraconazole in the single a.i. plate assay, and tebuconazole in the two a.i. plate assay; however, we did not compare these two compounds directly. Differing levels of sensitivity to the compounds between the *Colletotrichum* species were discussed in prior studies on *Colletotrichum* species from the Mid-Atlantic region (Chen et al. 2016; Hu et al. 2015b). Chen et al. (2016) observed a large variation in EC50 values among the tested species and even within isolates in a species in response to the six tested DMI fungicides. In our single a.i. plate assay, only the conidia of *C. aenigma*, and *C. fioriniae* genotype 2, and the mycelia of both *C. fioriniae* genotypes showed sensitivity to tetraconazole. Interestingly, when two active ingredients are combined, such as the combination of tebuconazole and mancozeb, the combination was successful in lowering the probability of both conidial germination and mycelial elongation. The variation in efficacy suggests that further investigation is required to evaluate the sensitivity of *Colletotrichum* species to multiple DMI compound, and sequence tentative resistance gene regions for mutations.

Limited information is available on the effects of SDHI fungicides on the inhibition of *Colletotrichum* species (Wedge et al. 2007). We tested four different SDHI materials (FRAC 7), which encompassed older compounds, such as boscalid, and newer compounds, such as benzovindiflupyr, fluopyram, and isofetamid. Prior research on boscalid demonstrated a lack of efficacy on inhibition of *Colletotrichum* growth (Glattli et al. 2005). Recent research on benzovindiflupyr suggested the SDHI class potentially could inhibit *Colletotrichum* growth (Ishii et al. 2016); however, our results showed that all tested SDHI materials exhibited EC50 values above 100 µg/mL, indicating their lack of efficacy against tested *Colletotrichum* isolates. The sequences that were obtained from the VA isolates were no more than 93% similar to accepted *Colletotrichum* reference isolates. In the protein sequence of *sdh*-B, no known resistance mutations were observed (Fig. 3.6), however, the protein sequence of the VA isolates of *Colletotrichum* and the *Colletotrichum* reference sequences from GenBank are not identical to the *Botrytis* GenBank references. Potentially, the inactivity the SDHI chemical class that was observed in these assays could be due to the differing structure of the *Colletotrichum* SDH subunits.

Polyoxin-D (FRAC 19) and pyriofenone (FRAC 50), exhibited no efficacy for inhibition of conidial germination or mycelial elongation of *Colletotrichum* species. Neither material is labeled for field application control of *Colletotrichum* species, however, prior field tests with polyoxin-D had shown fair to moderate efficacy for inhibition of *Colletotrichum* species on other host crops, such as apple and strawberry (Cordova et al. 2014; Yoder et al. 2018). Pyriofenone (FRAC 50) was made available in 2018 to commercial growers in the US. Since it is a material for powdery mildew, we did not expect it to work against *Colletotrichum* species. Also, the mode

of action of pyriofenone is inhibition of appressorium formation (FRAC 2018), therefore the artificial media-based assay such as the one in our study could provide false-negative results.

In our fungicide plate assays, we observed higher efficacy (e.g., lower EC50 or probability of successful growth) in inhibition of conidia as compared to mycelia as a type of inoculum. For example, captan inhibition of conidial germination produced an EC50 range of 3.2 µg/mL to 30.0 µg/mL for ten of the twelve tested species and genotypes whereas inhibition of mycelial elongation had an EC50 range of 9.4 µg/mL to 98.9 µg/mL for seven out of twelve species and genotypes tested (Fig. 3.3). This difference in sensitivity between the two inoculum types is due to the mode of action of the effective compounds. Both captan and mancozeb inhibit conidial germination by interfering with cellular respiration in multiple ways (Leroux 1996), but are known to have limited effect on mycelial elongation. Additionally, the DMI fungicide class affect sterol biosynthesis (FRAC 2018; Lepesheva & Waterman 2007) and thiophanate-methyl inhibits β-tubulin elongation during cell division, both of which are required for conidial germination and mycelial elongation.

In my other work (Chapter 2), an average of 2.5 *Colletotrichum* species within a vineyard was found, not including genotypes. *C. fioriniae* was ubiquitous among different wine regions in VA but the species belonging to the *C. gloeosporioides* species complex were more common in the warmer regions, closer to the coast. Additionally, I observed that these species can be isolated from the same cluster [i.e. KPTR01A12A (*C. fructicola*-like group) and KPTR01C13A (*C. aenigma*)]. In this study, I observed differences in sensitivity to fungicides for not only *Colletotrichum* species but also for the genotypes within a species. This suggests that the management practices in VA vineyards will have to be tailored to the location within the state to address all species within the area and potential fungicide insensitivities.

When the one a.i. and two a.i. assays were compared, several compounds, such as benzovindiflupyr, and polyoxin-D, where the individual a.i. EC50 was higher than 100 µg/mL, resulted in significantly lower probability of conidial germination or mycelial elongation than the overall mean probability. This trend shows the potential for an increase in efficacy with a combination of two MOA. In our Southwest VA vineyard field trials (Chapter 5), we observed benzovindiflupyr and polyoxin-D to be effective at reducing the presence of grape ripe rot in comparison to the grower's program. In the Southwest VA vineyard, the grape ripe rot treatments were applied in addition to the grower's program which contained mancozeb at the beginning of the season and captan at the end. However, the same materials performed poorly at the Alson H Smith Jr. Agricultural Research and Extension Center where these materials were applied alone. Thus the two a.i. assay effective compounds may work well in the field as a mixture with captan or mancozeb.

Results from the *in vitro* assay often do not agree with that from the field test (Chapter 5; Shephard 1987). *Colletotrichum* population dynamics (Chapter 2) and life cycle (Chapter 4) can be very complex in the field. Thus, further studies to examine more than one mode of action and considering realistic (i.e., abide by the law, economical, etc.) tank-mixes and rotations to manage this economically important disease of grape.

Acknowledgements

This research was financially supported by the Virginia Wine Board (VWB, 449036, 449204, and 449338), and Virginia Department of Agriculture and Consumer Services (VDACS, FYY-2015 544). We also thank Akiko Mangan, Amanda Bly, and Vanette Trumm, members of the Grape Pathology lab, for assisting with assay completion.

3.5. References

Altschul, S., Gish, W., Miller, W., Myers, E., & Lipman, D. (1990). Basic local alignment search tool. *Journal of Molecular Biology*, *215*, 403–410.

Amiri, A., Scherm, H., Brannen, P., & Schnabel, G. (2008). Laboratory evaluation of three rapid, agar-based assays to assess fungicide sensitivity in *Monilinia fructicola*. *Plant Disease*, *92*, 415–420.

Bolker, B., Brooks, M., Clark, C., Geange, S., Poulsen, J., Stevens, M., & White, J. (2009). Generalized linear mixed models: a practical guide for ecology and evolution. *Trends in ecology & evolution*, *24*, 127–135.

Chen, S., Luo, C., Hu, M., & Schnabel, G. (2016). Sensitivity of *Colletotrichum* species, including *C. fioriniae* and *C. nymphaeae*, from peach to demethylation inhibitor fungicides. *Plant Disease*, *100*, 2434–2441.

Colcol, J., & Baudoin, A. (2016). Sensitivity of *Erysiphe necator* and *Plasmopara viticola* in Virginia to QoI fungicides, boscalid, quinoxyfen, thiophanate-methyl, and mefenoxam. *Plant Disease*, *100*, 337–344.

Cordova, L., Zuniga, A., Mertely, J., & Peres, N. (2014). Evaluation of products for the control of Botrytis fruit rot in annual strawberry, 2013-14. *Plant Disease Management Reports, 8*, SMF028.

Damm, U., Cannon, P., Woudenberg, J., & Crous, P. (2012). The *Colletotrichum acutatum* species complex. *Studies in Mycology*, *73*, 37–113.

Fairchild, K., Miles, T., & Wharton, P. (2013). Assessing fungicide resistance in populations of *Alternaria* in Idaho potato fields. *Crop Protection*, *49*, 31–39.

Fernández-Ortuño, D., Grabke, A., Bryson, P., Amiri, A., Peres, N., & Schnabel, G. (2014). Fungicide resistance profiles in *Botrytis cinerea* from strawberry fields of seven southern US states. *Plant Disease*, *98*, 825–833.

Fitzell, R. & Peak, C. (1984). The epidemiology of anthracnose disease of mango: inoculum sources, spore production and dispersal. *Annals of Applied Biology*, *104*, 53–59.

FRAC. (2018). FRAC Code List 2018: Fungicides sorted by mode of action. In.: FRAC.

Glattli, A., Grote, T., & Stammler, G. (2005). SDH-Inhibitors: history, biological performance and molecular mode of action. in *Modern fungicides and antifungal compounds IV*, Dehne, H., Deising, H., Gisi, U., Kuck, K., Russell, P., & Lyr, H. eds. Braunschweig, Germany: British Crop Protection Council.

Greer, L., Harper, J., Savocchia, S., Samuelian, S., & Steel, C. (2011). Ripe rot of south-eastern Australian wine grapes is caused by two species of *Colletotrichum*: *C. acutatum* and *C. gloeosporioides* with differences in infection and fungicide sensitivity. *Australian Journal of Grape and Wine Research*, *17*, 123–128.

Halbrent, N., Ngugi, J., & Halbrent J. (2012). Evaluation of fungicides for management of bunch rots on Pinot Noir and Cabernet Franc in PA, 2011. *Plant Disease Management Report*, *6*, SMF027.

Higgins, B. (1926). Anthracnose of pepper (*Capsicum annuum* L.). *Phytopathology*, *16*, 333–345.

Hu, M., Grabke, A., Dowling, M., Holstein, H., & Schnabel, G. (2015)a. Resistance in *Colletotrichum siamense* from peach and blueberry to thiophanate-methyl and azoxystrobin. *Plant Disease*, *99*, 806–814.

Hu, M., Grabke, A., & Schnabel, G. (2015)b. Investigation of the *Colletotrichum gloeosporioides* species complex causing peach anthracnose in South Carolina. *Plant Disease*, *99*, 797–805.

SAS Institute (2012). *SAS/STAT® 9.4 User's Guide*. Cary, North Carolina: SAS Institute Inc.

Ishii, H. (2009). QoI fungicide resistance: current status and the problems associated with DNA-based monitoring. in *Recent Developments in Management of Plant Diseases*: Gisi, U., Chet, I., & Gullino, M. ed. Springer Netherlands, 37–45.

Ishii, H., Zhen, F., Hu, M., Li, X., & Schnabel, G. (2016). Efficacy of SDHI fungicides, including benzovindiflupyr, against *Colletotrichum* species. *Pest Management Science*, *72*, 1844–1853.

Kearse, M., Moir, R., Wilson, A., Stones-Havas, S., Cheung, M., Sturrock, S., Buxton, S., Cooper, A., Markowitz, S., Duran, C., Thierer, T., Ashton, B., Mentjies, P., & Drummond, A. (2012). Geneious Basic: an integrated and extendable desktop software platform for the organization and analysis of sequence data. *Bioinformatics*, *28*, 1647–1649.

Larkin, M., Blackshields, G., Brown, N., Chenna, R., McGettigan, P., McWilliam, H., Valentin, F., Wallace, I., Wilm, A., Lopez, R., Thompson, J., Gibson, T., & Higgins, D. (2007). Clustal W and Clustal X version 2.0. *Bioinformatics*, *23*, 2947–2948.

Lepesheva, G., & Waterman, M. (2007). Sterol 14α-demethylase cytochrome P450 (CYP51), a P450 in all biological kingdoms. *Biochimica et Biophysica Acta -General Subjects*, *1770*, 467–477.

Leroux, P. (1996). Recent developments in the mode of action of fungicides. *Pesticide Science*, *47*, 191–197.

Leroux, P., Gredt, M., Leroch, M., & Walker, A.S. (2010). Exploring mechanisms of resistance to respiratory inhibitors in field strains of *Botrytis cinerea*, the causal agent of gray mold. *Applied and Environmental Microbiology*, *76*, 6615–6630.

Littell, R., Milliken, G., Stroup, W., Wolfinger, R., & Schabenberger, O. 2006. SAS for mixed models. 2nd ed. *Cary, NC: SAS Institute*.

Melksham, K., Weckert, M., & Steel, C. (2002). An unusual bunch rot of grapes in sub-tropical regions of Australia caused by *Colletotrichum acutatum*. *Australasian Plant Pathology*, *31*, 193–194.

Miyamoto, T., Ishii, H., Stammler, G., Koch, A., Ogawara, T., Tomita, Y., Fountaine, J.M., Ushio, S., Seko, T. & Kobori, S. (2010). Distribution and molecular characterization of *Corynespora cassiicola* isolates resistant to boscalid. *Plant Pathology*, *59*, 873–881.

Mondal, S., Bhatia, A., Shilts, T., & Timmer, L. (2005). Baseline sensitivities of fungal pathogens of fruit and foliage of citrus to azoxystrobin, pyraclostrobin and fenbuconazole. *Plant Disease*, *89*, 1186–1194.

Peres, N., Souza, N., Peever, T., & Timmer, L. (2004). Benomyl sensitivity of isolates of *Colletotrichum acutatum* and *C. gloeosporioides* from citrus. *Plant Disease*, *88*, 125–130.

Pfeiffer, D., Baudoin, A., Bergh, J., & Nita, M. (2018). Grapes: diseases and insects in vineyards. in *Pest Management Guide: Horticultural and Forest Crops*. Hong, C., & Day, E. eds. Virginia Cooperative Extension. Pub. 456-017.

Shephard, M. (1987). Screening for Fungicides. *Annual Review of Phytopathology*, *25*, 189–206.

Sierotzki, H., & Scalliet, G. (2013). A review of current knowledge of resistance aspects for the next-generation succinate dehydrogenase inhibitor fungicides. *Phytopathology*, *103*, 880–887.

Smilanick, J., Mansour, M., Gabler, F., Margosan, D., & Hashim-Buckey, J. (2010). Control of postharvest gray mold of table grapes in the San Joaquin Valley of California by fungicides applied during the growing season. *Plant Disease*, *94*, 250–257.

Southworth, E. (1891). Ripe rot of grapes and apples. *The Journal of Mycology*, *6*, 164–173.

Steel, C., Greer, L., & Savocchia, S. (2007). Studies on *Colletotrichum acutatum* and *Greeneria uvicola*: Two fungi associated with bunch rot of grapes in sub-tropical Australia. *Australian Journal of Grape and Wine Research*, *13*, 23–29.

Sutton, T. (2015). Ripe rot. in *Compendium of Grape Diseases, Disorders, and Pests*. Wilcox, W., Gubler, W., & Uyemoto, J. eds. St. Paul, MN: American Phytopathological Society.

Travis, J., Halbrent, N., Lehman, B., & Jarjour, B. (2008). Evaluation of materials for control of grape cluster rots, 2007. *Plant Disease Management Reports, 2,* STF023.

Walter, H. (2011). New fungicides and new modes of action. in *Modern fungicides and antifungal compounds IV*, Dehne, H., Deising, H., Gisi, U., Kuck, K., Russell, P., & Lyr, H. eds. Braunschweig, Germany: British Crop Protection Council.

Wedge, D., Smith, B., Quebedeaux, J., & Constantin, R. (2007). Fungicide management strategies for control of strawberry fruit rot diseases in Louisiana and Mississippi. *Crop Protection*, *26*, 449–1458.

Weir, B., Johnston, P., & Damm, U. (2012). The *Colletotrichum gloeosporioides* species complex. *Studies in Mycology*, *73*, 115–180.

Wood, P., & Hollomon, D. (2003). A critical evaluation of the role of alternative oxidase in the performance of strobilurin and related fungicides acting at the Qo site of Complex III. *Pest management science*, *59*, 499–511.

Von Schmeling, B., & Kulka, M. (1966). Systemic fungicidal activity of 1,4-oxathiin derivates. *Science*, *152*, 659–660.

Xu, X., Lin, T., Yuan, S., Dai, D., Shi, H., Zhang, C., & Wang, H. (2014). Characterization of baseline sensitivity and resistance risk of *Colletotrichum gloeosporioides* complex isolates from strawberry and grape to two demethylation-inhibitor fungicides, prochloraz and tebuconazole. *Australasian Plant Pathology*, *43*, 605–613.

Yin, Y., Kim, Y., & Xiao, C. (2011). Molecular characterization of boscalid resistance in field isolates of *Botrytis cinerea* from apple. *Phytopathology*, *101*, 986–995.

Yoder, K., Cochran II, A., Royston Jr., W., Kilmer, S., & Kowalski, A. (2018). Evaluation of OMRI-approved and conventional products for disease management on three apple cultivars, 2017. *Plant Disease Management Reports*, *12*, PF040.

Table 3.1: Virginia survey representative isolates belonging to the *C. acutatum* and *C. gloeosporioides* species complexes for *in vitro* fungicide amended media testing and *sdh*-fragment sequencing.

Species[a]	Isolate[a]	Origin (County)	VA wine region
C. aenigma	ACPM01A13B	Frederick	Shenandoah
	BAPM01B13B	Nottoway	Central
	GMSB02A13A	Warren	Shenandoah
	PBCH04C13A	Northampton	Eastern Shore
	RMTR02A13B	Mecklenburg	Southern
C. conoides	BANN02A13A	Nottoway	Central
	GCVB02A13A	Rappahannock	Northern
C. fioriniae genotype 1	DEPM01A13B	Nelson	Central
	GMSB02D13A	Warren	Shenandoah
	GWCH03B13B	Halifax	Southern
	LNRG01A13A	Fauquier	Northern
	LNRG01B13A	Fauquier	Northern
	NECH04A13A	Loudoun	Northern
	TACH02A13A	Loudoun	Northern
C. fioriniae genotype 2	BAVR01C13A	Nottoway	Central
	GRVR02C13A	Albemarle	Central
	JRCH02D13B	Hanover	Central
C. fructicola-like genotype 1	AFCH02A13A	Halifax	Southern
	BXVR01C13A	Loudoun	Northern
	GRVR03A13A	Albemarle	Central
	JRCH06A13B	Hanover	Central
C. fructicola-like genotype 2	BXCH01B13A	Loudoun	Northern
	SSTR02C13A	Campbell	Central
C. fructicola-like genotype 3	HNPM01C13A	Orange	Central
	NECH04B13B	Loudoun	Northern
	PKCH01D13A	Albemarle	Central
	SSTR02B13A	Campbell	Central
C. fructicola-like genotype 4	SSVR02D13A	Campbell	Central
C. gloeosporioides sensu stricto	VECH01C13A	Nelson	Central
C. kahawae	GMSB02E13A	Warren	Shenandoah
C. nymphaeae genotype 1	TACH01D13B	Loudoun	Northern
C. nymphaeae genotype 2	TACH03A13A	Loudoun	Northern
	TACH04C13A	Loudoun	Northern

[a] Species identification and isolate name from Chapter 2 from the survey of Virginia vineyards.

[b] Genotypic grouping of *sdh*-fragments from alignment analysis. N/A = the fragment did not amplify. Indiv. = isolate did not genetically match the other tested isolates

Table 3.2: List of fungicide active ingredients tested, including trade name, company and FRAC group.

Active ingredients	Commercial Product	a.i. %	Company		FRAC[a]
azoxystrobin	Abound®	22.9	Syngenta Crop Protection, LLC	Greensboro, NC	11
benzovindiflupyr	Aprovia®	10.3	Syngenta Crop Protection, LLC	Greensboro, NC	7
boscalid	Endura®	70.0	BASF Corporation	Research Triangle Park, NC	7
captan	Captan Gold™ 80 WDG	78.2	Adama USA	Raleigh, NC	M4
copper hydroxide	Champ® Dry Prill	57.6	NuFarm Americas, Inc.	Alsip, IL	M1
copper octanoate	Cueva®	10.0	Certis USA	Columbia, MD	M1
fluopyram	Luna® Privilege	41.5	Bayer CropScience, LP	Research Triangle Park, NC	7
isofetamid	Kenja® 400SC	36.0	Summit Agro USA	Durham, NC	7
mancozeb	Dithane® 75DF Rainshield	75.0	Dow AgroScience	Indianapolis, IN	M3
polyoxin-D	OSO™ 5%SC	5.0	Certis USA	Columbia, MD	19
polyoxin-D	Ph-D®	11.3	Arysta LifeScience Corporation	Cary, NC	19
potassium phosphite	ProPhyt®	54.5	Luxembourg-Pamol Inc	Houston, TX	P07
pyriofenone	Prolivo® 400SC	27.3	Summit Agro USA	Durham, NC	50
tebuconazole	Elite® 45 DF	45.0	Bayer CropScience, LP	Research Triangle Park, NC	3
tetraconazole	Mettle® 125 ME	11.6	Gowan Company, LLC	Yuma, AZ	3
thiophanate-methyl	Topsin® M WSB	70.0	United Phosphorus Inc.	King of Prussia, PA	1

[a] Fungicide Resistance Action Committee (FRAC) codes

Table 3.3: Primers for *sdh* gene PCR amplification and sequencing.

Gene	Product name	Primer	Sequence (5'-3')	Reference
sdh-B	Succinate dehydrogenase subunit B	KES719	CTBCCNCACACCTACGTCGTCAAGGAC	Miyamoto et al. 2010
		KES729	CTTCTTRATCTCVGCRATVGCC	Miyamoto et al. 2010
sdh-C	Succinate dehydrogenase subunit C	CoCF	TGGGCGTGTCGGCCCT	Ishii et al. 2016
		CoCR	TACCACGCAAAGGCCAGGC	Ishii et al. 2016
sdh-D	Succinate dehydrogenase subunit D	CSD2F	CGWCAAGAGTCGCCGCYTTC	Ishii et al. 2016
		CSDR	ACGTCGCTGGTCTCRAACT	Ishii et al. 2016

Table 3.4: Estimated effective concentrations (EC50) for conidia and mycelia of two genotypes of *C. fioriniae*, and two genotypes of *C. nymphaeae* for fifteen fungicide active ingredients (a.i.) determined by an *in vitro* fungicide amended media assay.

		***C. fioriniae* genotype 1**			***C. fioriniae* genotype 2**			***C. nymphaeae* genotype 1**			***C. nymphaeae* genotype 2**		
		Intercept[a]	**Slope[a]**	**EC50[b]**	**Intercept[a]**	**Slope[a]**	**EC50[b]**	**Intercept[a]**	**Slope[a]**	**EC50[b]**	**Intercept[a]**	**Slope[a]**	**EC50[b]**
Conidia	azoxystrobin	1.83	-0.71	> 100.0	3.63	0.00	> 100.0	3.63	0.00	> 100.0	3.63	0.00	> 100.0
	benzovindiflupyr	1.09	15.84	> 100.0	3.63	0.00	> 100.0	1.00	-0.62	> 100.0	3.63	0.00	> 100.0
	boscalid	1.97	-0.46	> 100.0	3.63	0.00	> 100.0	3.63	0.00	> 100.0	3.63	0.00	> 100.0
	captan	27.71	-27.86	9.0	27.54	-27.77	8.2	30.49	-29.19	> 100.0	26.89	-27.46	8.6
	copper hydroxide	3.63	0.00	> 100.0	3.63	0.00	> 100.0	3.63	0.00	> 100.0	3.63	0.00	> 100.0
	copper octanoate	5.81	-2.34	> 100.0	3.63	0.00	> 100.0	3.63	0.00	> 100.0	3.63	0.00	> 100.0
	fluopyram	3.63	0.00	> 100.0	3.63	0.00	> 100.0	3.63	0.00	> 100.0	3.63	0.00	> 100.0
	isofetamid	3.63	0.00	> 100.0	3.63	0.00	> 100.0	3.63	0.00	> 100.0	3.63	0.00	> 100.0
	mancozeb	27.20	-27.61	8.8	18.87	-50.58	3.2	18.87	-50.58	3.2	26.89	-27.46	8.6
	polyoxin-D (OSO)	5.81	-2.34	> 100.0	3.63	0.00	> 100.0	3.63	0.00	> 100.0	3.63	0.00	> 100.0
	polyoxin-D (Ph-D)	3.63	0.00	> 100.0	6.08	-2.64	> 100.0	3.63	0.00	> 100.0	3.63	0.00	> 100.0
	potassium phosphite	3.63	0.00	> 100.0	3.63	0.00	> 100.0	3.63	0.00	> 100.0	3.63	0.00	> 100.0
	pyriofenone	3.63	0.00	> 100.0	3.63	0.00	> 100.0	3.63	0.00	> 100.0	3.63	0.00	> 100.0
	tetraconazole	3.73	-2.51	> 100.0	8.44	-4.90	87.8	3.63	0.00	> 100.0	3.63	0.00	> 100.0
	thiophanate-methyl	1.73	-0.52	> 100.0	1.60	-0.93	> 100.0	3.63	0.00	> 100.0	3.63	0.00	> 100.0
Mycelia	azoxystrobin	5.81	-2.34	> 100.0	3.63	0.00	> 100.0	3.63	0.00	> 100.0	3.63	0.00	> 100.0
	benzovindiflupyr	3.63	0.00	> 100.0	3.63	0.00	> 100.0	3.63	0.00	> 100.0	3.63	0.00	> 100.0
	boscalid	3.63	0.00	> 100.0	3.63	0.00	> 100.0	3.63	0.00	> 100.0	3.63	0.00	> 100.0
	captan	7.41	-3.91	98.9	1.71	-0.55	> 100.0	6.83	-3.36	> 100.0	6.83	-3.36	> 100.0
	copper hydroxide	3.63	0.00	> 100.0	3.63	0.00	> 100.0	3.63	0.00	> 100.0	3.63	0.00	> 100.0
	copper octanoate	3.63	0.00	> 100.0	6.08	-2.64	> 100.0	3.63	0.00	> 100.0	3.63	0.00	> 100.0
	fluopyram	3.63	0.00	> 100.0	1.19	1.29	> 100.0	3.63	0.00	> 100.0	3.63	0.00	> 100.0
	isofetamid	3.63	0.00	> 100.0	3.63	0.00	> 100.0	3.63	0.00	> 100.0	3.63	0.00	> 100.0
	mancozeb	8.63	-5.08	85.8	7.51	-4.01	97.6	6.83	-3.36	> 100.0	6.83	-3.36	> 100.0
	polyoxin-D (OSO)	3.63	0.00	> 100.0	3.63	0.00	> 100.0	3.63	0.00	> 100.0	3.63	0.00	> 100.0
	polyoxin-D (Ph-D)	3.63	0.00	> 100.0	3.63	0.00	> 100.0	3.63	0.00	> 100.0	3.63	0.00	> 100.0
	potassium phosphite	3.63	0.00	> 100.0	3.63	0.00	> 100.0	3.63	0.00	> 100.0	3.63	0.00	> 100.0
	pyriofenone	3.63	0.00	> 100.0	3.63	0.00	> 100.0	3.63	0.00	> 100.0	3.63	0.00	> 100.0
	tetraconazole	7.41	-3.91	98.9	7.51	-4.01	97.6	3.63	0.00	> 100.0	3.63	0.00	> 100.0
	thiophanate-methyl	7.41	-3.91	> 100.0	3.63	0.00	> 100.0	3.63	0.00	> 100.0	3.63	0.00	> 100.0

[a] Intercept and slope parameters of the non-linear mixed model with the complementary log-log link function.

[b] The effective concentration that suppresses 50% of growth of mycelia or germination of conidia (EC50) in µg/mL.

Table 3.5: Estimated effective concentrations (EC50) for conidia and mycelia of *C. aenigma*, *C. conoides*, *C. gloeosporioides sensu stricto*, and *C. kahawae* for fifteen fungicide active ingredients (a.i.) determined by an *in vitro* fungicide amended media assay.

		C. aenigma			***C. conoides***			***C. gloeosporioides sensu stricto***			***C. kahawae***		
		Intercept[a]	**Slope[a]**	**EC50[b]**	**Intercept[a]**	**Slope[a]**	**EC50[b]**	**Intercept[a]**	**Slope[a]**	**EC50[b]**	**Intercept[a]**	**Slope[a]**	**EC50[b]**
Conidia	azoxystrobin	3.63	0.00	> 100.0	3.63	0.00	> 100.0	3.63	0.00	> 100.0	3.63	0.00	> 100.0
	benzovindiflupyr	1.66	-0.65	> 100.0	3.63	0.00	> 100.0	3.63	0.00	> 100.0	3.63	0.00	> 100.0
	boscalid	3.63	0.00	> 100.0	3.63	0.00	> 100.0	3.63	0.00	> 100.0	3.63	0.00	> 100.0
	captan	1.85	-2.26	10.9	29.60	-28.78	10.0	44.16	-38.88	30.0	28.52	-28.25	9.4
	copper hydroxide	3.63	0.00	> 100.0	1.60	-0.93	> 100.0	3.63	0.00	> 100.0	3.63	0.00	> 100.0
	copper octanoate	3.63	0.00	> 100.0	3.63	0.00	> 100.0	3.63	0.00	> 100.0	3.63	0.00	> 100.0
	fluopyram	3.63	0.00	> 100.0	3.63	0.00	> 100.0	3.63	0.00	> 100.0	3.63	0.00	> 100.0
	isofetamid	6.03	-2.55	> 100.0	3.63	0.00	> 100.0	3.63	0.00	> 100.0	3.63	0.00	> 100.0
	mancozeb	0.97	-3.91	1.6	1.53	-3.64	3.3	30.49	-29.19	10.6	44.16	-38.88	9.6
	polyoxin-D (OSO)	3.63	0.00	> 100.0	3.63	0.00	> 100.0	3.63	0.00	> 100.0	3.63	0.00	> 100.0
	polyoxin-D (Ph-D)	6.03	-2.55	> 100.0	6.30	-2.85	> 100.0	3.63	0.00	> 100.0	3.63	0.00	> 100.0
	potassium phosphite	3.63	0.00	> 100.0	3.63	0.00	> 100.0	3.63	0.00	> 100.0	3.63	0.00	> 100.0
	pyriofenone	6.30	-2.85	> 100.0	3.63	0.00	> 100.0	3.63	0.00	> 100.0	3.63	0.00	> 100.0
	tetraconazole	2.12	-1.40	> 100.0	6.83	-3.36	> 100.0	3.63	0.00	> 100.0	3.63	0.00	> 100.0
	thiophanate-methyl	1.97	-1.77	> 100.0	1.99	-1.22	> 100.0	18.87	-50.58	> 100.0	3.63	0.00	> 100.0
Mycelia	azoxystrobin	3.63	0.00	> 100.0	6.83	-3.36	> 100.0	3.63	0.00	> 100.0	3.63	0.00	> 100.0
	benzovindiflupyr	1.84	-0.68	> 100.0	3.63	0.00	> 100.0	3.63	0.00	> 100.0	3.63	0.00	> 100.0
	boscalid	3.63	0.00	> 100.0	3.63	0.00	> 100.0	3.63	0.00	> 100.0	3.63	0.00	> 100.0
	captan	2.58	-1.60	76.0	1.99	-1.22	87.5	44.16	-38.88	30.0	28.52	-28.25	9.4
	copper hydroxide	6.03	-2.55	> 100.0	3.63	0.00	> 100.0	3.63	0.00	> 100.0	3.63	0.00	> 100.0
	copper octanoate	3.63	0.00	> 100.0	3.63	0.00	> 100.0	3.63	0.00	> 100.0	3.63	0.00	> 100.0
	fluopyram	3.63	0.00	> 100.0	3.63	0.00	> 100.0	3.63	0.00	> 100.0	3.63	0.00	> 100.0
	isofetamid	3.63	0.00	> 100.0	3.63	0.00	> 100.0	3.63	0.00	> 100.0	3.63	0.00	> 100.0
	mancozeb	0.78	-1.43	7.3	2.31	-1.62	53.1	30.49	-29.19	10.6	44.16	-38.88	9.6
	polyoxin-D (OSO)	3.63	0.00	> 100.0	3.63	0.00	> 100.0	3.63	0.00	> 100.0	3.63	0.00	> 100.0
	polyoxin-D (Ph-D)	3.63	0.00	> 100.0	3.63	0.00	> 100.0	3.63	0.00	> 100.0	3.63	0.00	> 100.0
	potassium phosphite	3.63	0.00	> 100.0	3.63	0.00	> 100.0	3.63	0.00	> 100.0	3.63	0.00	> 100.0
	pyriofenone	3.63	0.00	> 100.0	3.63	0.00	> 100.0	3.63	0.00	> 100.0	3.63	0.00	> 100.0
	tetraconazole	6.58	-3.12	> 100.0	6.30	-2.85	> 100.0	3.63	0.00	> 100.0	3.63	0.00	> 100.0
	thiophanate-methyl	1.84	-1.87	19.2	6.83	-3.36	> 100.0	18.87	-50.58	3.2	3.63	0.00	> 100.0

[a] Intercept and slope parameters of the non-linear mixed model with the complementary log-log link function.

[b] The effective concentration that suppresses 50% of growth of mycelia or germination of conidia (EC50) in µg/mL

Table 3.6: Estimated effective concentrations (EC50) for conidia and mycelia of 4 genotypes of *C. fructicola*-like isolates for fifteen fungicide active ingredients (a.i.) determined by an *in vitro* fungicide amended media assay.

		***C. fructicola*-like genotype 1**			***C. fructicola*-like genotype 2**			***C. fructicola*-like genotype 3**			***C. fructicola*-like genotype 4**		
		Intercept[a]	**Slope[a]**	**EC50[b]**	**Intercept[a]**	**Slope[a]**	**EC50[b]**	**Intercept[a]**	**Slope[a]**	**EC50[b]**	**Intercept[a]**	**Slope[a]**	**EC50[b]**
Conidia	azoxystrobin	3.63	0.00	> 100.0	3.63	0.00	> 100.0	3.63	0.00	> 100.0	3.63	0.00	> 100.0
	benzovindiflupyr	7.33	-3.84	100.0	3.63	0.00	> 100.0	6.30	-2.85	> 100.0	3.63	0.00	> 100.0
	boscalid	3.63	0.00	> 100.0	3.63	0.00	> 100.0	3.63	0.00	> 100.0	3.63	0.00	> 100.0
	captan	29.60	-28.78	10.00	18.87	-50.58	> 100.0	29.09	-28.52	> 100.0	3.63	0.00	> 100.0
	copper hydroxide	3.63	0.00	> 100.0	3.63	0.00	> 100.0	3.63	0.00	> 100.0	3.63	0.00	> 100.0
	copper octanoate	3.63	0.00	> 100.0	3.63	0.00	> 100.0	3.63	0.00	> 100.0	3.63	0.00	> 100.0
	fluopyram	3.63	0.00	> 100.0	3.63	0.00	> 100.0	3.63	0.00	> 100.0	3.63	0.00	> 100.0
	isofetamid	3.63	0.00	> 100.0	3.63	0.00	> 100.0	6.03	-2.55	> 100.0	3.63	0.00	> 100.0
	mancozeb	26.89	-27.46	8.6	12.21	-38.63	1.1	25.38	-26.72	7.9	44.16	-38.88	30.0
	polyoxin-D (OSO)	3.63	0.00	> 100.0	3.63	0.00	> 100.0	3.63	0.00	> 100.0	3.63	0.00	> 100.0
	polyoxin-D (Ph-D)	3.63	0.00	> 100.0	6.03	-2.55	> 100.0	3.63	0.00	> 100.0	3.63	0.00	> 100.0
	potassium phosphite	3.63	0.00	> 100.0	3.63	0.00	> 100.0	3.63	0.00	> 100.0	3.63	0.00	> 100.0
	pyriofenone	3.63	0.00	> 100.0	3.63	0.00	> 100.0	3.63	0.00	> 100.0	3.63	0.00	> 100.0
	tetraconazole	3.63	0.00	> 100.0	6.58	-3.12	> 100.0	3.63	0.00	> 100.0	3.63	0.00	> 100.0
	thiophanate-methyl	1.73	-1.20	> 100.0	1.54	-0.81	> 100.0	1.44	-0.88	> 100.0	6.83	-3.36	> 100.0
Mycelia	azoxystrobin	1.50	-0.29	> 100.0	3.63	0.00	> 100.0	3.63	0.00	> 100.0	3.63	0.00	> 100.0
	benzovindiflupyr	3.63	0.00	> 100.0	1.38	0.17	> 100.0	3.63	0.00	> 100.0	3.63	0.00	> 100.0
	boscalid	3.63	0.00	> 100.0	3.63	0.00	> 100.0	3.63	0.00	> 100.0	3.63	0.00	> 100.0
	captan	7.33	-3.84	> 100.0	2.12	-1.40	> 100.0	1.99	-1.22	> 100.0	3.63	0.00	> 100.0
	copper hydroxide	3.63	0.00	> 100.0	3.63	0.00	> 100.0	3.63	0.00	> 100.0	3.63	0.00	> 100.0
	copper octanoate	3.63	0.00	> 100.0	6.03	-2.55	> 100.0	6.03	-2.55	> 100.0	3.63	0.00	> 100.0
	fluopyram	3.63	0.00	> 100.0	3.63	0.00	> 100.0	3.63	0.00	> 100.0	3.63	0.00	> 100.0
	isofetamid	3.63	0.00	> 100.0	3.63	0.00	> 100.0	3.63	0.00	> 100.0	3.63	0.00	> 100.0
	mancozeb	1.92	-1.53	39.5	30.49	-29.19	10.6	2.43	-2.59	13.2	44.16	-38.88	30.0
	polyoxin-D (OSO)	3.63	0.00	> 100.0	3.63	0.00	> 100.0	3.63	0.00	> 100.0	3.63	0.00	> 100.0
	polyoxin-D (Ph-D)	3.63	0.00	> 100.0	3.63	0.00	> 100.0	3.63	0.00	> 100.0	3.63	0.00	> 100.0
	potassium phosphite	3.63	0.00	> 100.0	3.63	0.00	> 100.0	3.63	0.00	> 100.0	3.63	0.00	> 100.0
	pyriofenone	3.63	0.00	> 100.0	3.63	0.00	> 100.0	3.63	0.00	> 100.0	3.63	0.00	> 100.0
	tetraconazole	3.63	0.00	> 100.0	3.63	0.00	> 100.0	3.63	0.00	> 100.0	3.63	0.00	> 100.0
	thiophanate-methyl	3.63	0.00	> 100.0	1.21	-0.57	4.5	1.12	-0.62	> 100.0	6.83	-3.36	> 100.0

[a] Intercept and slope parameters of the non-linear mixed model with the complementary log-log link function.

[b] The effective concentration that suppresses 50% of growth of mycelia or germination of conidia (EC50) in µg/mL.

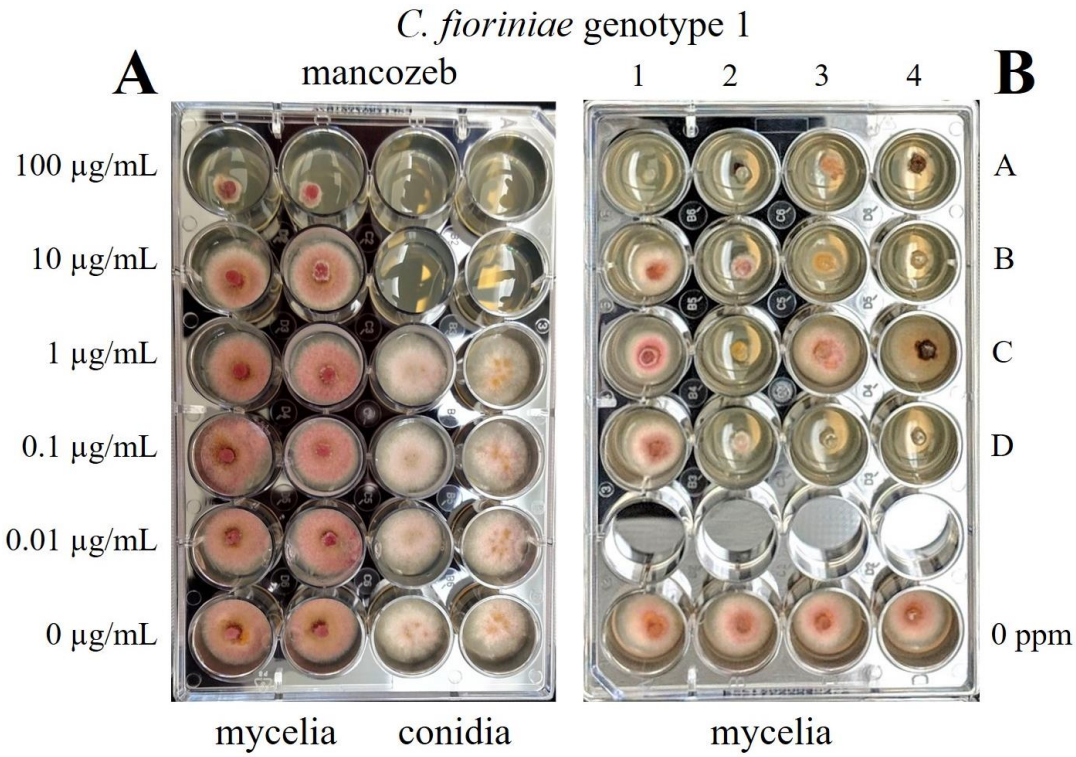

Figure 3.1: Layout of single active ingredient (a.i.) [A] and two a.i. [B] fungicide assay plate layouts. Panel A consists of a dilution of mancozeb (0 to 100) with agar plugs for mycelia in the left two columns of wells, and a conidial suspension in the right two columns of wells. Each well in the panel B plate contains a different combination of two active ingredients: A1 – copper octanoate + tebuconazole, A2 – captan+ tebuconazole, A3 – benzovindiflupyr + tebuconazole, A4 – azoxystrobin + tebuconazole, B1 – thiophanate-methyl + tebuconazole, B2 – potassium phosphite + tebuconazole, B3 – polyoxin-D + tebuconazole, and B4 – mancozeb + tebuconazole, C1 – copper octanoate + thiophanate-methyl, C2 – captan + thiophanate-methyl, C3 – benzovindiflupyr + thiophanate-methyl, C4 – azoxystrobin + thiophanate-methyl, D1 – tebuconazole + thiophanate-methyl, D2 – potassium phosphite + thiophanate-methyl, D3 – polyoxin-D + thiophanate-methyl, and D4 – mancozeb + thiophanate-methyl. The bottom row contains no fungicides.

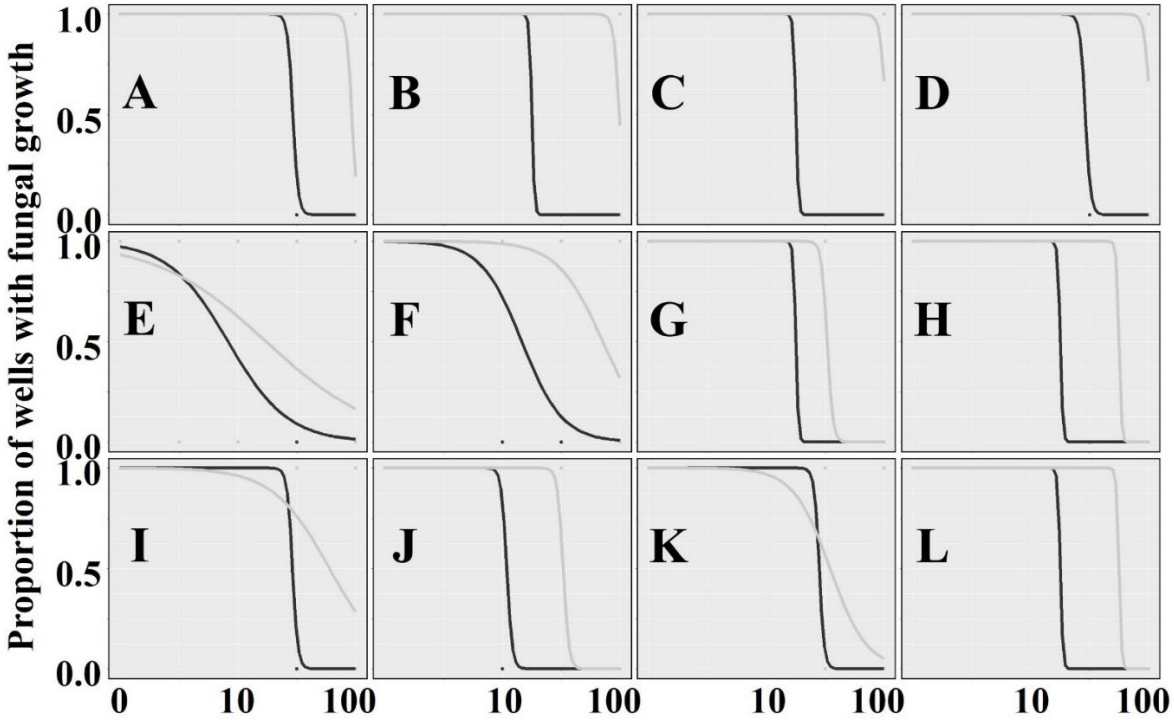

Figure 3.2: Percentage of wells with inhibition of fungal activity in mancozeb (0.0 to 100 µg/mL) from the single a.i. plate assay for twelve *Colletotrichum* species and species genotypes. Each graph represents a species or species genotype; *C. fioriniae* genotype 1 [A] and 2 [B], *C. nymphaeae* genotype 1 [C] and 2 [D], *C. aenigma* [E], *C. conoides* [F], *C. gloeosporioides*[G], *C. kahawae* [H] and *C. fructicola*-like genotype 1 [I], 2 [J], 3 [K], and 4 [L]. The black dots represent the mean proportion of wells with inhibition of conidial germination, and the gray dots and represent wells with inhibition of mycelial expansion. The black and gray lines represent the curvature of the concentration that effectively suppresses 50% of growth (EC50) using the intercept and slope using the best-fit link function obtained from PROC NLMIXED (SAS Studio, ver. 3.7).

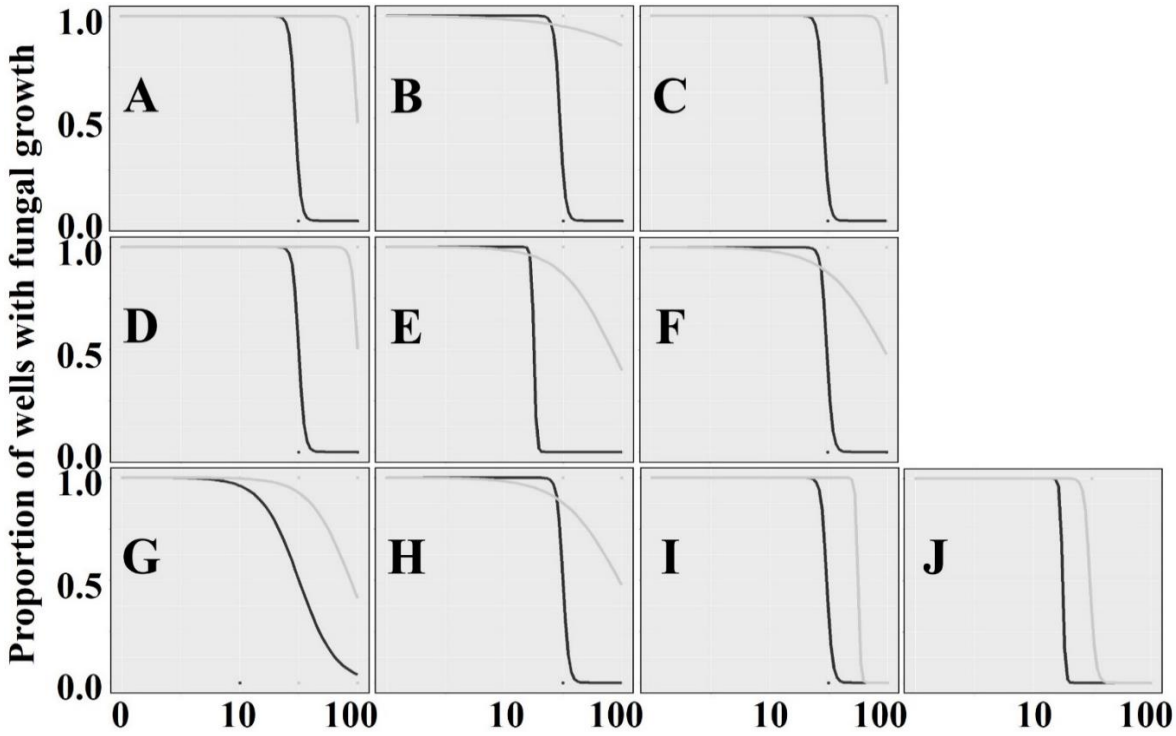

Figure 3.3: Percentage of wells with inhibition of fungal activity in captan (0.0 to 100 µg/mL) from the single a.i. plate assay for ten *Colletotrichum* species and species genotypes. Each graph represents a species or species genotype; *C. fioriniae* genotype 1 [A] and 2 [B], *C. nymphaeae* genotype 2 [C], *C. fructicola*-like genotype 1 [D], 2 [E], and 3 [F], *C. aenigma* [G], *C. conoides* [H], *C. gloeosporioides*[I], and *C. kahawae* [J]. The black dots represent the mean proportion of wells with inhibition of conidial germination, and the gray dots and represent wells with inhibition of mycelial expansion. The black and gray lines represent the curvature of the concentration that effectively suppresses 50% of growth (EC50) using the intercept and slope using the best-fit link function obtained from PROC NLMIXED (SAS Studio, ver. 3.7).

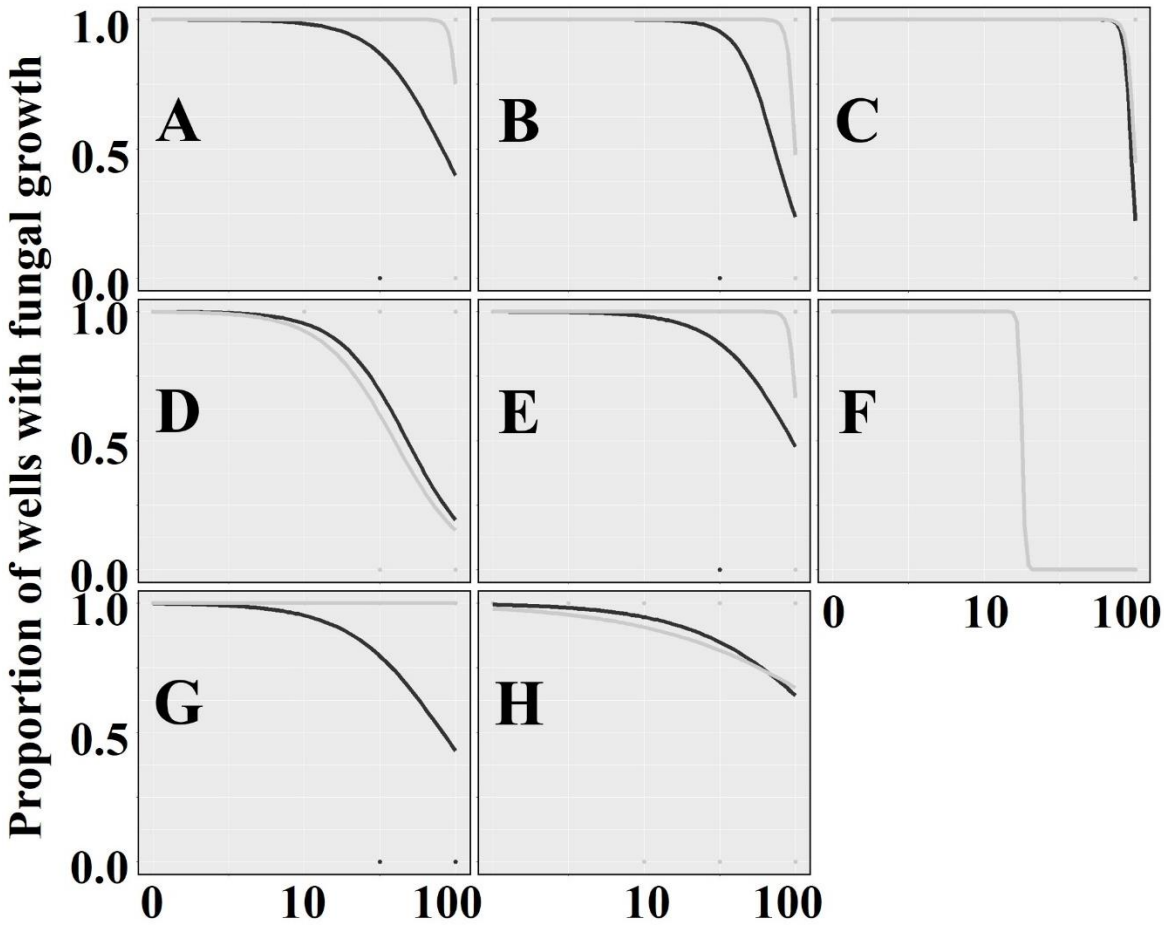

Figure 3.4: Percentage of wells with inhibition of fungal activity to tetraconazole [A-C] and thiophanate-methyl [D-H] (0.0 to 100 µg/mL) from the single a.i. plate assay for *Colletotrichum* species and species genotypes. Each graph represents a species or species genotype; *C. aenigma* [A], *C. fioriniae* genotype 1 [B] and 2 [C], in tetraconazole, and *C. aenigma* [D], *C. conoides* [E], *C. gloeosporioides*[F], *and C. fructicola*-like genotype 1 [G] and 2 [H] in thiophanate-methyl. The black dots represent the mean proportion of wells with inhibition of conidial germination, and the gray dots and represent wells with inhibition of mycelial expansion. The black and gray lines represent the curvature of the concentration that effectively suppresses 50% of growth (EC50) using the intercept and slope using the best-fit link function obtained from PROC NLMIXED (SAS Studio, ver. 3.7).

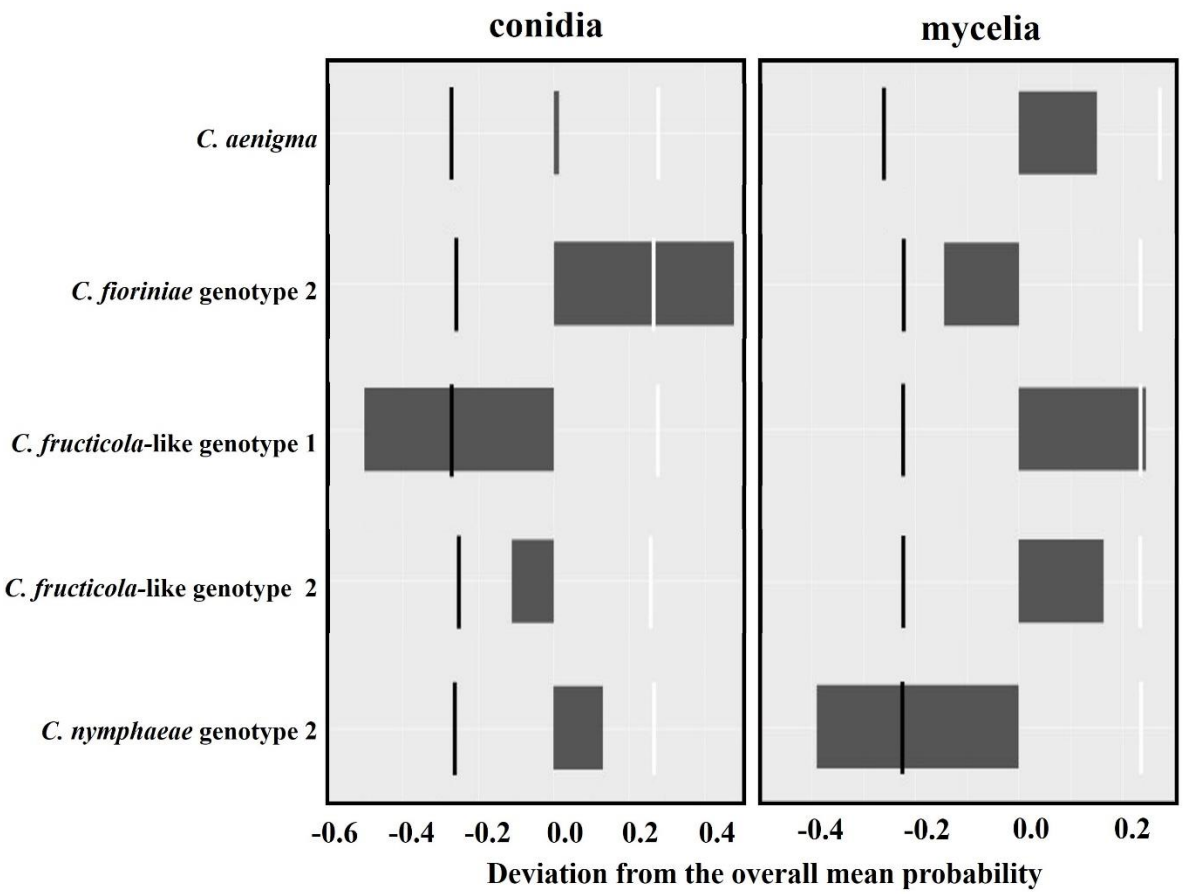

Figure 3.5: Analysis of means plot on the effect of species on the probability of successful growth in the two a.i. amended media assay. The mean value that deviate from the overall mean (set at 0 in the figure), and lower than the 95% confidence interval (i.e., left hand side of the black vertical line below 0) indicates that species had significantly lower probability of successful growth than the overall mean across all species. Two inoculum types, conidia [A] and mycelia [B], are shown.

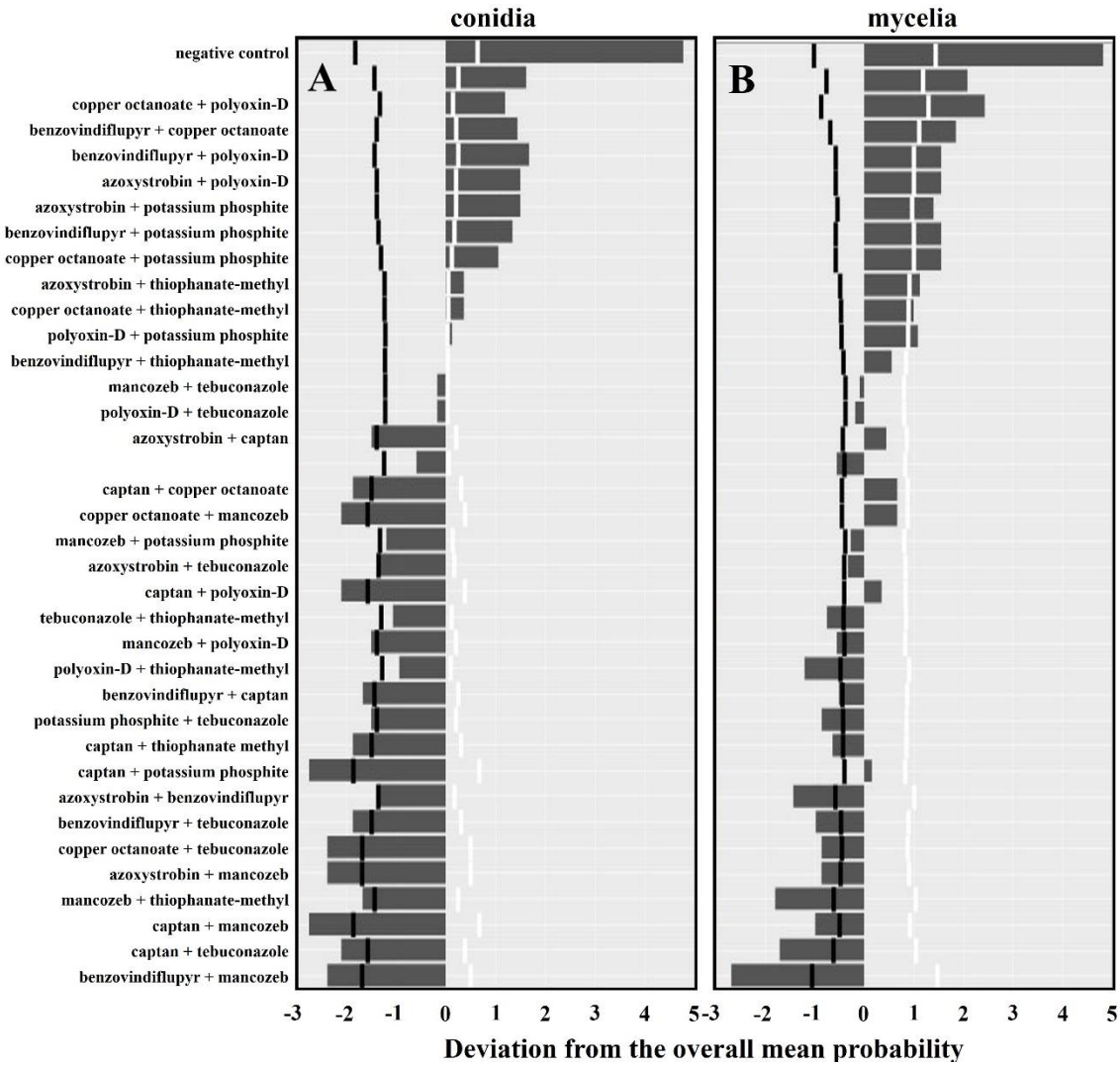

Figure 3.6: Analysis of means plot on the effect of two a.i. combination on the probability of successful growth. The mean probability value (all *Colletotrichum* species combined) that deviate from the overall mean (set at 0 in the figure), and lower than the 95% confidence interval (i.e., left hand side of the vertical line below 0) indicates that species had significantly lower probability of successful growth than the overall mean across all species. The response of the two inoculum types, conidia [A] and mycelia [B], are represented separately.

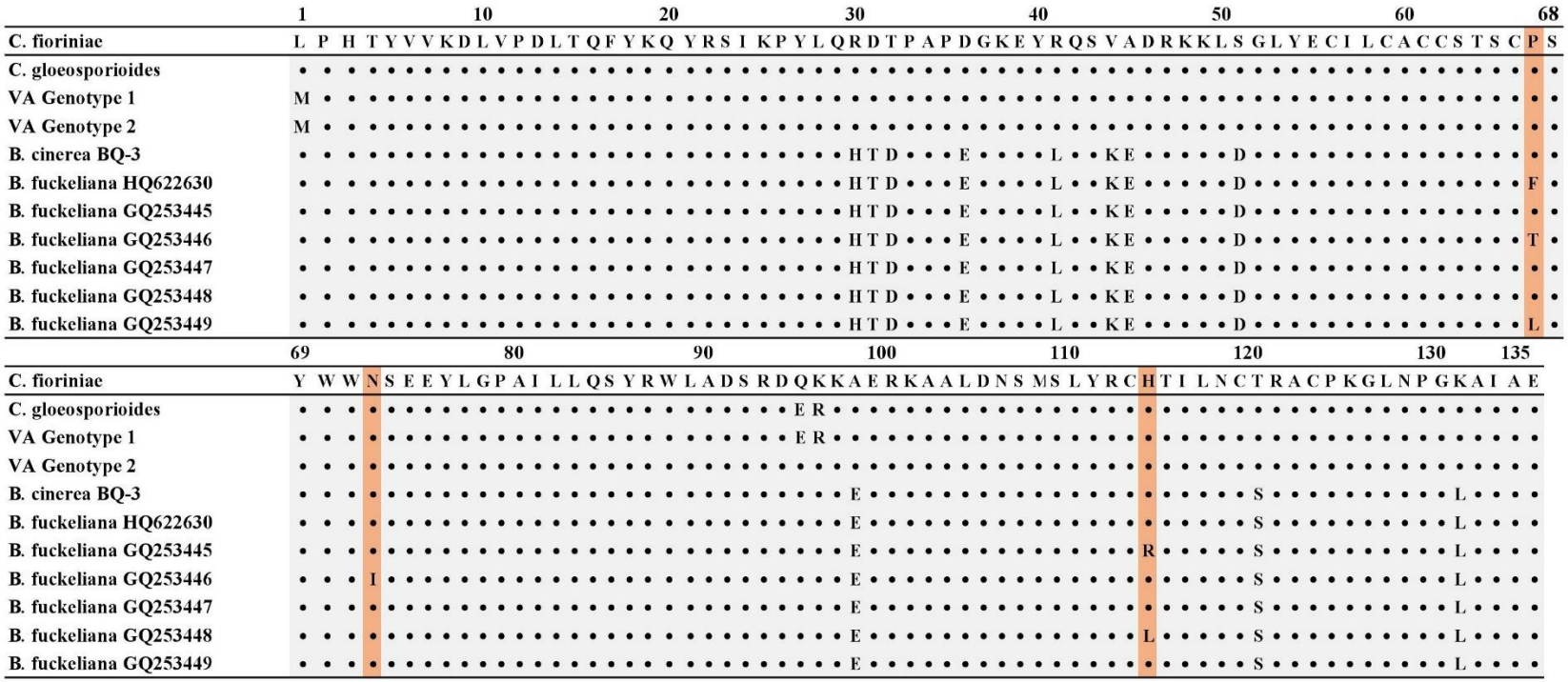

Figure 3.7: Alignment of *sdh*-B protein sequences from the selected VA tested isolates, two *Colletotrichum* GenBank sequences; *C. gloeosporioides* XM 007276209, and *C. acutatum* XM 00759612 (Ishii et al. 2016), one sensitive isolate; *B. cinerea* BQ-3 KR866382, and six SDHI resistant *B. fuckeliana*; GenBank accessions HQ622630, GQ253445, GQ253446, GQ253447, GQ253448, and GQ253449 (Leroux et al. 2010, Yin et al. 2011). Each SDHI-resistant accession corresponds to a different resistance mutation; HQ622630 with P225F, GQ253445 with H272R, GQ253446 with P225F, GQ253447 with N230I, GQ253448 with H272L, and GQ253449 with P225L. Mutation locations are highlighted in orange. Dots represent exact letter matches to the *C. acutatum* XM 00759612 reference sequence.

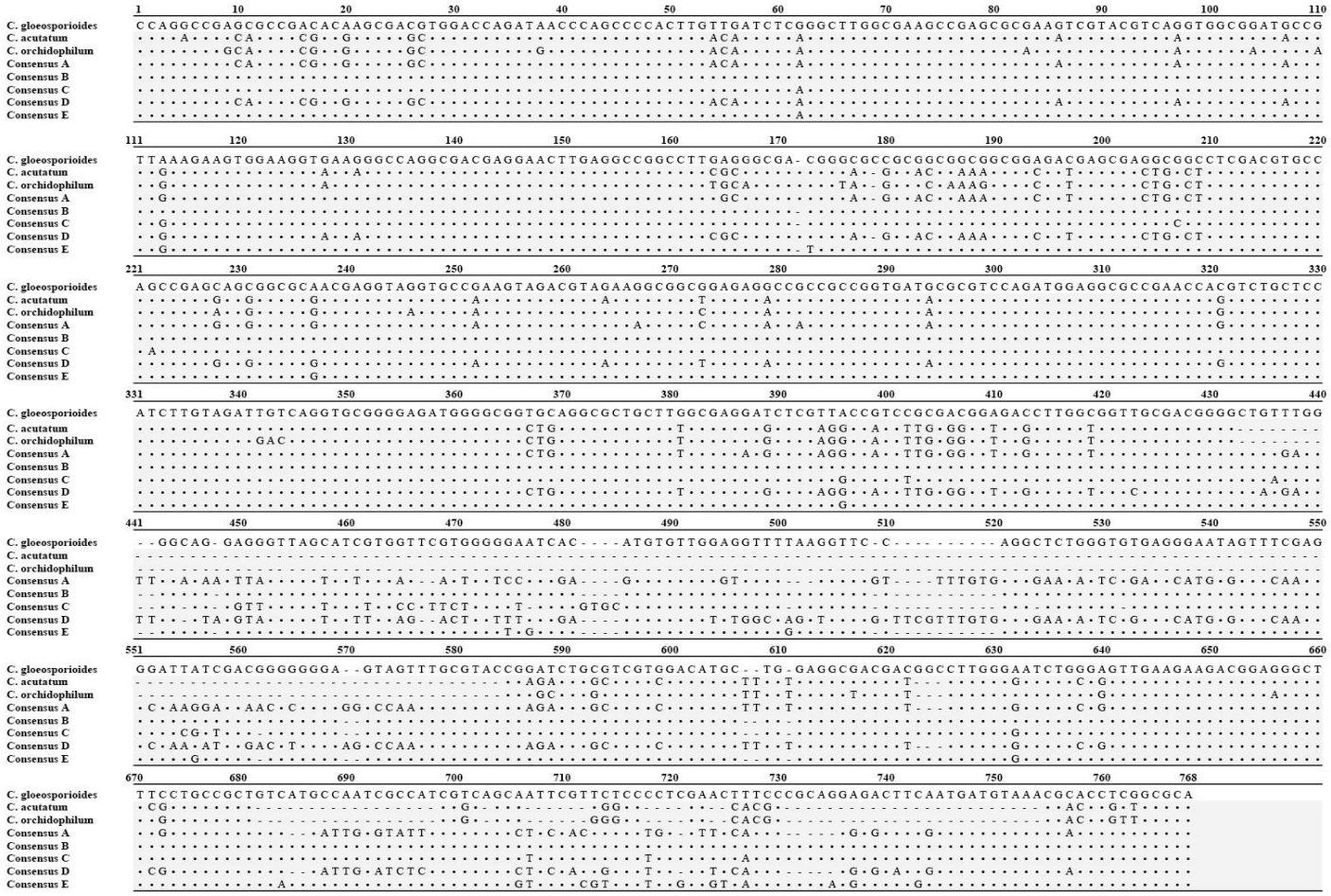

Figure 3.8: Alignment of *sdh*-C consensus sequences from the selected VA tested isolates and three *Colletotrichum* GenBank reference sequences; *C. gloeosporioides* CSLL11 KU873022, *C. acutatum* HHBY48 XM 00759612, and *C. orchidophilum* CORC01 02719 XM 022614369. Dots represent exact letter matches to the *C. gloeosporioides* CSLL11 KU873022 reference sequence. Dashes correspond to alignment gaps.

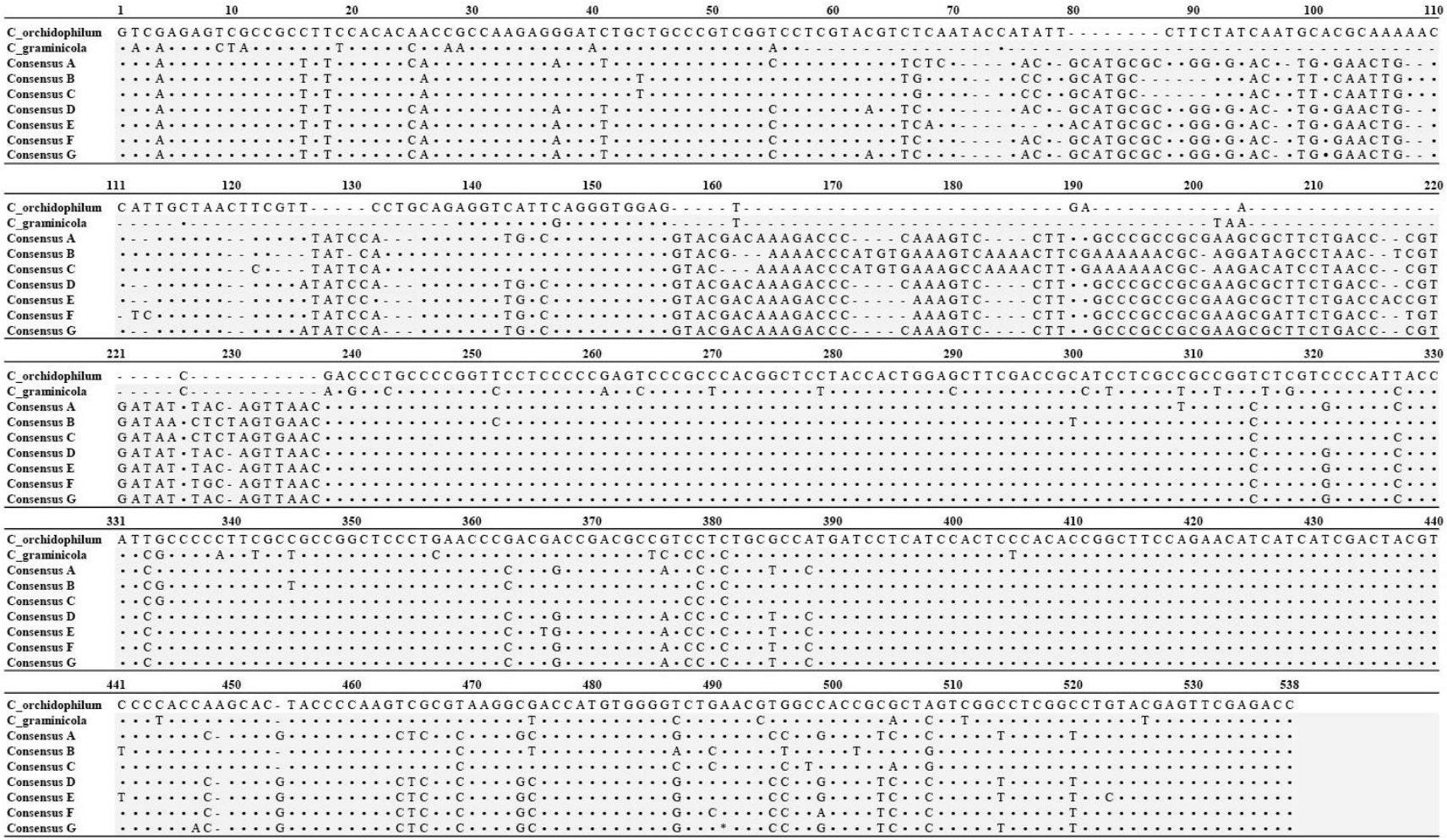

Figure 3.9: Alignment of *sdh*-D consensus sequences from the selected VA tested isolates and two *Colletotrichum* GenBank reference sequences; *C. orchidophilum* CORC01 11017 XM 022622644, and *C. graminicola* M1.001 XM 008091315. Dots represent exact letter matches to the *C. orchidophilum* CORC01 11017 XM 022622644 reference sequence. Dashes correspond to alignment gaps.

Chapter 4.

Potential survival phases of *Colletotrichum* species in three wine grape tissues

Abstract

Ripe rot of grape in VA is mainly caused by the four separate *Colletotrichum* species: *Colletotrichum fioriniae, C. nymphaeae* [*C. acutatum* complex], *C. aenigma,* and two genotypes of *C. fructicola*-like isolates [*C. gloeosporioides* complex]. The disease cycle of grape ripe rot is missing information on the sources of initial inoculum and latency survival during the growing season. The objectives of my study were to investigate the susceptibility of three grapevine tissues, canes, clusters, and leaves, to four *Colletotrichum* species and observe potential infection structures before and after the application of fungicides. In my studies, I observed germination and production of melanized appressoria by *C. fioriniae* on leaves. I also observed conidial germination, mycelial extension, and mycelial mat formation by each of the tested *Colletotrichum* species on blooms, pea-size berries, and berries at veraison. Appressorium formation on blooms was observed for *C. fructicola*-like genotypes 1 and 3, and *C. nymphaeae,* and secondary conidiation on blooms was observed for *C. aenigma*, *C. fructicola*-like genotype 3, and *C. nymphaeae*. This is the first report of infection structure formation by *C. fioriniae* on grape leaves, by *C. aenigma*, *C. fructicola*-like isolates, and *C. nymphaeae* on blooms, and mycelial extension of all five species at three phenological stages of wine grape.

4.1. Introduction

Colletotrichum acutatum and *C. gloeosporioides* are considered cosmopolitan pathogens (Dean et al. 2012), with a wide range of hosts including apple (Southworth 1891), strawberry (Freeman 2008; Xiao et al. 2004), pepper (Higgins 1923), and grape (Greer et. al 2011). Though generally referred to as anthracnose pathogens, these fungi are known as ripe rot on grapes (Greer et. al 2011). *Colletotrichum* species prefer humid, temperate climates, such as the Mid-Atlantic USA (Bailey & Jeger 1992). In Virginia (VA), which is part of the Mid-Atlantic USA, *Colletotrichum* species are considered to be endemic and have been reported on apple since the late 1800s (Southworth 1891). Ripe rot of grape in VA has been found to be mainly caused by the five separate species *Colletotrichum fioriniae, C. nymphaeae* [*C. acutatum* complex], *C. aenigma,* and two genotypes of *C. fructicola*-like isolates [*C. gloeosporioides* complex] (Chapter 2; Damm et al. 2012; Weir et al. 2012).

Wine grape cluster infection can occur anytime between bloom and harvest (Oliver, 2016); however, symptoms will not appear until after veraison, when fruits begin to change color. Additionally, *Colletotrichum* species cause identical symptoms on mature grape berries (Chapter 2; Kummuang et al. 1996a; Kummuang et al. 1996b). Symptoms begin as tan lesions that can be easily mistaken for sunburn on white-fruited cultivars. As the symptoms progress on white-fruited cultivars, the tan lesion spreads over the berry and concentric rings of acervuli with salmon-colored conidia begin to appear. Symptoms are less apparent on red-fruited cultivars and acervuli formation is generally the first observable symptom. Over time, symptomatic fruits of both red- and white-fruited cultivars will shrivel and become a soft, raisin-like rot.

The disease cycle of grape ripe rot is not well described. Particularly, the disease cycle is missing information on the source of inoculum. There are several months between the formation

of symptoms on berries and infection at bloom. For example, the initial sources of strawberry anthracnose inoculum can be infected transplants or remnants of infected tissues from the previous season (Maas 1998). With blueberry anthracnose, the primary inoculum source is overwintering conidia in dormant buds (Wharton & Dieguez-Uribeondo, 2004). This allows conidia to be spread by water splash to new tissues such as, leaf, blooms, and immature fruit, and to neighboring healthy plants after the season begins (Maas 1998; Wharton & Dieguez-Uribeondo, 2004).

Colletotrichum species are known for the ability to form asymptomatic and latent infections. Previous studies have found asymptomatic infections on strawberry, apple, and sweet cherry leaves (Borve et al. 2010; Borve & Stensvand 2017; Leandro et al. 2003). Additionally, grape ripe rot is known to infect wine and muscadine grapes at bloom, without symptoms appearing until the fruit begins to mature (Daykin & Milholland 1984; Greer et al. 2014; Oliver 2016), but there is limited information on how they behave between the initial infection to the time of symptom development.

Since these fungi were considered to be minor pathogens in wine grape, chemical controls are still limited. Currently, the active ingredients suggested for application in the state of VA are ethylene-bis-dithiocarbamates, such as mancozeb (Fungicide Resistance Action Committee code (FRAC) M3), phthalimides, such as captan (FRAC M4), and quinone outside inhibitors, such as azoxystrobin (FRAC 11). Each of these materials have shortcomings as *Colletotrichum* species controls. In the case of mancozeb, the pre-harvest interval, or amount of time between application and harvest, is a minimum of 66 days. This means that the material cannot be applied when the symptoms appear at the end of the season. Additionally, *Colletotrichum gloeosporioides* captan insensitivity has been reported (Greer et al. 2011) as well

as *Colletotrichum* species resistance to quinone outside inhibitors (Forcelini et al. 2016; Hu et al. 2015). Therefore, additional options for chemical control are required.

The objectives of this study were to investigate 1) initial infection stages of *Colletotrichum* species on grape leaf, flowers, and young berries, 2) the effect of fungicide on flower infection, and 3) capability of *Colletotrichum* species to infect woody grape tissues as a potential means of winter survival.

4.2. Materials and methods

4.2.1 Fungal isolate preparation

A representative isolate of each of the four commonly found species in VA vineyards were selected; BAVR01C13A (*C. fioriniae*), GRVR03A13A (*C. fructicola*-like genotype 1), PBCH04C13A (*C. aenigma*), PKCH01D13A (*C. fructicola*-like genotype 3), and TACH03A13A (*C. nymphaeae*) (Chapter 2). Cultures were maintained as dry-agar plugs as described in Chapter 3. The isolates were revived for experimentation by placing dried agar plugs into sterile potato dextrose broth (BD Difco™, Becton, Dickinson and Company, Franklin Lakes, NJ) in 15 mL conical tubes. Broth cultures were placed in an incubator (Precision™ 818, Thermo Scientific Inc, Waltham, MA) on a benchtop rocker (BenchRocker™ 3D, Benchmark Scientific, Edison, NJ) at 25 °C with a diurnal light cycle (12 h light /12 h dark). After 4 days, mycelia were pulled from the tubes and grown on antibiotic amended [streptomycin and chloramphenicol (100 mg/mL each)] quarter strength potato dextrose agar (amended-¼ PDA) (Acumedia®, Neogen Company Lansing, MI) for 14 days. Cultures were grown for 7-14 days at 25 °C with a diurnal light cycle (12 h light /12 h dark) before use. In order to harvest conidia, plates were flooded with 2 mL sterile distilled water and rubbed with a glass rod to suspend conidia. The suspension

was filtered through two layers of autoclaved Miracloth (EMD Millipore, Germany) to remove mycelia. The conidial suspension was then adjusted $5x10^5$ conidia/mL with an aid of a hemocytometer (Neubauer Bright-line™, Hausser Scientific, Horsham, PA).

4.2.2 Leaf inoculations

In 2014, one-year old cv. 'Chardonnay' grafted grapevines grown in one-gallon pots (16.6 cm in top diameter, 12.4 cm in bottom diameter, and 16.5 cm in depth, 6:2:1 topsoil, peat moss, and Perlite) were pruned to produce four shoots with 2 to 4 clusters per plant. Vines were maintained in a polyethylene film (Sun Master®, Farmtek, Dyersville, IA) covered high tunnel at the AHS AREC. To reduce light intensity and heat accumulation, a 30% reflective shade cloth (Farmtek, Dyersville, IA) was applied to the structure on 16 June until the end of the experiment.

Leaves were marked with paper tags labeled with a date of unfolding (Avery 12204, Avery Dennison, Glendale, CA). For each vine, two leaves of approximately two weeks (2wo) and four weeks (4wo) after unfolding were selected. On each leaf, while still attached to the vine, four areas were arbitrarily selected, and an approximately 1 cm circle was gently drawn with a waxed pencil. In the center of the wax circle, a 10 µL of a 5×10^5 conidia/mL *Colletotrichum fioriniae* suspension prepared as described above, was applied with a pipette. A quart-sized plastic bag (0.96 L Ziploc, SC Johnson, Racine, WI) containing a wet paper towel was placed to cover the leaf during the time of incubation. Inside of the bag, a 17-gauge wire was placed under the leaf and wrapped around above the top surface, to provide support for the inoculated leaf and keep the wet plastic bag off the inoculated surface (Fig. 4.1, A). The experiment took place in an environmental chamber (E-75L Percival, Perry, IA) set to 25 °C with constant light (Fig. 4.1, B). At 3, 10, and 24 h after inoculation (hai), a leaf was detached from the vine for the microscopy. For each inoculated circle, 25 random conidia were examined for germination. A conidium was

considered germinated when the length of the germ tube was longer than twice the length of the longitudinal length of the conidium. There were four internal replications (i.e., four circles per leaf) and the experiment was repeated three times. Thus, a total of 300 conidia were counted per leaf age.

To observe the presence of appressoria, grape leaves of cv. 'Chardonnay' grown as described above were used for the experiment. Three leaves that were less than 3 weeks old were randomly selected within a vine, and on each leaf, 10 μL of *Colletotrichum fioriniae* conidia suspension (5×10^5 conidia/mL) prepared as described earlier, was applied with a pipette. Then the leaf was placed in a plastic bag with a wet paper towel, and the whole vine was placed in an environmental chamber set to 30 °C with constant light. At 3, 6 and 10 hai, a bag was removed, and an individual leaf was detached from the vine. Then, 25 random conidia per inoculated circle were examined for conidial germination, and presence of non-melanized, and melanized appressoria. There were four internal replications and the experiment was repeated twice for a total of 200 conidia per hai.

4.2.3 Cluster inoculations

Cluster inoculations were performed in 2016 and 2017 in the experimental vineyard at the Alson H. Smith, Jr. Agricultural Research and Extension Center (AHS AREC) in Winchester, VA (39°N6'33.6", -78°W16'56.1"). The AHS AREC vineyard contains spur-pruned, vertical shoot positioned (VSP) cv. 'Chardonnay' vines that were planted in 2009. The spacing between vines within a row was 1.5 m and between two rows was 3 m.

Clusters were inoculated at three phenological stages: bloom, pea-size (when fruit was approximately 1 cm in diameter), and veraison (when fruit begins to change color). Before bloom, grapevines were treated with a mixture of mancozeb (Dithane® 75DF Rainshield, Dow

Agro Science, Indianapolis, IN, rate of 3.4 kg/ha) and sulfur (Microthiol® Disperss®, United Phosphorus, Inc., King of Prussia, PA, rate of 3.4 kg/ha) weekly until the start of the experiment. Also before bloom, clusters were bagged with wax-coated protective fruit bags (Grape No. 19., Hoshino Co. Ltd., Niigata, Japan) to serve as a physical barrier and prevent non-target pathogen infection. The day before inoculation, shade tents were placed over the vineyard row to prevent the clusters from overheating during incubation after inoculation (Fig. 4.2, A). Rectangular, plastic, food storage containers (Deep Dish, 1.89 L, The Glad Products Company, Oakland, CA) with an opening for the rachis was placed on clusters during the time of incubation. Floral wire (22-gauge) was added to the long sides to affix the box to the vineyard wires as a support structure (Fig. 4.2, B). The box contained wet paper towels in the bottom placed around the bag-protected cluster to keep high relative humidity during the incubation period. A sheet of plastic screen was placed underneath the cluster to keep it off of the towel (Fig. 4.2, B). Hereafter, we will refer to these containers as “moist chambers”.

On the day of inoculation, the fruit bags were removed from clusters, and then the clusters were inoculated with a conidial suspension of each species. For pea-size, and veraison inoculations, sterile water-thinned latex paint was used to paint a ring on the surface of the berry. For all cluster inoculations, 5 μL droplet of a 5×10^5 conidia/mL was placed in the center of the paint circle (Fig. 4.2, B). After inoculation, the cluster was incubated inside the moist chamber and berries were collected at 24 h, 48 h, 7 days, and 14 days after inoculation.

To assess the effect of fungicide application on conidial germination, mycelial elongation, and the production of *Colletotrichum* species survival structures, fungicides were applied before and after bloom inoculations in 2017. Four commercial fungicides, benzovindiflupyr (Aprovia®, Syngenta Crop Protection, LLC, Greensboro, NC), captan (Captan

Gold™ 80 WDG, Adama USA, Raleigh, NC), copper octanoate (Cueva®, Certis USA, Columbia, MD), and thiophanate-methyl (Topsin® M 70 WDG, United Phosphorus, Inc., King of Prussia, PA) were used. Each cluster was visually longitudinally split into two sections, using a strip of flagging tape placed between the blooms. One section was inoculated 24 h prior to a treatment application, and the other section was inoculated 24 h after the treatment application. After each inoculation, the cluster was incubated inside the moist chamber. For the berries inoculated before the treatment application, samples were collected 24 h and 72 h after the fungicide application. For the berries inoculated after the treatment application, samples were collected 24 h and 72 h after the inoculation.

The amount of fungal presence on berries from inoculated clusters was visually estimated and rated on a 0 to 4 scale where: "0" was no conidia or mycelia observed, "1" was conidial germination was observed, "2" was elongating mycelia, "3" was overlapping, elongated mycelia and "4" was formation of a mycelial mat (Fig. 4.3).

4.2.4 Light Microscopy

Cluster and leaf tissues were sliced into 5 x 5 mm pieces and fixed in Karnovsky's fixative [3% formaldehyde/glutaraldehyde, in 0.1M sodium cacodylate buffer] (Electron Microscopy Sciences, Hatfield, PA). Once fixed, tissues were transferred onto clean slides and a drop of 0.05% aniline blue stain was placed on top of the inoculated area. Slides were incubated at room temperature (20-21 ℃) for 10-15 min then washed in sterile distilled water three times before the final mounting. Slides were observed and images taken with an Eclipse Ci upright microscope with the NIS-Elements 4.0 software (Nikon Instruments Inc., Melville, NY).

4.2.5 Scanning Electron Microscopy

Cluster and leaf tissues were sliced, seeds or veins removed, and fixed in a modified Karnovsky's fixative (3% glutaraldehyde, 2% paraformaldehyde solution in a 0.1M phosphate buffer adjusted to pH 7.2) based on instructions from the Molecular and Cellular Imaging Center of the Ohio State University, Wooster, OH. Samples were subjected to a vacuum via a vacuum pump to ensure fixative penetration of interior tissues. Fixed samples were then stained with a 1% osmium tetroxide and 1% uranyl acetate solution for one hour with constant, slow agitation. Stained samples were dehydrated through a series of graded alcohol solutions (25, 50, 70, 90, and 100%), and were critical point dried using a home freeze dryer (Medium, Harvest Right, North Salt Lake, UT). Samples were mounted on aluminum stubs with double-sided carbon adhesive tabs and coated with gold-palladium using a sputter coater (SC 7620, Emitech, Quorum Technologies, Ltd, Kent, UK). Images were captured using a JCM-5000 NeoScope™ Table Top scanning electron microscope (JEOL USA, Inc., Peabody, MA) with an acceleration voltage of 10 kV.

4.2.6 Cane inoculations

Two-month-old cv. 'Chardonnay' self-rooted cuttings were used. Vines were planted with three vines per pot in a 3:1 mix of vermiculite and mushroom compost. Vines were watered twice a week and MiracleGro® water soluble all-purpose plant food (The Scotts Company LLC, Marysville, OH) was applied once a month at the recommended indoor plant rate. Three pots were used per isolate for a total of nine vines per isolate. An agar core (3 mm dia) was obtained from 7- to 14-day old plates of each of the five isolates on amended-¼ PDA. The negative control was a non-inoculated amended-¼ PDA plate agar core. A 6 mm hole was drilled into the pith of each the vines and filled with one 3 mm agar core. The hole was wrapped in parafilm and

the vines were left for three months in a temperature controlled greenhouse with a 30% reflective shade cloth (Farmtek, Dyersville, IA).

After three months, the canes were cut at the soil line and 25 mm above the inoculation drill hole. Bark was removed from the cane sections. Canes sections were halved vertically for visual observation of internal necrotic lesions (Fig. 4.4). Lesions were measured with a digital caliper (Electron Microscopy Sciences, Hatfield, PA) and four chips per cane were cut. Chips were surface sterilized in 5% bleach, cut in half, and placed cut edge down into amended-¼ PDA in 24-well plates for re-isolation. Plates were incubated for 14 days at 25 ℃ with a diurnal light cycle, then colony morphology was visually assessed for16-20 colonies per *Colletotrichum* species.

4.2.7 Statistical analysis

The effect of *Colletotrichum* species, cluster phenological stage, treatment, and treatment timing on the presence/absence and relative quantity of mycelia was determined by a non-parametric Kruskal-Wallis rank sum method since the measurement was in an ordinal scale (R, ver. 3.5, R Core Team 2014). *C. nymphaeae* was removed from the analysis due to the limited number of samples available. When the effect of the factor was found to be significant ($P \leq 0.05$), Dunn's multiple comparison test was computed (R, ver. 3.5 package 'FSA'). The effect of leaf age on the rate of mean germination per hai was determined using a one-way ANOVA (JMP 14 Pro, SAS Institute, Cary, NC). The effect of *Colletotrichum* species on the mean cane lesion length was analyzed using the non-parametric Kruskal-Wallis rank sum method because the data was not normally distributed when subjected to the Bartlett's test (K-score = 23.46, $P < 0.01$). When the effect of the factor was found to be significant ($P \leq 0.05$), Dunn's multiple comparison test was computed (R, ver. 3.5 package 'FSA').

4.3. Results

4.3.1 Leaf inoculations

We observed conidial germination, mycelial extension, and appressorial formation (Fig. 4.6). Within 24 hai, we observed multiple melanized appressoria on inoculated leaf surfaces via light microscopy and SEM (Fig. 4.6, A, B, C, E). Additionally, secondary conidiation was observed on SEM samples after 24 hai (Fig. 4.6, F). No visual symptoms of fungal infection were observed when samples were collected for microscopic observation.

At 3 hai, the mean rate of germination was 27% and 16% for 2wo and 4wo, respectively (Fig. 4.7, A). At 10 hai, 2wo resulted in 56% and 4wo resulted in 64% mean germination rate (Fig. 4.7, A). At 24 hai, leaves were covered with mycelia, thus, we were not able to count germination rate. Lesion formation on the spot of inoculation at 24 hai was not observed. At 3 hai, the mean germination rate on 2wo was significantly higher ($F = 5.70$, $P = 0.03$), but at 10 hai, the effect of leaf age was not significant on the germination rate ($F = 0.46$, $P = 0.51$).

The rate of appressorium formation was examined in a separate experiment. The mean germination rate at 3 hai was 68%, and increased to 95% at 6 hai, and 100% at 10 hai. The mean number of non-melanized appressoria increased to 19% at 6 hai, then become 0% at 10 hai; on the other hand, the mean number of melanized appressoria increased to 19% at 10 hai (Fig. 4.7, B).

4.3.2 Cluster inoculations

We observed conidial germination, and mycelial extension on all tested cluster growth stages for all *Colletotrichum* species (Fig. 4.8). Appressorium formation was observed on blooms by *C. fructicola*-like genotype 3 (Fig. 4.8, E), *C. fructicola*-like genotype 1 (Fig. 4.8, I),

and *C. nymphaeae* (Fig. 4.8, Q), on pea-size fruit by *C. aenigma* (Fig. 4.8, A) within 48 h after inoculation. Secondary conidiation was observed for *C. aenigma*, *C. fructicola*-like genotype 3, and *C. nymphaeae* on blooms within 24 h (Fig. 4.8, B, F, G, R). *C. fioriniae* produced setae on pea-sized berries within 7 days (Fig. 4.8, O). *C. aenigma* was observed exiting the stomata of a bloom within 48 h of inoculation (Fig. 4.8, D). After 48 h, *Colletotrichum* species would begin to form thick mycelial mats on pistils and stamens (Fig. 4.8, H, K, L, P, S, T). Additionally, conidia still germinated on fungicide treated blooms and formed infection structures (Fig. 4.8, B, D, F-L, N, R, T).

Even though appressorial formation was observed on blooms for *C. fructicola*-like genotype 1, there was a selection of samples without observable conidia or conidial germination (Fig. 4.9, B). This lack of infection is in part due to blooms overheating during incubation, causing cluster abortions. The high temperature conditions within the moist chamber would reduce the survival rate of the *C. fructicola*-like genotype 1conidia and potentially damage tissues, even samples that appeared healthy when collected.

Relative mycelial quantity was classified into five groups. Based on the visual classification of mycelial quantity within an image, the effect of phenological stage (Chi-square = 16.87, $P < 0.01$) was significant, but that of *Colletotrichum* species was not (Chi-square = 8.7, $P = 0.07$). The median visual classification for inoculated blooms, pea-size berries, and veraison berries images was 3, 2, and 4, respectively. Twenty-four hr samples of tissues inoculated at veraison resulted in significantly the higher median rating scale than 24 hr samples inoculated at bloom ($z = -4.1$, $P < 0.01$) or pea size ($z = -2.5$, $P = 0.02$), but there were no significant differences between the at bloom and the at pea size inoculation ($z = -1.4$, $P = 0.15$).

The effect of fungicide treatment and timing of application on the development of mycelia on the grape surface tissue was examined only with inoculation at bloom. The effect of *Colletotrichum* species (Chi-square = 4.42, $P = 0.22$), and the timing of fungicide application (Chi-square = 5.7, $P = 0.06$) did not significantly affect the approximated median visual classification. When fungicide treatment and the timing of application was combined as a treatment factor, it significantly affected (Chi-square = 15.23, $P = 0.05$) the approximated median visual classification. The median visual classification for fungicide treated blooms was 1 for all fungicide treatments with the exception of blooms inoculated prior to applications of benzovindiflupyr were the median visual classification was 2. Captan applied at either pre- or post-inoculation resulted in a significantly lower approximated median visual classification than the negative check which did not receive any fungicide application (Fig. 4.9). There no other treatments significantly different ($P > 0.05$) from the negative check, indicating no significant reduction in the approximated median visual classification with other materials, benzovindiflupyr, copper octanoate, and thiophanate-methyl.

4.3.3 Cane inoculations

No visual symptoms or external fungal structures were observed three months after the initial inoculation (Fig. 4.4, A). Dark lesions were only observed after the cane had been stripped of bark and split longitudinally. The overall mean lesion length among five *Colletotrichum* species was 16.1 mm, with a range of 7.6 to 53.0 mm (Fig. 4.10). There was a significant difference of the median lesion length (Chi-square = 10.90, $P = 0.05$); however, the difference was only significant with comparison of a negative check and *Colletotrichum* species. There were no significant differences ($P > 0.05$) between the species (Fig. 4.10).

4.4. Discussion

We observed conidial germination, and mycelial extension on all tested cluster growth stages for the four *Colletotrichum* species tested. Appressorium formation was observed with two genotypes of *C. fructicola*-like isolates, and *C. nymphaeae*. Secondary conidiation on blooms was observed with *C. aenigma*, *C. fructicola*-like genotype 3, and *C. nymphaeae.* To our knowledge, this is the first report to demonstrate colonization of *C. aenigma, C. fioriniae, C. fructicola*-like isolates, and *C. nymphaeae* on grape blooms, pea-size berries, and veraison berries. The other *Colletotrichum* species might produce appressoria and secondary conidia on blooms; however, due to limitations in sample size and timing of sample collection (i.e., mycelial mat formation could obscure appressoria and secondary conidia), we were not able to confirm (Fig. 4.6, B). For example, *C. aenigma* produced appressoria on pea-size fruit, but it also tended to produce mats of mycelia by 24 hai (Fig. 4.6, B).

There was very limited information on the infection process of *Colletotrichum* species on grape tissues. Prior studies with *Colletotrichum acutatum* bloom inoculations observed germination and mycelial mat formation on pistils and stamens within 24 h (Greer et al. 2014). Our studies observed similar behavior for *C. aenigma*, *C. fioriniae,* two genotypes of *C. fructicola*-like isolates, and *C. nymphaeae* on all three tested grape phenological stages (blooms, pea-size berries, and berries at veraison).

When fungicides were applied before and after inoculation with the *Colletotrichum* species, conidia still germinated. Applications of captan either before or after inoculation provided a significant reduction ($P < 0.05$) in colonization of blooms from no fungicide treatments. This suggests that benzovindiflupyr, copper octanoate, and thiophanate-methyl were not effective at controlling conidial germination when applied either before or after inoculation

with *Colletotrichum* species. Since both benzovindiflupyr and copper octanoate provided a certain level of protection in the field (Chapter 5), there may be other factors involved (e.g., environmental condition, differences in species, etc.), but it needs further research. We did not find strong species effect on the germination and development of mycelia on grape tissues, but in both experiments, species effect was significant at the 90% confidence level. Since our sample size is small (1-7 tissues per combination of *Colletotrichum* species, phenological stage, fungicide treatment, and sample collection time), it is possible that difference among species may become more apparent with a larger sample size.

Although significantly more conidia germinated on the surface of 2wo leaves than 4wo leaves at 3 hai, the difference between two age groups was not significant at 10 hai, indicating that the germination rate of *C. fioriniae* did not differ based on the tested leaf age. In other pathogens such as *Diaporthe ampelina*; syn. *Phomopsis viticola* (Sutton 2015) and *Erysiphe necator* (Doster & Schnathorst 1985) younger leaves were found to be more susceptible than older ones. When we examined the rate of germination over time at 30 ℃, by 6 hai, nearly all conidia had germinated, with some producing non-melanized appressoria. By 10 hai, all the conidia germinated, and the appressoria formed by 6 hai had melanized. Within 24 hai, melanized appressoria will form and leaf surfaces would be covered with mycelia; however, there was no observable symptom development. Similar behavior has been observed for *C. acutatum* on apple, strawberry, and sweet cherry leaves (Borve et al. 2010; Borve & Stensvand 2017; Leandro et al. 2003). To our knowledge, this is the first report of *C. fioriniae* colonization and appressorial formation on grape leaves.

Although these were two independent experiments, when the rate of germination from the leaf age trial was compared to the rate of germination and appressorial formation trial, the

latter resulted in higher mean germination rates at both 3 and 10 hai, probably due to a higher incubation temperature (25 ℃ vs 30 ℃). Prior studies with *C. acutatum* and *C. gloeosporioides* on grape (Steel et al. 2007; Steel et al. 2012) and other crop hosts such as strawberry (Leandro et al. 2003; Wilson & Madden 1990) and blueberry (Miles et al. 2013) suggest an optimum germination rate between 25- 30 ℃ on slides or detached clusters or fruit. Once the temperature exceeded 30 ℃, there was a sharp drop off in conidial germination such that few spores would germinate at 35 ℃ (Wilson & Madden 1990). Additionally, Miles et al, (2013) observed an increase in germination rate of *C. acutatum* as temperature increased, until it hit the optimum above 30 ℃.

The scale our lab used to evaluate the images taken of *Colletotrichum*-inoculated blooms was useful in describing the observed differences in fungal mass between the different cluster phenological stages and the effects of the fungicide treatments. Our scale progressed from no germination to formation of mycelial mat; however, the importance of the formation of a mycelial mat on the exterior of the grape epidermal tissue is uncertain. Although it shows that the fungi were able to grow on the outside of the grape epidermal tissue, the formation of the mat could be due to an inability of the fungi to penetrate into the epidermal tissues, therefore they are left to colonize the surface. For instance, there was a lower proportion of samples with fungal mat formation during the bloom phenological stage, especially when compared to the veraison berries (Fig. 4.6, A). Since we observed appressorial formation for the majority of the *Colletotrichum* species at bloom, it is possible that, at bloom, the fungi proliferate inside the tissue, thus resulted in less development at the outside. On the other hand, at veraison, infection structures were not observed, and what we observed are mycelial mats. The mycelial mat could have obscured the structures, or the structures were not formed at all, leaving the fungi to

proliferate on the exterior of the epidermal tissue instead. Within the three months of the experiment, we did not observe any fruiting body formed outside of the infected canes. A different type of measurement, such as transmission electron microscopy, to observe changes in the inside of the epidermal cell would be the topic of the future research.

The survival of the fungi within wounded canes suggests that these *Colletotrichum* species could survive inside grapevine woody tissue, if they enter through a wound. Survival of cluster rot pathogens within woody tissues has been reported for other fungal grape pathogens. For example, *Botryosphaeria* spp. is known to cause extensive interior trunk lesions within grape vines (Botryosphaeria dieback) as well as a late season cluster rot disease (Macrophoma rot) (Sutton 2015). Some cluster rot pathogens such as *Elsinoe ampelina* (grape anthracnose) are known to form exterior cane lesions for overwintering (Thind 2015). To our knowledge, this is the first report of *Colletotrichum* species successfully surviving within the canes of wine grapes.

These findings illustrate that *Colletotrichum* species can colonize berries at three phenological stages, form appressoria and secondary conidia on blooms, and survive in wounded canes. *C. fioriniae* can form appressoria and secondary conidiation asymptomatically on grape leaves. Additionally, all fives species were found to germinate on blooms that have been treated with fungicides. This information suggests that fungicide spray programs should be adjusted to provide season-long pre-infection protection of clusters and suggests captan still has some efficacy against the *Colletotrichum* species tested in this study.

Future studies are required to validate the effect of leaf infection on the level of disease development on fruit. Also, further studies are needed to demonstrate whether *Colletotrichum* species in woody grape tissue can produce conidia in the field, serving as a source of spring inoculum.

Acknowledgements

This research was financially supported by the Virginia Wine Board (VWB, 449036, 449204, and 449338), Southern Region Small Fruit Consortium (#2014-17) and Virginia Department of Agriculture and Consumer Services (VDACS, FYY-2015 544). We would like to thank Dr. Tea Meulia and Andrea Kaszas of the OSU MCIC for sample preparation training and Dr. Jon Eisenback of VT for use of his SEM. We also would like to thank Morgan Gannon, and Alex Wong, members of the Grape Pathology lab, for assisting with cluster inoculations.

4.5. References

Bailey, J., & Jeger, M. (1992). *Preface.* in *Colletotrichum: biology, pathology and control*, Bailey, J., & Jeger, M. eds. Melksham, UK: CAB International.

Børve, J., Djønne, R., & Stensvand, A. (2010). *Colletotrichum acutatum* occurs asymptomatically on sweet cherry leaves. *European Journal of Plant Pathology*, *127*, 325–332.

Børve, J., & Stensvand, A. (2017). *Colletotrichum acutatum* occurs asymptomatically on apple leaves. *European Journal of Plant Pathology*, *147*, 943–948.

Damm, U., Cannon, P., Woudenberg, J., & Crous, P. (2012). The *Colletotrichum acutatum* species complex. *Studies in Mycology*, *73*, 37–113.

Daykin, M., & Milholland, R. (1984). Histopathology of ripe rot caused by *Colletotrichum gloeosporioides* on muscadine grape. *Phytopathology*, *74*, 1339–1341.

Dean, R., Van Kan, J., Pretorius, Z., Hammond-Kosack, K., Di Pietro, A., Spanu, P., Rudd, J., Dickman, M., Kahmann, R., Ellis, J. & Foster, G. (2012). The Top 10 fungal pathogens in molecular plant pathology. *Molecular Plant Pathology*, *13*, 414–430.

Doster, M., & Schnathorst, W. (1985). Effects of leaf maturity and cultivar resistance on development of the powdery mildew fungus on grapevines. *Phytopathology, 75*, 318-321.

Freeman, S. (2008). Management, survival strategies, and host range of *Colletotrichum acutatum* on strawberry. *HortScience, 43*, 66–68.

Forcelini, B., Seijo, T., Amiri, A., & Peres., N. (2016). Resistance in strawberry isolates of *Colletotrichum acutatum* from Florida to quinone-outside inhibitor fungicides. *Plant Disease, 100*, 2050–2056.

Greer, L., Harper, J., & Steel, C. (2014). Infection of *Vitis vinifera* (cv. Chardonnay) inflorescences by *Colletotrichum acutatum* and *Greeneria uvicola*. *Journal of Phytopathology, 162*, 407–410.

Greer, L., Harper, J., Savocchia, S., Samuelian, S., & Steel, C. (2011). Ripe rot of South-Eastern Australian wine grapes is caused by two species of *Colletotrichum*: *C. acutatum* and *C. gloeosporioides* with differences in infection and fungicide sensitivity." *Australian Journal of Grape and Wine Research, 17*, 123–128.

Higgins, B. (1926). Anthracnose of pepper (*Capsicum annuum* L.). *Phytopathology, 16*, 333–345.

Hu, M., Grabke, A., Dowling, M., Holstein, H., & Schnabel, G. (2015). Resistance in *Colletotrichum siamense* from peach and blueberry to thiophanate-methyl and azoxystrobin. *Plant Disease, 99*, 806–814.

Kummuang, N., Diehl, S., Smith, B., & Graves Jr., C. (1996)a. Muscadine grape berry rot diseases in Mississippi: Disease epidemiology and crop reduction. *Plant Disease, 80*, 244–247.

Kummuang, N., Smith, B., Diehl, S., & Graves Jr., C. (1996)b. Muscadine grape berry rot diseases in Mississippi: Disease identification and incidence. *Plant Disease, 80*, 238–243.

Leandro, L., Gleason, M., Nutter, F., Wegulo, S., & Dixon, P. (2003). Ecology and population biology strawberry plant extracts stimulate secondary conidiation by *Colletotrichum acutatum* on symptomless leaves. *Phytopathology*, *93*, 1285–1291.

Maas, J. (1998). Anthracnose fruit rot (black spot). in *Compendium of Strawberry Diseases*. 2nd ed. Maas, J. ed. St. Paul, MN: American Phytopathological Society.

Miles, T., Gillett, J., Jarosz, A., & Schilder, A. (2013). The effect of environmental factors on infection of blueberry fruit by *Colletotrichum acutatum*. *Plant Pathology*, *62*, 1238–1247.

Oliver, C. (2016). Effects of cultivar and cluster developmental stage of wine grapes to infection by ripe rot of grape, caused by *Colletotrichum gloeosporioides* and *C. acutatum* species complexes. Ch. 2. (Master's Thesis, Virginia Tech).

R Core Team (2014). R: A language and environment for statistical computing. *R Foundation for Statistical Computing*, Vienna, Austria. URL http://www.R-project.org/.

Southworth, E. (1891). Ripe rot of grapes and apples. *The Journal of Mycology*, *6*, 164–173.

Steel, C., Greer, L., & Savocchia, S. (2007). Studies on *Colletotrichum acutatum* and *Greeneria uvicola*: Two fungi associated with bunch rot of grapes in sub-tropical Australia. *Australian Journal of Grape and Wine Research*, *13*, 23–29.

Steel, C., Greer, L., & Savocchia, S. (2012). Grapevine inflorescences are susceptible to the bunch rot pathogens, *Greeneria uvicola* (bitter rot) and *Colletotrichum acutatum* (ripe rot). *European Journal of Plant Pathology*, *133*, 773–778.

Sutton, T. (2015). Macrophoma rot. in *Compendium of Grape Diseases, Disorders, and Pests*. Wilcox, W., Gubler, W., & Uyemoto, J. eds. St. Paul, MN: American Phytopathological Society.

Thind, T. (2015). Anthracnose. in *Compendium of Grape Diseases, Disorders, and Pests*. Wilcox, W., Gubler, W., & Uyemoto, J. eds. St. Paul, MN: American Phytopathological Society.

Weir, B., Johnston, P., & Damm, U. (2012). The *Colletotrichum gloeosporioides* species complex. *Studies in Mycology*, *73*, 115–180.

Wharton, P., & Dieguez-Uribeondo, J. (2004). The biology of *Colletotrichum acutatum*. *Anales Del Jardín Botánico de Madrid*, *61*, 3–22.

Wilson, L., Madden, L., & Ellis, M. (1990). Influence of temperature and wetness duration on infection of immature and mature strawberry fruit by *Colletotrichum acutatum*. *Phytopathology*, *80*, 111–116.

Xiao, C., Mackenzie, S., & Legard, D. (2004). Genetic and pathogenic analyses of *Colletotrichum gloeosporioides* isolates from strawberry and noncultivated hosts. *Phytopathology*, *94*, 446–453.

Figure 4.1: *C. fioriniae* leaf inoculation in the environmental chamber. Leaves were marked with a wax pencil, inoculated with 5×10^5 conidia/mL *Colletotrichum fioriniae* suspension, and placed inside a humid plastic bag with wire supports above and below the inoculated leaf [A]. Vines with inoculated leaves were placed inside the environmental chamber for 24 h of incubation at either 25 or 30 ℃ [B].

Figure 4.2: Field setup for cluster inoculations in 2016 and 2017 at the Alson H. Smith Jr. Agriculture Research and Extension Center (AHS AREC). Tents were erected over the vineyard rows to the temperature within the moist chambers [A]. Clusters were placed inside moist chambers and circles for inoculation were painted with sterile water-thinned latex onto the berries [B].

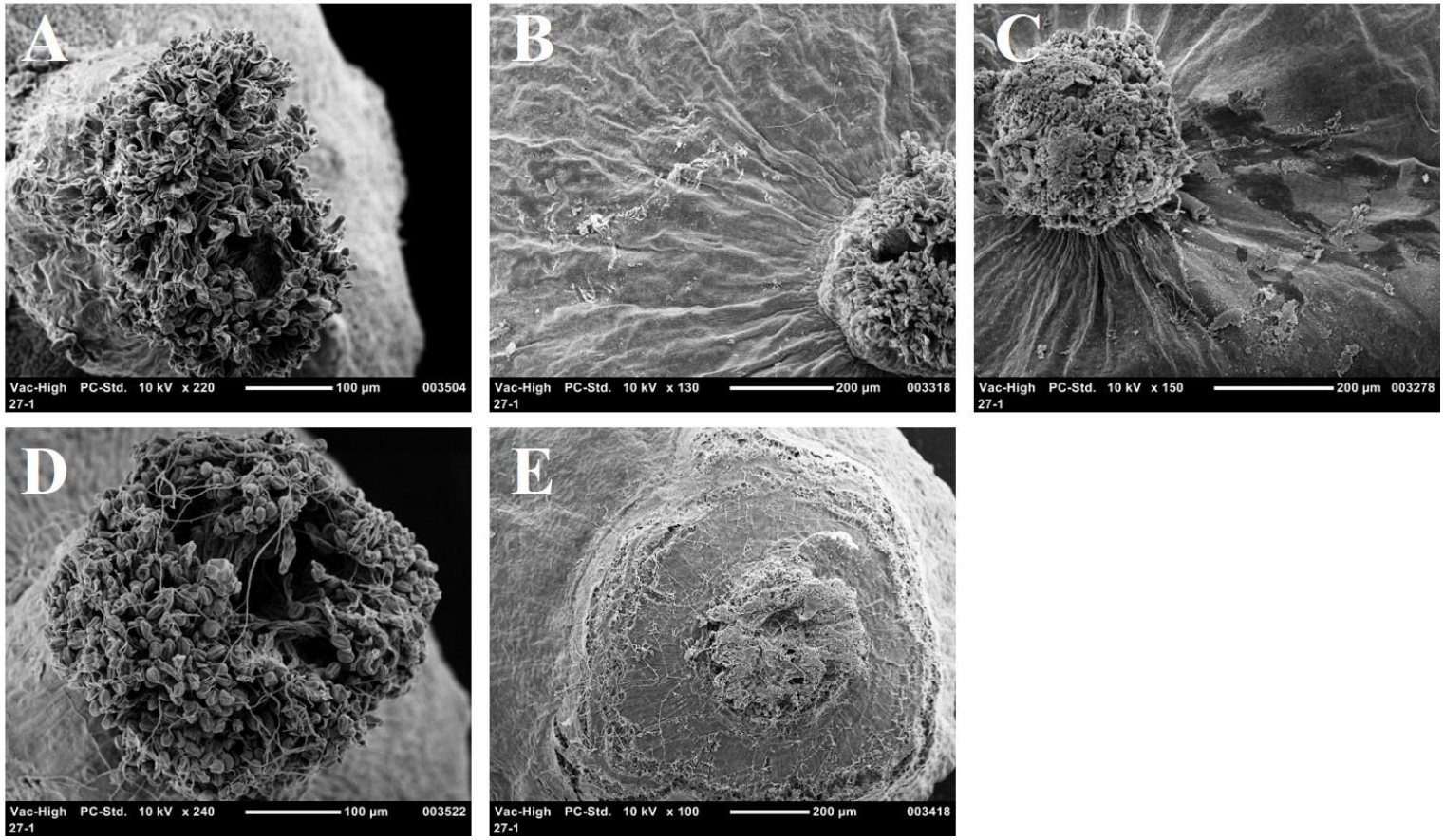

Figure 4.3: Scanning electron microscopy inoculated berry image rating scale. Berries with no conidia or mycelia were rated a "0" [A]. Berries with sporulating conidia were rated "1" [B]. Berries with elongating mycelia were rated "2" [C]. Berries with multiple, long, overlapping mycelia were rated "3" [D]. Berries covered with a mycelial mat were rated "4" [E].

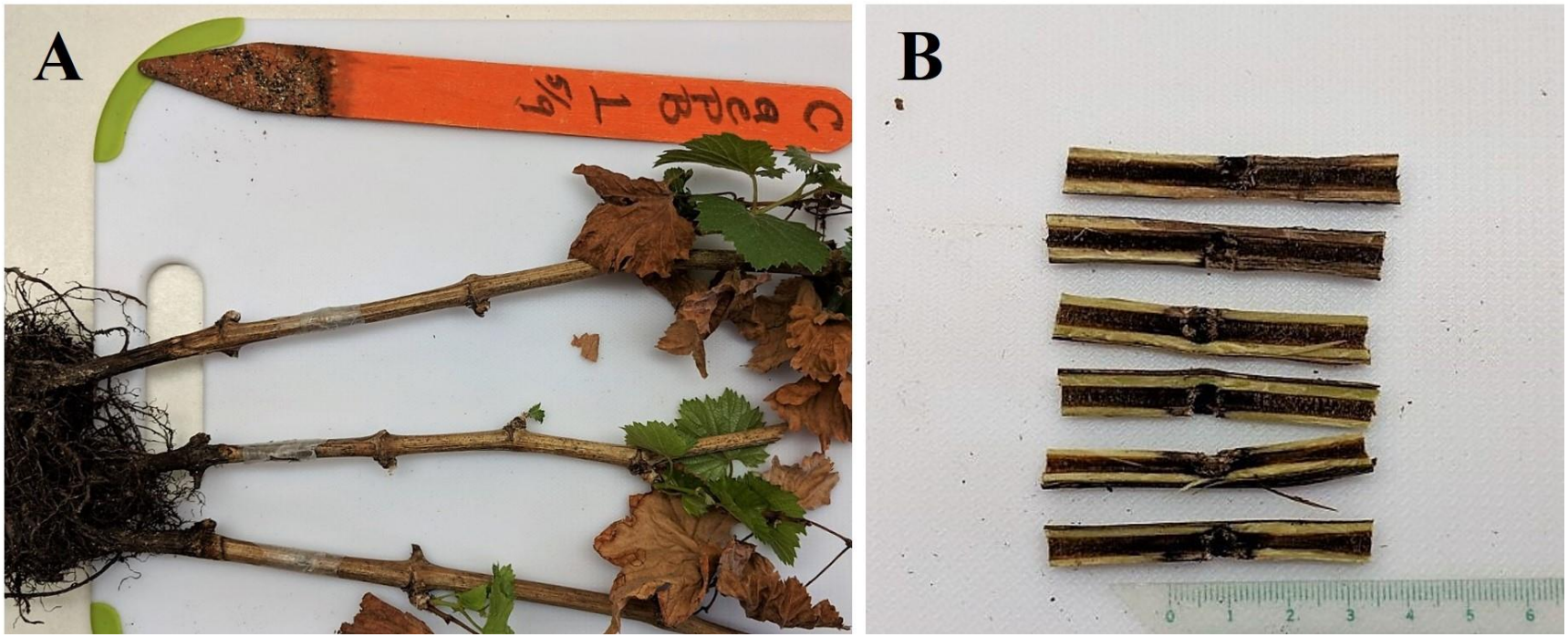

Figure 4.4: Canes inoculated with agar plugs of *Colletotrichum* species. Canes were pulled from the soil and cleaned [A] before the bark was removed and canes split [B]. The measurement tool in the bottom right of panel B is in cm.

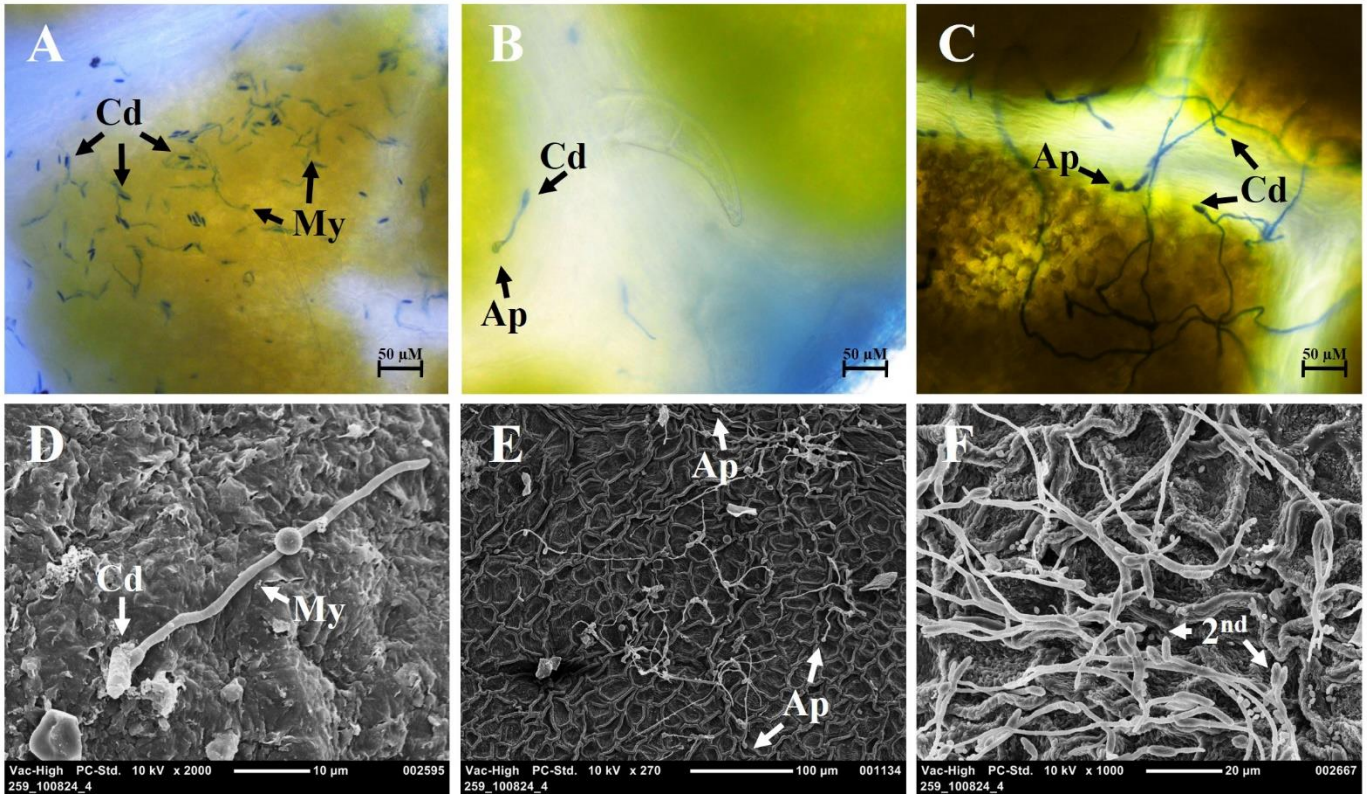

Figure 4.5: Light microscopy and scanning electron microscopy images of *C. fioriniae*-inoculated leaves. Light microscopy images are shown in the top row [A-C], and scanning electron microscopy images are shown in the bottom row [D-F]. Appressoria (Ap), conidium (Cd), mycelium (My), and secondary conidiation (2^{nd}) were observed. Measurement bars are represented at the bottom of each image in µm. Examples of *C. fioriniae* germinating conidia and elongating mycelia [A, D], appressoria formation [B, C, E], and secondary conidiation [F].

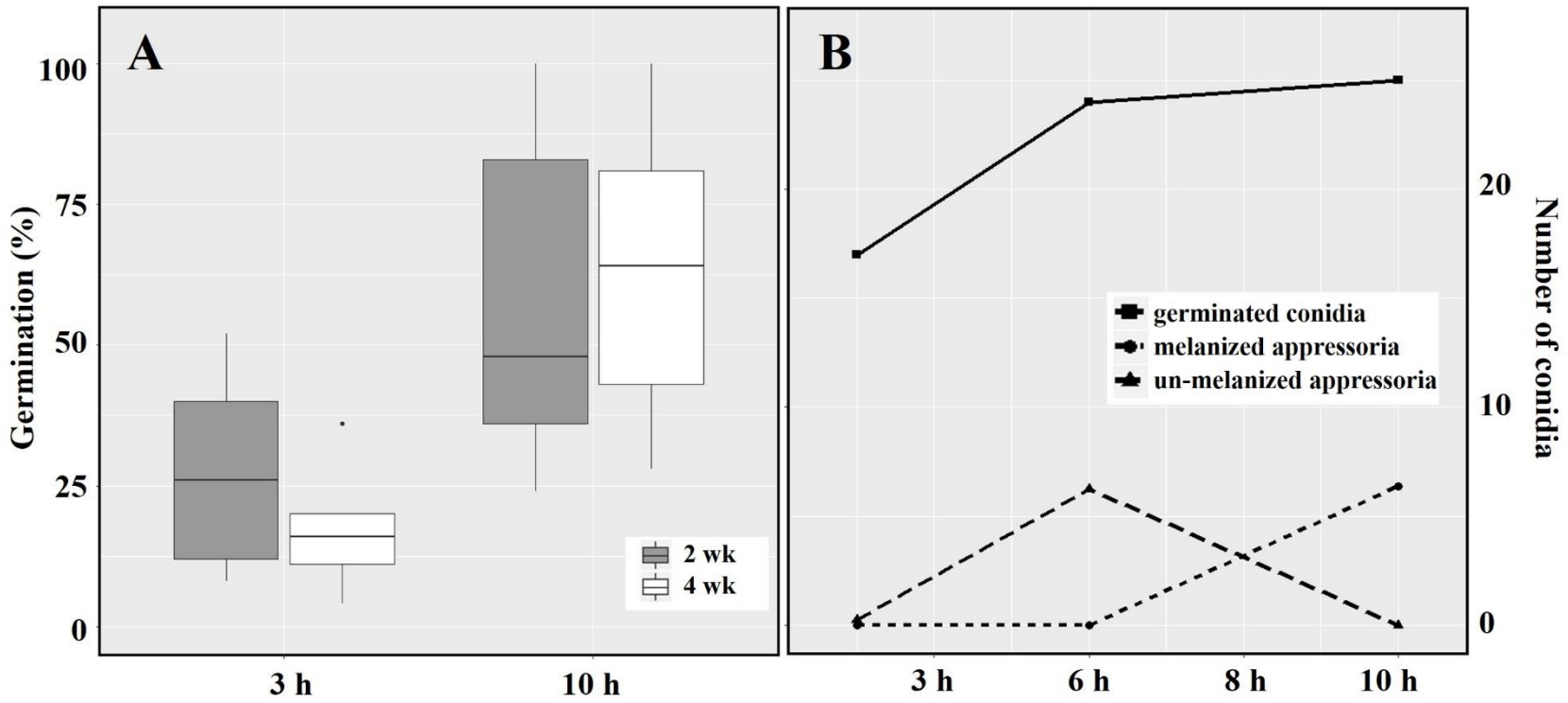

Figure 4.6: Germination of *C. fioriniae* conidia on cv. Chardonnay leaves. Percent of conidial germination on leaves after 3 or 10 hours on leaves of two ages: 2 week old leaves (gray boxes) and 4 week old leaves (white boxes) [A]. Number of *C. fioriniae* conidia that germinated (square points), formed non-melanized appressoria (triangle points), and formed melanized appressoria (circle points) by four time points.

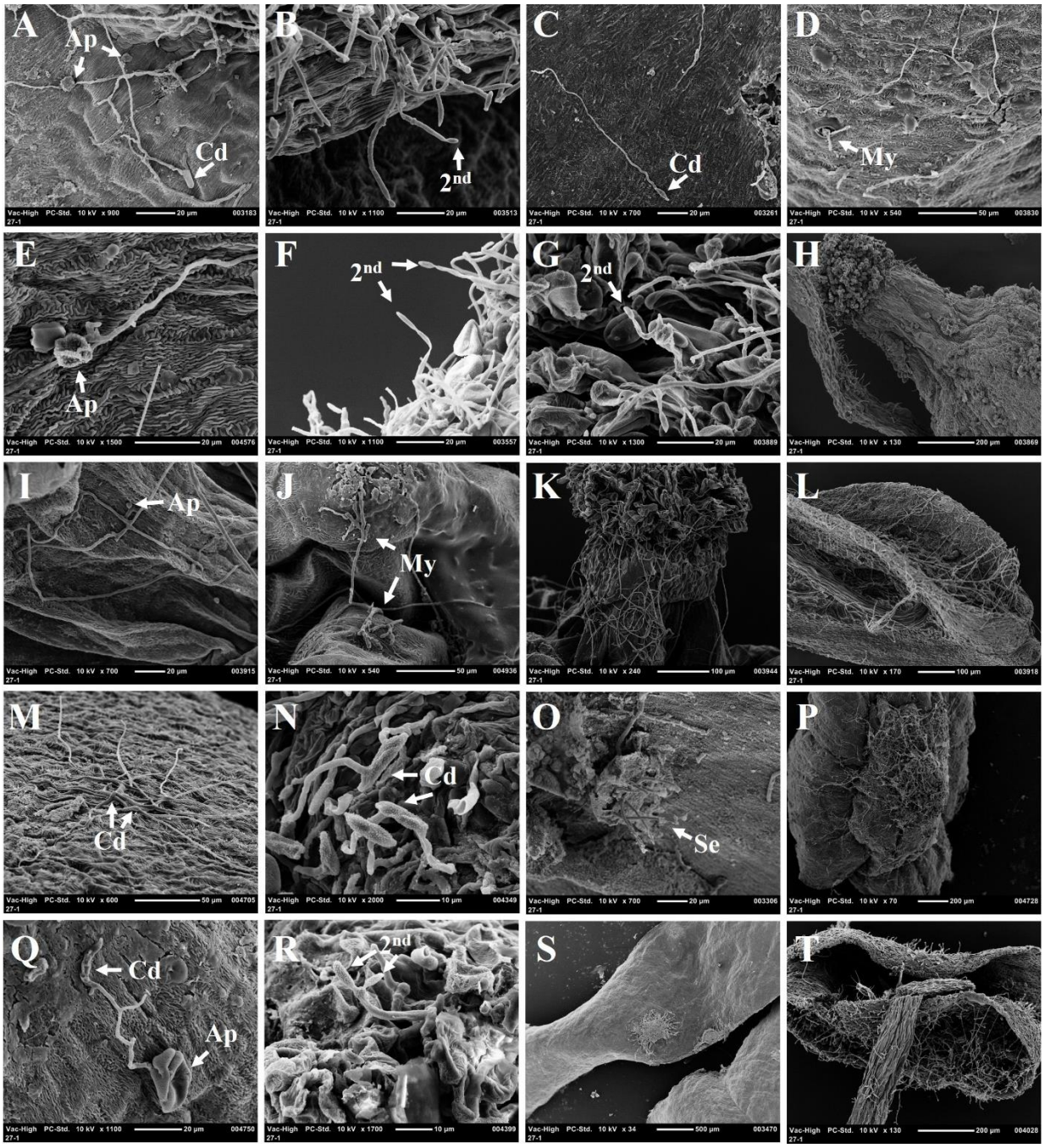

Figure 4.7: Scanning electron microscopy images of inoculated berries. Berries were inoculated with *C. aenigma* [A-D], *C. fructicola*-like genotype 3 [E-H], *C. fructicola*-like genotype 1 [I-L], *C. fioriniae* [M-P], and *C. nymphaeae* [Q-T]. Appressoria (Ap), conidium (Cd), mycelium (My), secondary conidiation (2^{nd}), and setae (Se) were observed. Measurement bars are represented at the bottom of each image in µm. Examples of germinating conidia [C, N] and mycelial

elongation [J]. Appressorium was observed for *C. aenigma* [A], *C. fructicola*-like genotype 3 [E], *C. fructicola*-like genotype 1 [I], and *C. nymphaeae* [Q]. Secondary conidiation was observed for *C. aenigma* [B], *C. fructicola*-like genotype 3 [F, G], and *C. nymphaeae* [R]. *C. fioriniae* produced setae on pea-sized berries [O]. *C. fructicola*-like genotype 3 [H], *C. fructicola*-like genotype 1 [K], *C. fioriniae* [P], and *C. nymphaeae* [S] formed mycelial mats on berry tissues with *C. fructicola*-like genotype 1 [L], and *C. nymphaeae* [T] also forming mats on stamens. *C. aenigma* was observed exiting the stomata of blooms [D].

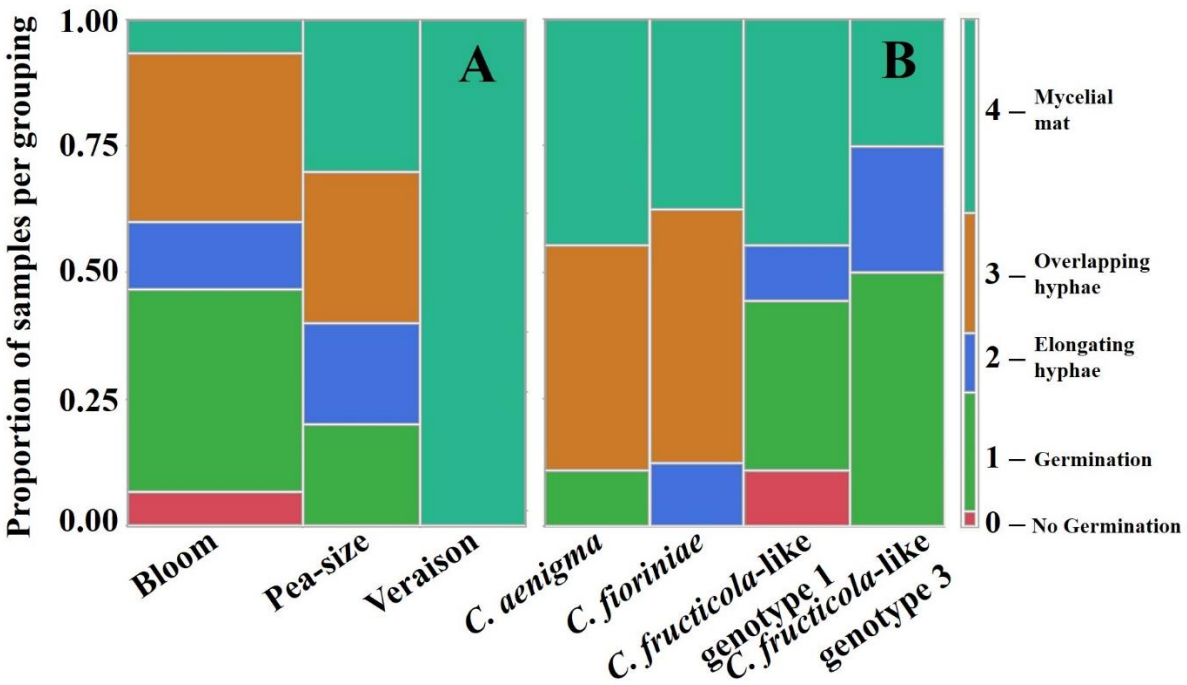

Figure 4.8: Proportion of samples within each image rating category (0-4) per the total number of samples. The width of each bar corresponds to the number of samples within each cluster developmental stage [A] or *Colletotrichum* species and genotype [B] per the total number of samples collected. The colors of the bars correspond to the image rating with no germination (0) as red, germination (1) as green, elongating hyphae (2) as blue, overlapping hyphae (3) as orange, and mycelial mat formation (4) as teal.

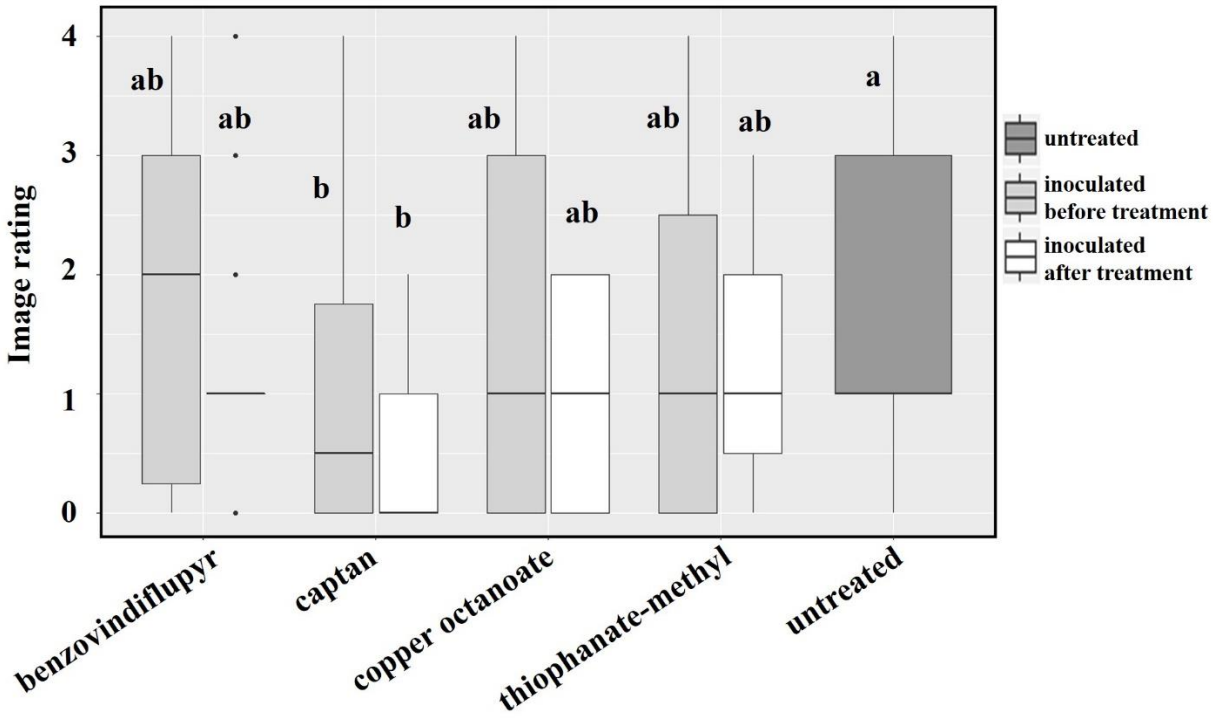

Figure 4.9: Median image rating of fungicide-treated blooms 24 hours after inoculation. Boxes represent the combination of five *Colletotrichum* species. The dark gray box represents blooms without fungicides, light gray boxes represent blooms inoculated prior to fungicide application, and white boxes represent blooms inoculated after fungicide application. Significant mean separations ($P \leq 0.05$) between treatments from Dunn's Multiple comparison test (package 'FSA', R version 3.5) are denoted by non-overlapping lettering.

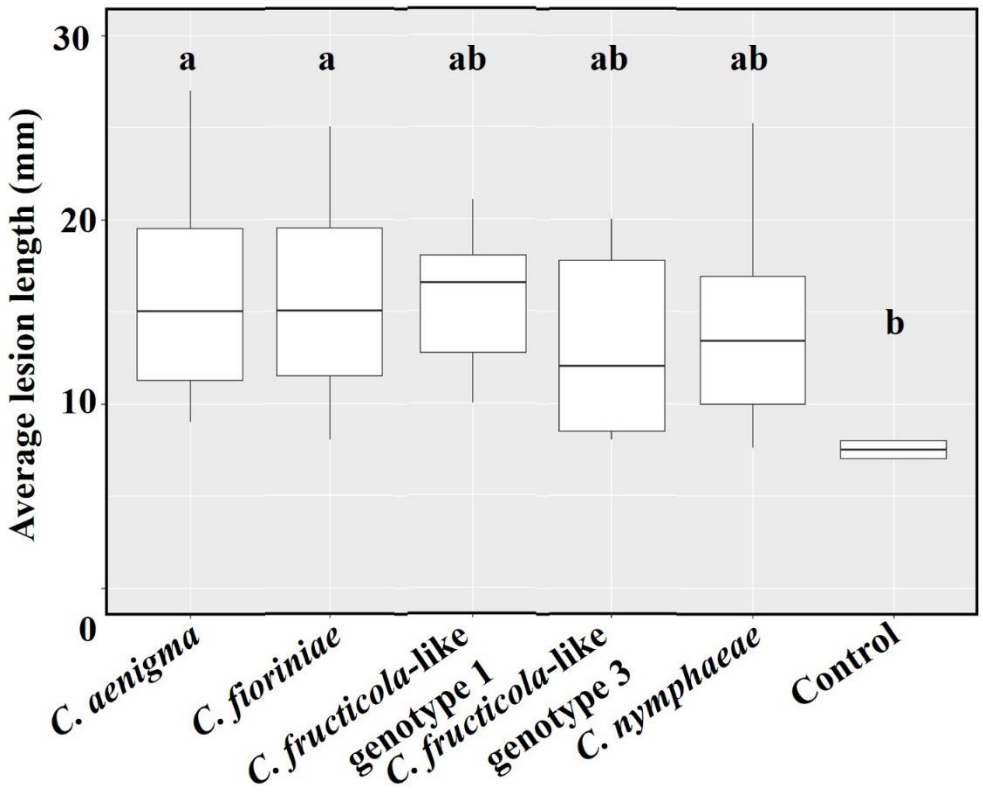

Figure 4.10: Average cane lesion length (mm) for four species of *Colletotrichum* from VA vineyards. Significant mean separations ($P \leq 0.05$) between treatments from Dunn's Multiple comparison test (package 'FSA', R version 3.5) are denoted by non-overlapping lettering.

Chapter 5.

Evaluation of commercial fungicides at different wine grape phenological stages for control of grape ripe rot caused by the *Colletotrichum acutatum* and *C. gloeosporioides* species complexes

Abstract

Grape ripe rot is caused by multiple fungal species in the *Colletotrichum acutatum* and *C. gloeosporioides* complexes. The current recommendations for chemical management are ethylene-bis-dithiocarbamate, phthalimide, and quinone outside inhibitor fungicides. These materials suffer from multiple limitations such as, long pre-harvest intervals and insensitive species. Currently, there is little information on the efficacy of additional commercial fungicides. The objectives of this study were to evaluate the efficacy of ten potential commercial fungicides for control of grape ripe rot, and determine the most advantageous timing of applications. These trials were conducted in 2015-2017 at two locations: an experimental vineyard at the Alson H. Smith Jr. Agricultural Research and Extension Center in Winchester, VA, and a commercial vineyard in Southwest VA near Abingdon, VA. Between the two trial locations, benzovindiflupyr, cyprodinil + fludioxonil, and potassium phosphite + tebuconazole were identified as candidates for chemical control options for grape ripe rot. Additionally, variable results from fenhexamid alt w/ iprodione, fluopyram + tebuconazole, and four applications of polyoxin-D (11.3% a.i.) indicate these could be effective in tank-mixes with the above listed materials but further investigation is required.

5.1. Introduction

Ripe rot of grape, caused by multiple fungal species within the *Colletotrichum acutatum* and *C. gloeosporioides* species complexes (Damm et al. 2012; Weir et al. 2012), is endemic to the Mid-Atlantic USA region (Southworth 1891). These pathogens thrive in warm, humid climates (Greer et al. 2011). Symptoms on fruit often appear on the skin surface as round to irregularly shaped tan to brown lesions for white-fruited cultivars and limited or no symptom on red-fruited cultivars. As the disease progresses, salmon-colored, conidial masses form in concentric rings of acervuli, and infected berry shrivel to raisin-like texture. On wine grape, fruit infection can occur anytime between bloom and harvest, but symptoms tend to appear after the fruit begins to color (veraison) (Melksham et al. 2002; Steel et al. 2007; Sutton 2015). Thus, it is difficult to encourage growers to apply fungicides months before symptoms are visible in the field.

In the USA, the recommended fungicides for grape ripe rot are the ethylene-bis-dithiocarbamate (EBDC) fungicides (e.g., mancozeb, FRAC M3), the phthalimide (e.g., captan, FRAC M1), and quinone outside inhibitor (QoI) (e.g. azoxystrobin, FRAC 11) fungicides (Pfeiffer et al. 2018). However, mancozeb has a 66-day for grapes grown in the US; thus, growers cannot use these materials late in the season when grape ripe rot symptoms appear. In addition, there is some evidence indicating some *C. gloeosporioides* isolates are not sensitive to captan (Greer et al. 2011). A vineyard in Southeast Virginia (VA) experienced 30% crop loss when they relied on captan for the late season disease management (Nita, *personal communication*). Moreover, there are known instances of QoI resistance in *Colletotrichum* species found in other fruit crops in the Mid-Atlantic and Southern USA (Forcelini et al. 2016; Hu et al. 2015a).

Demethylase inhibitor (DMI, FRAC 3) materials are the largest class of fungicides available for growers (Morton & Straub 2008) and variable *Colletotrichum* sensitivity has been observed in recent years (Chen et al. 2016; Xu et al. 2014). In the work by Chen et al. (2016), sensitivity differences were observed between species to the six tested fungicides, for example, *C. nymphaeae* was insensitive to fenbuconazole and flutriafol while *C. fioriniae* and *C. fructicola* were sensitive. Additionally, differences in sensitivity were observed within *C. fioriniae* where one of the sub-groups was found to be less sensitive to all tested fungicides compared to the other sub-group (Chen et al. 2016).

Succinate dehydrogenase inhibitor (SDHI, FRAC 7) materials such as boscalid are commonly used against late-season rots, such as Botrytis gray mold caused by *Botrytis cinerea*. In recent years, a number of new materials have become available in the USA (i.e. benzovindiflupyr, fluopyram, pydiflumetofen). Recent studies have found that benzovindiflupyr is capable of controlling *Colletotrichum* sp. on apple and peach; therefore, information about the efficacy of these materials against grape ripe rot is required (Ishii et al. 2016).

Polyoxin-D is a peptidyl pyrimidine nucleoside with chitin-synthase inhibition as the mode of action (FRAC 19). Introduced in 1965 in Japan (Endo et al. 1970), polyoxin-D has been revived in the USA with a line of new products available for grape production since early 2012. It has efficacy against a wide range of pathogens that cause late-season rots, such as *Botryosphaeria dothidea* on apple (Yoder et al. 2018), *Botrytis cinerea* on strawberry (Cordova et al. 2014; Mertely et al. 2015), and *Colletotrichum* spp. on apple and strawberry (Cordova et al. 2014; Yoder et al. 2018).

The developmental stages of wine grape clusters can have varying levels of sensitivity to grape ripe rot infection during the season. For example, for black rot of grape, caused by

Phyllosticta ampelicida; syn. *Guignardia bidwellii*, clusters become resistant to infection as they mature, three to five weeks after bloom (Hoffman et al. 2002). For Phomopsis cane and leaf spot, caused by *Diaporthe ampelina*; syn. *Phomopsis viticola*, the berries and rachis are susceptible throughout the growing season, from bloom to harvest (Erincik et al. 2001).

The objectives of this study were to evaluate the efficacy of ten commercial fungicides and examine the most advantageous timing of applications.

5.2. Materials and methods

5.2.1 Vineyards

Trials were conducted in two locations: the experimental vineyard at the Alson H. Smith Jr. Agricultural Research and Extension Center (AHS AREC) in Winchester, VA (39°N6'33.6", -78°W16'56.1") in 2016 and 2017 and a commercial vineyard in Southwest VA near Abingdon, VA (36°N39'37.3", 81°W53'32.5") from 2015-2017. The AHS AREC vineyard contained spur-pruned, vertical shoot positioned (VSP) cv. 'Chardonnay' vines that were planted in 2009. The spacing between vines within a row was 1.5 m and between two rows was 3 m. The Southwest VA vineyard contained VSP-trained cv. 'Traminette' vines planted in 1998. Rows were spaced 3 m apart with 2.1 m between vines within a row. The experimental design was a randomized complete block design (RCBD) with four blocks for both locations. Each block included a complete set of treatments randomly assigned to two consecutive vines at the AHS AREC and three consecutive vines at the Southwest VA vineyard. Fungicides used in these trials are listed in Table 5.1.

5.2.2 AHS AREC trial

Treatment applications were made with a backpack sprayer (SP3, Jacto Inc, Tualatin, OR) with output pressure regulated at 21 psi (using Jacto EcoValve regulator), and a flat-fan nozzle (TeeJet XR8002, TeeJet Technologies, Springfield, IL). The tested fungicides were; benzovindiflupyr, cyprodinil + fludioxonil (pre-mix), fenhexamid alternated with iprodione (= fenhexamid alt. w/ iprodione), fluopyram + tebuconazole (pre-mix), polyoxin-D (5% a.i.), polyoxin-D (11.3% a.i.), and pydiflumetofen (Table 5.1). Tested timing of applications are bloom (= BL), berry touch (= BT), veraison (= V), and two weeks after veraison (= LM). Cyprodinil + fludioxonil, fluopyram + tebuconazole, polyoxin-D (5% a.i.), and pydiflumetofen were applied at three phenological stages (BL, BT, and V). Fenhexamid alt. w/ iprodione treatment consisted of a rotation of two fenhexamid applications (BL and V) and a single application of iprodione at BT. The relevance of application timing was tested with benzovindiflupyr and polyoxin-D (11.3% a.i.). For benzovindiflupyr, three different treatments were tested; applications at BL, BT, and V, applications at BL and V, and applications at BL and BT in 2016 or BT and V in 2017. Polyoxin-D (11.3% a.i.) had four different treatments; the three listed above for benzovindiflupyr, and applications at BL, BT, V, and LM. The maintenance program served as a negative check treatment.

The maintenance fungicide program applied at the AHS ARE vineyard suppressed all disease infections such as black rot, downy mildew (*Plasmopara viticola*), and powdery mildew (*Erysiphe necator*) (Table 5.2). Applications were made with a backpack sprayer with output pressure regulated at 21 psi, and a flat-fan nozzle in 2016, and a three-point hitch air blast sprayer (AF100-32, Durand-Wayland, Inc., LaGrange, GA) at 240 psi in 2017. In 2016, the maintenance program was tank-mixed with the treatment applications and applied at the time of treatment application (Table 5.2). In 2017, the treatment applications were made after the

application of the maintenance program. For both years, the weather was recorded with a CR206X weather station with a CS215-L temperature and relative humidity sensor and TE525WS-L rain gauge (Campbell Scientific, Logan, UT) that was located in the vineyard.

5.2.3 Southwest VA trial

As with the AHS AREC trials, treatment applications were made with a backpack sprayer with a 21 psi output pressure with a flat-fan nozzle in all three years. In 2015, there three treatments; two copper octanoate treatments with two different rates; 5.62 L/ha and 2.81 L/ha, and a potassium phosphite + tebuconazole (pre-mix) treatment. All three treatments were applied four times; BL, BT, V and LM (Table 5.2). In 2016 and 2017, the applications of copper octanoate and potassium phosphite + tebuconazole were applied at BL, BT, and V. In addition, benzovindiflupyr or polyoxin-D (11.3% a.i.) was applied at BL, or at BL, BT, and V. The grower's spray program was considered as a negative check treatment.

At the Southwest VA vineyard, the grower's spray was applied with a three-point hitch air blast sprayer (Bravo 300, Tifone Ambiente s.r.l., Italy) at 240 psi to control multiple diseases including grape ripe rot (Table 5.2). The treatments were applied within five days of the maintenance applications. Weather data was accessed from the Country Club Estates KVAABING station (6N36°41'33", W81°58'7") which was 4.8 km from the vineyard via WeatherUnderground weather archives.

5.2.4 Disease assessment

For each vine, twenty clusters were visually evaluated for disease incidence and severity within five days before harvest (Table 5.2). Clusters were harvested at 20 °Brix (percent soluble sugar content) in AHS AREC and 21-22 °Brix and 2.9 - 3.1 pH in Southwest VA (Table 5.2). The percent of cluster disease severity was estimated with a zero to 100 scale, where a single

instance of disease was rated as 1% and all the other levels were estimated using intervals of five. Clusters were rated once per season. With four blocks, the total number of clusters assessed for grape ripe rot per treatment was 160 and 240 at the AHS AREC and Southwest VA vineyard, respectively.

5.2.5 Statistical analysis

The effect of application timing and commercial material on the median cluster disease incidence and on the median percentage of symptomatic berries per cluster were analyzed using the non-parametric Kruskal-Wallis rank sum method (R version 3.5.0) for all studies. Each year was analyzed separately since the maintenance and grower's spray programs, as well as weather, differed in each year. The non-parametric method was used due to significant deviation from the normal distribution. Results from Bartlett test were strongly significant ($P < 0.01$) for both median disease incidence and severity, both locations, and all three years. If the effect of the factor was found to be significant ($P \leq 0.05$), the median cluster disease incidence and the median disease severity among treatments were compared using Dunn's multiple comparison test (Dunn 1961) (R version 3.5.0, 'FSA' package). A percent reduction in median disease incidence and severity was determined as a difference of the median percent disease of the negative check and of a treatment divided by the median percent disease of the negative check.

5.3. Results

5.3.1 AHS AREC trial

The effect of treatment on the median disease incidence was significant in 2017, and, for both years, the effect of treatment on the median disease severity was significant ($P \leq 0.05$) (Table 5.3). In 2016, the median disease incidence was 100% for all treatments, i.e., every cluster

had at least one symptomatic berry, thus, the treatment effect was not significant (Fig. 5.1, A). The benzovindiflupyr at BL and BT, benzovindiflupyr at BL and V, cyprodinil + fludioxonil, and fluopyram + tebuconazole resulted in a significantly lower median disease severity ($P \leq 0.05$) with more than 40% reduction (Fig. 5.1, B). Polyoxin-D (11.3% a.i.) applied four times did not significantly differ in the median disease severity ($P > 0.05$) from the negative check (Fig. 5.2, B).

In 2017, only cyprodinil + fludioxonil treatment was significantly lower in the median disease incidence than the negative check ($P \leq 0.05$), with more than 20% reduction (Fig. 5.2, C). Differences of median disease incidence between the negative check and all other treatments were 6% or less (Fig. 5.2, C). Benzovindiflupyr applied three times, cyprodinil + fludioxonil, and polyoxin-D (11.3% a.i.) applied four times resulted in a significantly lower median disease severity, with more than 43% reduction (Fig. 5.2, D).

5.3.2 Southwest VA trial

The effects of treatment on the median disease incidence and severity were significant ($P \leq 0.05$) for all three years (Table 5.3). In 2015, copper octanoate applied at 5.62 L/ha resulted in significantly lower median disease incidence and severity than all other treatments with a reduction of 62% and 70%, respectively, from the negative check (Fig. 5.3). There was a significantly lower median disease incidence and severity with copper octanoate applied at 2.81 L/ha with a percent reduction of the disease incidence and severity by 38% and 47%, respectively, from the negative check (Fig. 5.2).

In 2016, potassium phosphite + tebuconazole treatment resulted in the lowest median disease incidence and severity (Fig. 5.3, A, B). Both disease incidence and severity were significantly lower than the negative check ($P \leq 0.05$), with 80% and 95% reduction,

respectively (Fig. 5.3, A, B). Two benzovindiflupyr treatments (three applications and BL) were also significantly lower in the median disease incidence and severity than the negative check, with a percent reduction of 60% and 75%, respectively (Fig. 5.4, A, B).

In 2017, a significant difference ($P \leq 0.05$) between the potassium phosphite + tebuconazole and the negative check was found, with 100% percent reduction for both the median disease incidence and severity (Fig. 5.4, C, D). Both copper octanoate treatments, benzovindiflupyr, and polyoxin-D (11.3% a.i.) were also significantly lower than the negative check ($P \leq 0.05$), with a percent reduction in the median disease incidence by more than 53% (Fig. 5.4, C), and in the median disease severity by 70% (Fig. 5.4, D). However, the benzovindiflupyr application at BL resulted in a median disease incidence and severity that was not significantly different from the negative check (Fig. 5.4, C, D).

5.3.3 Weather evaluation

Of the two years at the AHS AREC, 2016 had the most rainfall. At the Southwest VA vineyard, 2015 had the highest rainfall and 2016 and 2017 were similar (Fig. 5.5, D). There were minimal differences between the two locations with the exception of a large variation in rainfall in 2015 (Fig. 5.5). The 2015 season was the driest of the three seasons (483 mm) at the AHS AREC but was the wettest (646 mm) at the Southwest VA vineyard, creating a 163 mm difference in rainfall (Fig. 5.5, C, D). On the year where there was the highest variability, there were no materials that were repeated in both locations.

5.4. Discussion

Grape ripe rot is a common issue among Mid-Atlantic wine grape growers and has large economic impacts, but current chemical management options are limited. This study's goal was

to identify potential treatment (either as individual a.i. or combinations of active ingredients) that would provide effective control. With some treatments, timing of application was examined to identify important periods to protect clusters from grape ripe rot infection.

The a.i. that we investigated had limited prior field testing for control of *Colletotrichum* sp., especially as single product applications. The majority of studies utilized these materials as rotation partners. For example, the potassium phosphite + tebuconazole reduced the percentage of disease incidence of apple bitter rot on Golden Delicious by 91% when applied from pink until after third cover then followed by applications of captan + potassium phosphite, and fluxapyroxad + pyraclostrobin pre-mix + captan (Yoder et al. 2017). Fenhexamid alone and cyprodinil + fludioxonil as a late season rotation partner for metconazole and pyraclostrobin resulted in lower disease incidence of blueberry anthracnose (Schilder et al. 2015) by 41% and 75%, respectively.

At the AHS AREC, the vineyard maintenance program was planned to have limited to no effect on the development of grape ripe rot, thus, the observed incidence and severity should reflect the effect of the product, whether individual a.i. or pre-mix of two a.i., alone. The benzovindiflupyr treatments, cyprodinil + fludioxonil, and fenhexamid alt. w/ iprodione treatment provided a consistent level of disease reduction. Four applications of polyoxin-D (11.3% a.i.) treatment resulted in variable efficacy between years.

At the Southwest vineyard, the BL application was compared with three applications (BL, BT, V) with both benzovindiflupyr and polyoxin D (11.3% a.i.) treatments. In 2016, there was no significant difference in both the median disease incidence and severity with the benzovindiflupyr treatment, whether it was applied just at BL or three times. On the other hand, in 2017, benzovindiflupyr applied at BL resulted in a significantly higher median disease

incidence and severity, despite the fact that captan and pyraclostrobin where applied by the grower at veraison. This indicates that, although protection of blooms is important, it alone is not enough to be able to control grape ripe rot reliably. Fenhexamid alt. w/ iprodione, the standard management program for Botrytis was also examined at the AHS AREC. It was included because in preliminary study (data not shown), this treatment resulted in a significantly lower median disease incidence and severity than a polyoxin-D treatment applied three times (BL, BT, V). Fenhexamid alt w/ iprodione significantly reduced the median disease severity in 2016, but not in 2017. The low level of reduction was likely due to the effect of iprodione which lists suppression of *Colletotrichum* species on the product label. However, in 2017, this treatment did not significantly differ from the negative control in 2017, in both median disease incidence and severity.

The benzovindiflupyr treatment applied three times in 2017, resulted in a numerically lower median disease incidence and severity than the two application treatments, but the difference was not significant. Moreover, benzovindiflupyr applied at BL and V and at BT and V did not significantly differ in either the median disease incidence or severity in both years. Although polyoxin-D (11.3% a.i.) applied four times resulted in significantly lower median disease severity in 2017, polyoxin-D (11.3% a.i.) treatment generally did not provide efficacy, regardless of the number or timing of application. In addition, in 2016, the polyoxin-D (11.3% a.i.) applied three times at the Southwest vineyard did not significantly differ from the negative check. Since there was a significant reduction in 2016 with both BL and three applications of polyoxin-D (11.3% a.i.), this product may have some efficacy, but probably not enough to be recommended as a solo application.

There were two pre-mixed materials contained tebuconazole. Potassium phosphite + tebuconazole, tested at the Southwest VA vineyard, was the most effective control in both 2016 and 2017; Although, it was not as effective as copper octanoate applied at 5.62 L/ha, in 2015. Potassium phosphite + tebuconazole resulted in a significantly lower median disease incidence and severity than both rates of copper octanoate (Fig. 5. 3, C, D). The efficacy of DMI fungicides can be heavily dependent on the species present and the fungicides applied (Chen et al. 2016; Hu et al. 2015b). Hu et al. (2015b) observed at least two species can be present in a single orchard, and Chen et al. (2016) observed a large variation in EC50 values among the tested species and even within isolates in a species in response to the six tested DMI fungicides. Our lab confirmed the presence of at two species of *Colletotrichum* in the AHS AREC vineyard (*C. aenigma*, and *C. fructicola*-like isolates) and at least four in the Southwest VA (*C. fioriniae, C. fructicola*-like isolates, *C. kahawae, C. nymphaeae*) vineyard in 2013 and 2014 (Chapter 2). This mixture of species could greatly affect the efficacy of the tebuconazole applications. Our lab is investigating species of *Colletotrichum* in both locations.

Overall, benzovindiflupyr, cyprodinil + fludioxonil, and potassium phosphite + tebuconazole were identified as candidates for chemical control options for grape ripe rot. However, our study also indicated that none of materials provided consistent results alone, and worked better when it was applied with captan or mancozeb (i.e. Southwest VA), that has efficacy against grape ripe rot pathogens.

Limited or variable results from fenhexamid alt w/ iprodione, fluopyram + tebuconazole, and four applications of polyoxin-D (11.3% a.i.) indicate these materials can be used in combinations with the other mode of action, including the materials listed above, but further investigation is required. With the prevalence of resistance and the potential for insensitive

species, these materials should be used carefully and tank-mixing and/or rotation of different FRAC groups is the best approach to manage grape ripe rot in the field.

In summary, we were able to identify several materials that can be used as a part of a grape ripe rot management program. The variability in the efficacy between locations and years, and consistently lower median disease incidence and severity at the Southwest VA vineyard where treatments were applied in addition to grower's spray program, indicated that the best approach is to use two or more modes of action. We also examined potential effect of timing of applications (BL, BT, and V) with two materials, especially focused on the protection of BL; however, consistently better reduction in median disease incidence and severity provided by three or four applications indicated that a thorough protection from BL to V most likely produces consistent control of grape ripe rot.

Acknowledgements

This research was financially supported by the Virginia Wine Board (VWB) (449036, 449204, 449338, 449504, and 449663). We would like to thank Sabrina Hartley, Amanda Bly and Dana Melby, members of the Grape Pathology lab, for assisting with spray applications and field evaluations at the Alson H Smith Jr Agricultural Research and Extension Center. We would also like to thank Kevin Sutherland and his field crew for assisting with spray applications at the Southwest VA vineyard.

5.5. References

Chen, S., Luo, C., Hu, M., & Schnabel, G. (2016). Sensitivity of *Colletotrichum* species, including *C. fioriniae* and *C. nymphaeae*, from peach to demethylation inhibitor fungicides. *Plant Disease*, *100*, 2434–2441.

Cordova, L., Zuniga, A., Mertely, J., & Peres, N. (2014). Evaluation of products for the control of Botrytis fruit rot in annual strawberry, 2013-14. *Plant Disease Management Reports*, *8*, SMF028.

Damm, U., Cannon, P., Woudenberg, J., & Crous, P. (2012). The *Colletotrichum acutatum* species complex. *Studies in Mycology*, *73*, 37–113.

Dunn, O. (1961) Multiple comparisons among means. *Journal of the American Statistical Association*, *56*, 54–64.

Endo, A., Kakiki, K., & Tomomasa, M. (1970). Mechanism of action of the antifungal agent polyoxin D. *Journal of Bacteriology*, *104*, 189–196.

Erincik, O., Madden, L., Ferree, D., & Ellis, M. (2001). Effect of growth stage on susceptibility of grape berry and rachis tissues to infection by *Phomopsis viticola*. *Plant Disease, 85,* 517–520.

FRAC. (2018). FRAC Code List 2018: Fungicides sorted by mode of action. In.: FRAC.

Forcelini, B., Seijo, T., Amiri, A., & Peres., N. (2016). Resistance in strawberry isolates of *Colletotrichum acutatum* from Florida to quinone-outside inhibitor fungicides. *Plant Disease, 100,* 2050–2056.

Greer, L., Harper, J., Savocchia, S., Samuelian, S., & Steel, C. (2011). Ripe rot of south-eastern Australian wine grapes is caused by two species of *Colletotrichum*: *C. acutatum* and *C. gloeosporioides* with differences in infection and fungicide sensitivity. *Australian Journal of Grape and Wine Research, 17,* 123–128.

Hoffman, L., Wilcox, W., Gadoury, D., & Seem, R. (2002). Influence of grape berry age on susceptibility to *Guignardia bidwellii* and its incubation period length. *Phytopathology, 92,* 1068–1076.

Hu, M., Grabke, A., Dowling, M., Holstein, H., & Schnabel, G. (2015)a. Resistance in *Colletotrichum siamense* from peach and blueberry to thiophanate-methyl and azoxystrobin. *Plant Disease, 99,* 806–814.

Hu, M., Grabke, A., & Schnabel, G. (2015)b. Investigation of the *Colletotrichum gloeosporioides* species complex causing peach anthracnose in South Carolina. *Plant Disease, 99,* 797–805.

Ishii, H., Zhen, F., Hu, M., Li, X., & Schnabel, G. (2016). Efficacy of SDHI fungicides, including benzovindiflupyr, against *Colletotrichum* species. *Pest Management Science, 72,* 1844–1853.

Melksham, K., Weckert, M., & Steel, C. (2002). An unusual bunch rot of grapes in sub-tropical regions of Australia caused by *Colletotrichum acutatum*. *Australasian Plant Pathology, 31*, 193–194.

Mertely, J., Seijo, T., & Peres, N. (2015). Evaluation of products for anthracnose and Botrytis fruit rot control in annual strawberry, 2013-14. *Plant Disease Management Reports*, *9*, SMF007.

Morton, V., & Staub, T. (2008). A short history of fungicides. *APSnet Features*. doi: 10.1094/APSnetFeature-2008-0308.

Pfeiffer, D., Baudoin, A., Bergh, J., & Nita, M. (2018). Grapes: diseases and insects in vineyards. in *Pest Management Guide: Horticultural and Forest Crops*. Hong, C., & Day, E. eds. Virginia Cooperative Extension. Pub. 456-017.

Schilder, A., Gillett, J., & Sysak, R. (2015). Evaluation of fungicides for control of post-harvest anthracnose fruit rot in blueberries, 2014. *Plant Disease Management Reports*, *9*, SMF037.

Southworth, E. (1891). Ripe rot of grapes and apples. *The Journal of Mycology*, *6*, 164–173.

Steel, C., Greer, L., & Savocchia, S. (2007). Studies on *Colletotrichum acutatum* and *Greeneria uvicola*: Two fungi associated with bunch rot of grapes in sub-tropical Australia. *Australian Journal of Grape and Wine Research*, *13*, 23–29.

Sutton, T. (2015). Ripe rot. in *Compendium of Grape Diseases, Disorders, and Pests*. Wilcox, W., Gubler, W., & Uyemoto, J. eds. St. Paul, MN: American Phytopathological Society.

Weir, B., Johnston, P., & Damm, U. (2012). The *Colletotrichum gloeosporioides* species complex. *Studies in Mycology*, *73*, 115–180.

Xu, X., Lin, T., Yuan, S., Dai, D., Shi, H., Zhang, C., & Wang, H. (2014). Characterization of baseline sensitivity and resistance risk of *Colletotrichum gloeosporioides* complex isolates from strawberry and grape to two demethylation-inhibitor fungicides, prochloraz and tebuconazole. *Australasian Plant Pathology*, *43*, 605–613.

Yoder, K., Cochran II, A., Royston Jr., W., Kilmer, S., Engelman, A., Kowalski, A., & Repass, J. (2017). Disease control by experimental and registered fungicide schedules on Golden Delicious and Idared, 2016. *Plant Disease Management Reports, 11*, PF010.

Yoder, K., Cochran II, A., Royston Jr., W., Kilmer, S., & Kowalski, A. (2018). Evaluation of OMRI-approved and conventional products for disease management on three apple cultivars, 2017. *Plant Disease Management Reports, 12*, PF040.

Table 5.1: Fungicides applied as treatments and general vineyard maintenance programs at Alson H. Smith Jr. Agricultural Research and Extension Center (AHS AREC) and the Southwest VA vineyard from 2015-2017.

Fungicide Treatments

Active ingredients	Commercial Product	a.i. %	Company		FRAC	rate /ha
benzovindiflupyr	Aprovia®	10.3	Syngenta Crop Protection, LLC	Greensboro, NC	7	0.66 L
copper octanoate	Cueva®	10	Certis USA	Columbia, MD	M1	2.81 L
copper octanoate	Cueva®	10	Certis USA	Columbia, MD	M1	5.62 L
cyprodinil + fludioxonil	Switch® 62.5 WG	37.5, 25.0	Syngenta Crop Protection, LLC	Greensboro, NC	9, 12	0.98 kg
fenhexamid	Elevate® 50 WDG	50	Arysta LifeScience Corporation	Cary, NC	17	0.84 kg
fluopyram + tebuconazole	Luna® Experience	17.6, 17.6	Bayer CropScience, LP	Research Triangle Park, NC	7, 3	0.58 L
iprodione	Rovral® 4 Flowable	41.6	FMC Corporation	Philadelphia, PA	2	2.11 L
polyoxin-D	OSO™ 5%SC	5	Certis USA	Columbia, MD	19	0.46 L
polyoxin-D	Ph-D®	11.3	Arysta LifeScience Corporation	Cary, NC	19	0.43 kg
potassium phosphite + tebuconazole	Viathon®	49. 0, 3.3	Luxembourg-Pamol Inc	Houston, TX	33, 3	2.81 L
pydiflumetofen	Miravis®	18.3	Syngenta Crop Protection, LLC	Greensboro, NC	7	0.96 kg

Maintenance Program Products

Active ingredients	Commercial Product	a.i. %	Company		FRAC	rate /ha
ametoctradin + dimethomorph	Zampro®	26.9, 20.2	BASF Corporation	Research Triangle Park, NC	45, 40	0.88 kg
captan	Captan Gold™ 80 WDG	78.2	Adama USA	Raleigh, NC	M4	1.41 kg
copper hydroxide	Champ® Dry Prill	57.6	NuFarm Americas, Inc.	Alsip, IL	M1	3.40 kg
copper octanoate	Cueva®	10	Certis USA	Columbia, MD	M1	9.44 L
cyazofamid	Ranman® 400SC	34.5	Summit Agro USA	Durham, NC	21	0.16 kg
cyflufenamid	Torino®	10	Gowan Company, LLC	Yuma, AZ	U6	0.25 L
mancozeb	Dithane® 75DF Rainshield	75	Dow Agro Science	Indianapolis, IN	M3	3.40 kg
mancozeb	Manzate® Pro-Stick™	75	United Phosphorus Inc.	King of Prussia, PA	M3	2.25 kg
mancozeb + mefenoxam	Ridomil Gold® MZ WG	64.0, 4.0	Syngenta Crop Protection, LLC	Greensboro, NC	M3, 4	2.82 kg
mandipropamid + difenoconazole	Revus Top®	21.9, 21.9	Syngenta Crop Protection, LLC	Greensboro, NC	40, 3	0.24 kg
mandipropamid	Revus®	23.3	Syngenta Crop Protection, LLC	Greensboro, NC	40	0.58 L
metrafenone	Vivando®	25	BASF Corporation	Research Triangle Park, NC	U8	0.76 L
phosphorous acid	Rampart®	53	Loveland Products, Inc.	Greeley, CO	P07	2.36 L
phosphorous acid	Phostrol®	53.6	NuFarm Americas, Inc.	Alsip, IL	P07	4.26 L
potassium bicarbonate	EcoMate Armicarb®	85	Luxembourg-Pamol Inc	Houston, TX	NC	2.27 kg
potassium phosphite	ProPhyt®	54.5	Luxembourg-Pamol Inc	Houston, TX	P07	2.84 L
pyraclostrobin + boscalid	Pristine®	12.8, 25.2	BASF Corporation	Research Triangle Park, NC	7, 11	0.56 kg
pyrimethanil	Scala® SC	54.6	Bayer CropScience, LP	Research Triangle Park, NC	9	1.13 kg
quinoxyfen	Quintec®	22.5	Dow Agro Science	Indianapolis, IN	13	0.29 L
sulfur	Microthiol® Disperss®	80	United Phosphorus Inc.	King of Prussia, PA	M2	3.40 L
tebuconazole	TebuStar® 45WP	45	Albaugh, LLC	Ankeny, IA	3	0.28 kg

Table 5.2: Application, rating, and harvest dates for field trials at Alson H. Smith Jr. Agricultural Research and Extension Center (AHS AREC) and the Southwest VA vineyard for 2015-2017.

			AHS AREC[a]		Southwest VA		
			2016	**2017**	**2015**	**2016**	**2017**
Application time	**Bloom**	**Weather**	22.2 ℃, 28.2 mm	18.4 ℃, 2.5 mm	21.4 ℃, 5.6 mm	17.9 ℃, 38.6 mm	19.4 ℃, 26.4 mm
		Treatment	6 Jun.	8 Jun.	1 Jun.	6 Jun.	24 May
		Maintenance	6 Jun. mandipropamid + sulfur	8 Jun. mandipropamid + metrafenone	30 May mancozeb, sulfur + tebuconazole	2 Jun. pyraclostrobin + boscalid, pyrimethanil + sulfur	24 May mancozeb, phosphorous acid, pyraclostrobin + boscalid, pyrimethanil + sulfur
	Berry touch	**Weather**	23.0 ℃, 19.6 mm	24.0 ℃, 24.1 mm	22.1 ℃, 30.2 mm	23.6 ℃, 30.7 mm	22.1 ℃, 62.2 mm
		Treatment	8 Jul.	11 Jul.	30 Jun.	29 Jun.	23 Jun.
		Maintenance	8 Jul. cyazofamid, cyflufenamid + sulfur	8 Jul. mandipropamid + metrafenone	28 Jun. mancozeb + sulfur	29 Jun. captan, sulfur + quinoxyfen	23 Jun. mancozeb + sulfur
	Veraison	**Weather**	26.4 ℃, 6.1 mm	21.5 ℃, 34.8 mm	23.1 ℃, 6.1 mm	24.5 ℃, 7.4 mm	21.3 ℃, 0.8 mm
		Treatment	15 Aug.	9 Aug.	5Aug.	4 Aug.	2 Aug.
		Maintenance	15 Aug. cyazofamid + sulfur	4 Aug. mandipropamid + quinoxyfen	24 Jul. captan, cyflufenamid + pyrimethanil	1 Aug. captan, fenhexamid + tebuconazole	2 Aug. captan, fenhexamid, phosphorous acid + pyraclostrobin + boscalid
	2 weeks after	**Weather**	23.2 ℃, 0.8 mm	19.1 ℃, 13.7 mm	23.0 ℃, 42.7 mm	NA[b]	NA[b]
		Treatment	26 Aug.	30 Aug.	21 Aug.		
		Maintenance	26 Aug. phosphorous acid	30 Aug. phosphorous acid	21 Aug. captan + fenhexamid		
		Rating date	27 Sep.	28 Sep.	9 Sep.	8 Sep.	8 Sep.
		Harvest date	27 Sep.	28 Sep.	10 Sep.	12 Sep.	12 Sep.

[a] Average temperature (℃) and total rainfall (mm) for the seven days before treatment application

[b] No applications were made.

Table 5.3: Fungicide Spray programs in two locations, Alson H. Smith Jr. Agricultural Research and Extension Center (AHS AREC) and the Southwest VA vineyard, for the 2015-2017 seasons.

AHS AREC vineyard						Southwest VA vineyard			
2016		2017		2015		2016		2017	
		22 Apr.	mancozeb + sulfur	20 Apr.	mancozeb	19 Apr.	mancozeb + sulfur	18 Apr.	mancozeb + sulfur
26 Apr.	mancozeb + sulfur	29 Apr.	mancozeb + sulfur	28 Apr.	mancozeb + sulfur	29 Apr.	mancozeb + sulfur	28 Apr.	mancozeb + sulfur
		6 May	mancozeb + sulfur	5 May	mancozeb + sulfur	8 May	mancozeb, phosphorous acid + sulfur	3 May	mancozeb + sulfur
10 May	mancozeb, potassium phosphite + sulfur	13 May	mancozeb + sulfur	13 May	mancozeb + sulfur	16 May	mancozeb, phosphorous acid + sulfur	14 May	mancozeb + sulfur
20 May	mancozeb, potassium phosphite + sulfur	20 May	cyazofamid + cyflufenamid	20 May	mancozeb + sulfur			24 May	mancozeb, phosphorous acid, pyraclostrobin + boscalid, pyrimethanil + sulfur
		24 May	cyazofamid + metrafenone	30 May	mancozeb, sulfur + tebuconazole				
1 Jun.	cyflufenamid + metrafenone	3 Jun.	mandipropamid + quinoxyfen			2 Jun.	pyraclostrobin + boscalid, pyrimethanil + sulfur	7 Jun.	mancozeb, sulfur + tebuconazole
6 Jun.	mandipropamid, sulfur + quinoxyfen	8 Jun.	mandipropamid + metrafenone	10 Jun.	pyraclostrobin + boscalid + sulfur	10 Jun.	mancozeb, sulfur + tebuconazole	16 Jun.	mancozeb + sulfur
21 Jun.	cyazofamid, cyflufenamid + metrafenone	14 Jun.	cyazofamid + quinoxyfen	19 Jun.	mancozeb, sulfur + tebuconazole	18 Jun.	mancozeb + sulfur	23 Jun.	mancozeb + sulfur
30 Jun.	mandipropamid, sulfur + quinoxyfen	20 Jun.	cyazofamid + cyflufenamid	28 Jun.	mancozeb + sulfur	29 Jun.	captan, sulfur + quinoxyfen	30 Jun.	captan + sulfur
		1 Jul.	mandipropamid + quinoxyfen						
		8 Jul.	mandipropamid + metrafenone	7 Jul.	cyflufenamid + ametoctradin + dimethomorph	10 Jul.	captan	8, Jul.	captan + sulfur
19 Jul.	mandipropamid + sulfur	15 Jul.	cyazofamid + cyflufenamid	16 Jul.	captan + sulfur	20 Jul.	captan + pyraclostrobin + boscalid		
		24 Jul.	cyazofamid + metrafenone	24 Jul.	captan, cyflufenamid + pyrimethanil			20, Jul.	captan, cyflufenamid + sulfur
1 Aug.	mandipropamid + sulfur	4 Aug.	mandipropamid + quinoxyfen			1 Aug.	captan, fenhexamid + tebuconazole	2 Aug.	captan, fenhexamid, phosphorous acid + pyraclostrobin + boscalid
		21 Aug.	mandipropamid + quinoxyfen	21 Aug.	captan + fenhexamid	14 Aug.	captan, phosphorous acid + quinoxyfen	14 Aug.	captan + quinoxyfen
		30 Aug.	phosphorous acid	28 Aug.	captan	22 Aug.	captan, cyflufenamid + phosphorous acid	25 Aug.	captan + fenhexamid
						30 Aug.	captan + phosphorous acid		
7 Sep.	cyazofamid + sulfur	9 Sep.	copper octanoate					1 Sep.	captan
20 Sep.	mandipropamid + sulfur	23 Sep.	copper octanoate						

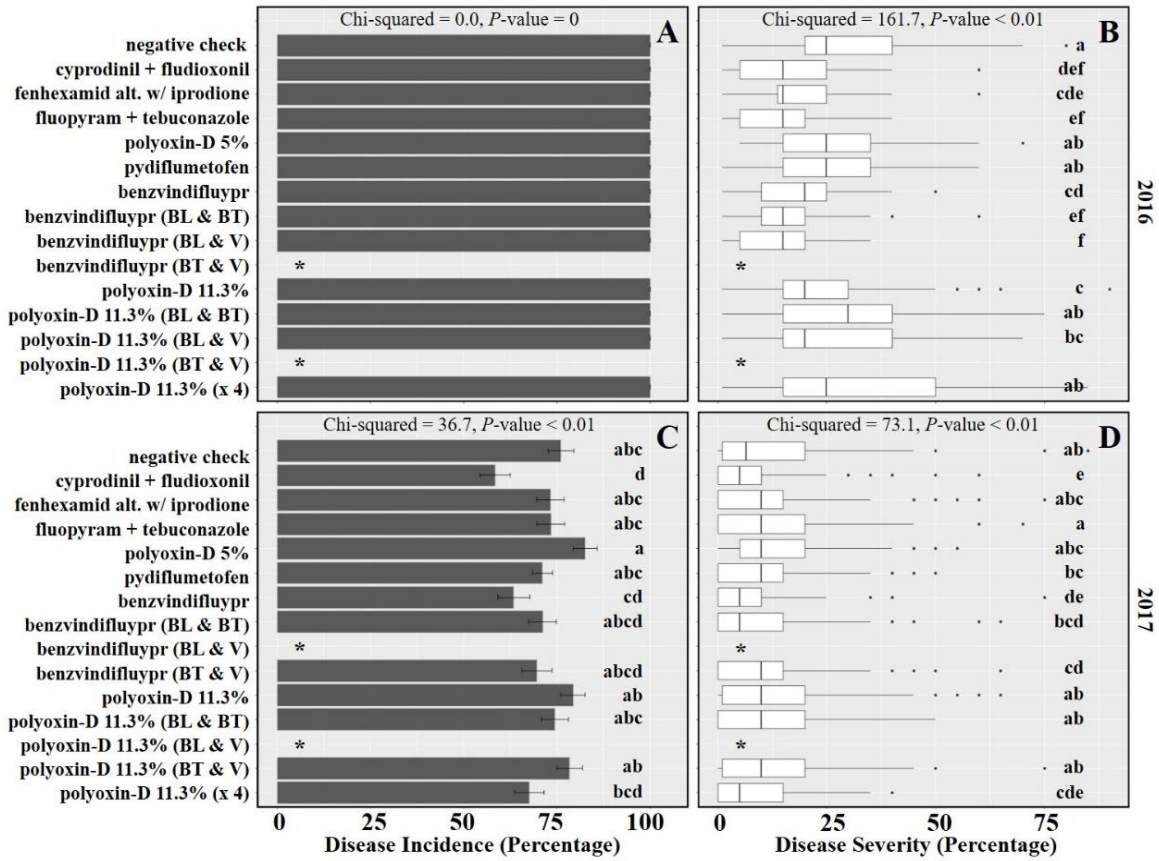

Figure 5.1: Percentage of grape ripe rot disease incidence and disease severity from the AHS AREC field trials. The two years are shown horizontally [2016 (A and B), 2017 (C and D)] with black bars representing the mean disease incidence [A and C] and the white box plots representing the upper and lower quantiles of disease severity [B and D] with the median marked by a horizontal line. The error bars represent one standard error from the median. The Chi-squared and *P*-values were calculated using the non-parametric Kruskal-Wallis rank sum method (R version 3.5.0) in the top of each panel. Significant mean separations ($P \leq 0.05$) between treatments from Dunn's Multiple comparison test (package 'FSA', R version 3.5.0) are denoted by non-overlapping lettering. Not all treatments were applied in both 2016 and 2017, therefore no data was collected (*) for specific treatments.

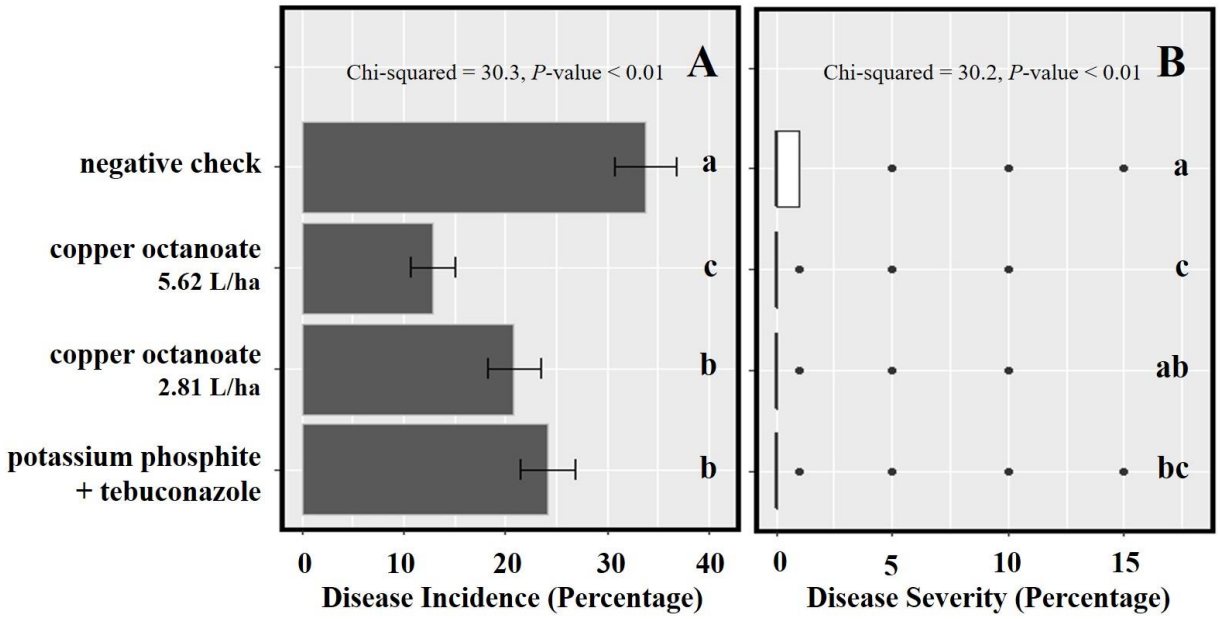

Figure 5.2: Percentage of grape ripe rot disease incidence and disease severity from the Southwest VA vineyard 2015 trials. The four a.i. treatments are shown horizontally with black bars representing the mean disease incidence [A] and the white box plots representing the upper and lower quantiles of disease severity [B] with the median marked by a horizontal line. The error bars represent one standard error from the median. The Chi-squared and *P*-values were calculated using the non-parametric Kruskal-Wallis rank sum method (R version 3.5.0) in the top of each panel. Significant mean separations ($P \leq 0.05$) between treatments from Dunn's Multiple comparison test (package 'FSA', R version 3.5.0) are denoted by non-overlapping lettering.

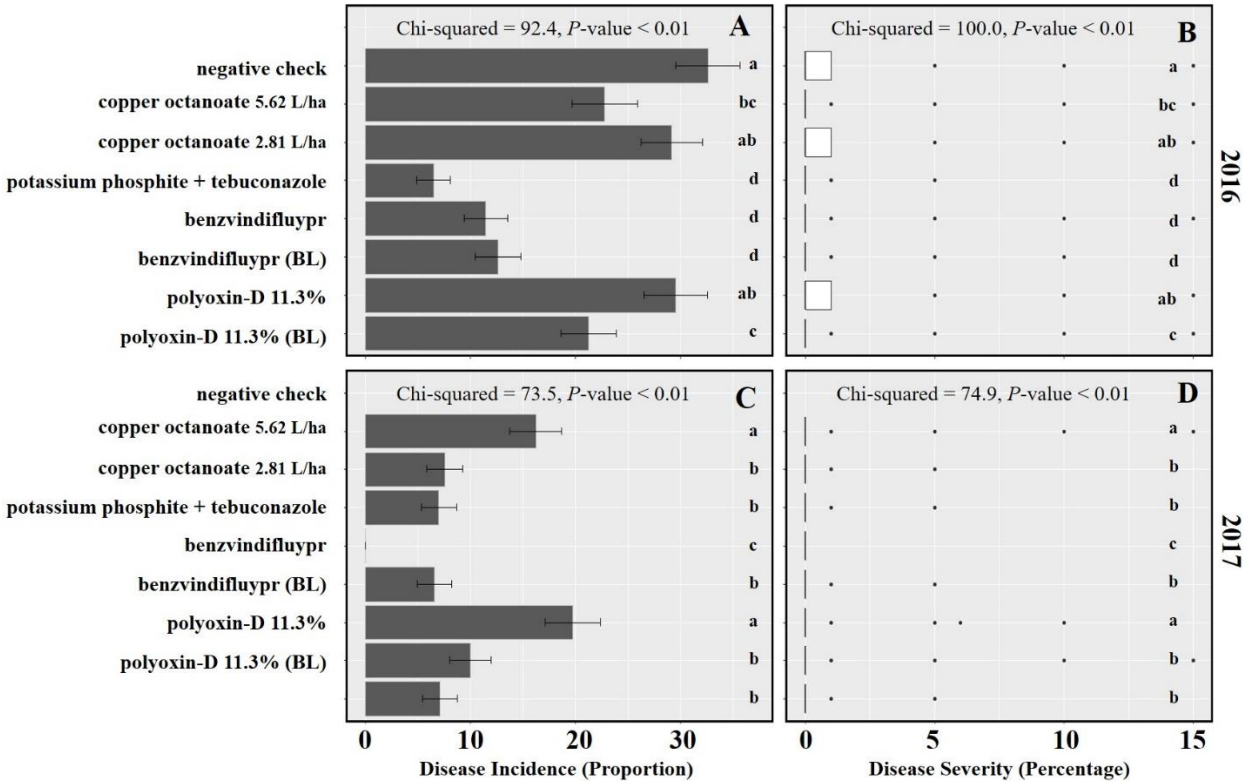

Figure 5.3: Percentage of grape ripe rot disease incidence and disease severity from the Southwest VA vineyard 2015 trials. The two years are shown horizontally [2016 (A and B), 2017 (C and D)] with black bars representing the mean disease incidence [A] and the white box plots representing the upper and lower quantiles of disease severity [B] with the median marked by a horizontal line. The error bars represent one standard error from the median. The Chi-squared and *P*-values were calculated using the non-parametric Kruskal-Wallis rank sum method (R version 3.5.0) in the top of each panel. Significant mean separations ($P \leq 0.05$) between treatments from Dunn's Multiple comparison test (package 'FSA', R version 3.5.0) are denoted by non-overlapping lettering.

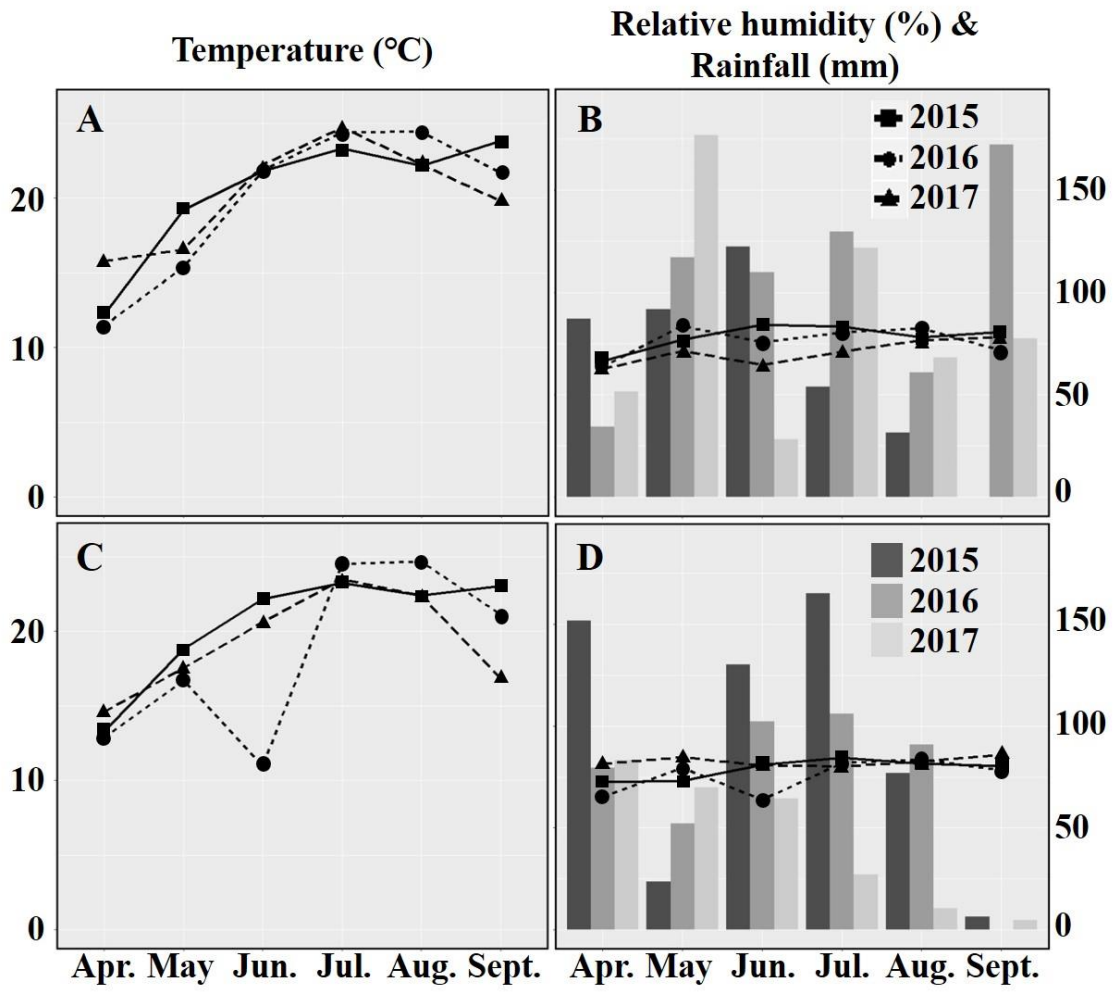

Figure 5.4: Temperature, relative humidity, and rainfall totals for both the Alson H. Smith Jr. Agricultural Research and Extension Center and Southwest VA vineyard from Apr. to harvest (early-mid. Sept.) in 2015-2017. Locations are shown horizontally with AHS AREC as the top two panels [A, B], and the Southwest vineyard as the bottom two panels [C, D]. The monthly average temperatures are displayed as a line graph in ℃ (left-hand vertical axis) [A, C], average monthly rainfall as a bar graph in mm (right-hand vertical axis) [B, D] with the average relative humidity overlaid as line graphs (percentage via right-hand vertical axis). Years are represented within each panel: 2015 as a solid line with squares or dark gray bars, 2016 as a dotted line with circles or gray bars, and 2017 as a dashed line with triangles or light gray bars.